ABSTRACT

Title of Document: STEADY STATE MODELING AND OPTIMIZATION FOR PERFORMANCE AND ENVIRONMENTAL IMPACT OF ADVANCED VAPOR COMPRESSION SYSTEMS

Mohamed Hassan Beshr
Doctor of Philosophy, 2016

Directed By: Reinhard Radermacher, Professor
Department of Mechanical Engineering

The use of heating, ventilation, air conditioning, and refrigeration (HVACR) systems is always increasing. This is because the HVACR systems are necessary for food production and ability to inhabit buildings that otherwise would be inhabitable. The basic vapor compression (VC) cycle which is still the main underlying HVACR technology worldwide, has already reached its limits and researchers are investigating more creative and complex cycles to improve capacity and efficiency. This motivates the development of a generalized vapor compression system simulation platform.

This thesis presents a comprehensive vapor compression system steady state solver which has several novel features compared to the existing solvers. Firstly, this solver is capable of simulating large number of different vapor compression system designs. This includes system configurations comprising more than 500 components, multiple air and refrigerant paths, and user defined refrigerants. Also, the solver uses a component-based solution scheme in which the component models are treated as black box objects. This allows a system engineer to quickly assemble and simulate a system

where-in the component models and performance data comes from disparate sources. This allows different vapor compression systems design engineers, and manufacturers to use the solver without the need to expose the underlying component model complexities. We validate the solver using a residential air source heat pump system, a vapor injection heat pump system with a flash tank, and a CO_2 two-stage supermarket refrigeration system with mechanical subcooler.

Moreover, designing a HVACR system while primarily considering its environmental impact requires an evaluation of the system's overall environmental impact as a function of its design parameters. The most comprehensive metric proposed for this evaluation is the system's Life Cycle Climate Performance (LCCP). Hence, this thesis presents an open-source and modular framework for LCCP based design of vapor compression systems. This framework can be used for, not only evaluation, but also LCCP-based design and optimization of vapor compression systems to minimize the environmental impact of such systems. Furthermore, the framework provides insights into various other challenges such as selection of appropriate systems for various climates and the choice of next generation lower global warming potential (GWP) refrigerants.

STEADY STATE MODELING AND OPTIMIZATION FOR PERFORMANCE AND ENVIRONMENTAL IMPACT OF ADVANCED VAPOR COMPRESSION SYSTEMS

By

Mohamed Hassan Beshr

Dissertation submitted to the Faculty of the Graduate School of the
University of Maryland, College Park, in partial fulfillment
of the requirements for the degree of
Doctor of Philosophy
2016

Advisory Committee:
Professor Reinhard Radermacher, Chair
Professor Jungho Kim
Professor Jelena Srebric
Associate Professor Bao Yang
Associate Professor Peter Sunderland
Associate Research Scientist Vikrant Aute

Acknowledgements

I would like to express my deep gratitude to Dr. Reinhard Radermacher for his help, support, and patience during this work. His continuous guidance has enriched this work. I would also like to offer heartfelt thanks to Dr. Vikrant Aute for his patience and providing me all the time and assistance I needed to complete this work. His insightful comments were of great significance for this work. I learned a lot of lessons, and developed many skills through my day to day interactions with him. I would like to thank my other committee members: Dr. Jungho Kim, Dr. Jelena Srebric, Dr. Bao Yang, and Dr. Peter Sunderland.

I would like to thank Hongtao Qiao for taking the time to guide me through VapCyc code during my first two years. I would like to thank my colleague Daniel Bacellar for his help and advice.

I would also like to thank all the past and current MOC faculty, staff, and students for their support and for creating a motivating and friendly work atmosphere throughout my PhD studies.

My greatest and deepest gratefulness goes to my parents who gave me infinite love, care, and support through my whole life and my career. My mother passed away ten months before my defense, but she is in our hearts every day. Her motivation and encouragement gave me the power to go on every day. I would also like to express my love to my family and thank them for their care and encouragement.

Finally, I would like to express my heartfelt gratefulness to my wife, Radia Eldeeb, for her care, patience, tolerance, encouragement, and support during my PhD journey.

Table of Contents

List of Tables

List of Figures

Nomenclature

Symbol	Quantity	Units
C	HX Cost	$
E	Energy	kWh/kg
Em	Emissions	Tons CO_{2eq}
Em_R	Emission rate for electricity production	kg CO_2/kWh
FA	Face Area	m^2
h	Enthalpy	kJ/kg
Life	Lifetime	years
LR	Leak Rate	%
m	Mass	kg
MC	Material Cost per unit mass	$ kg^{-1}
N	Number	
ρ	Density	kg m^{-3}
P	Pressure	Pa
R	Percentage of reused refrigerant	%
V	Volume	m^3

Subscripts

acc	Accidents
air	Air
con	Consumed
cond	Condenser
direct	Direct

elec	Electric energy consumption
eq	Equivalent
evap	Evaporator
fin	Fin
guess	Guess value
h	Hourly
in	Inlet
indirect	Indirect
input	Input
mat	Material
reaction	Reaction byproduct of the atmospheric breakdown of the refrigerant
recyc	Recycling
ref	Refrigerant
ref,disp	Refrigerant recycling and disposal at end-of-life
ref,EOL	Refrigerant leakage at end-of-life
ref,leak	Refrigerant leakage
ref,man	Energy used to manufacture the refrigerant
ref,prod	Refrigerant production and transportation
out	Outlet
SC	Subcooling
serv	Servicing
SH	Superheat

sys	System
sys,EOL	Energy required to recycle the system
sys,man	Energy required to manufacture the system
sys,trans	Energy used to transport the system
total	Total
tube	Tube

Abbreviations

AREP	Alternative Refrigerants Evaluation Program
ASHP	Air Source Heat Pump
CO_2	Carbon Dioxide
COP	Coefficient of Performance
DX	Direct Expansion
EMS	Enthalpy Marching Solver
GWP	Global Warming Potential
HVAC	Heating, Ventilation, and Air Conditioning
HVACR	Heating, Ventilation, Air Conditioning, and Refrigeration
HX	Heat Exchanger
LCCP	Life Cycle Climate Performance
LT	Low Temperature
MAC	Mobile Air Conditioners
MCHX	Micro-channel Heat Exchanger
MOGA	Multi-Objective Genetic Algorithm
MT	Medium Temperature

SEER	Seasonal Energy Efficiency Ratio
SLHX	Suction Line Heat Exchanger
TMY	Typical Meteorological Year
VC	Vapor Compression
VRF	Variable Refrigerant Flow

1. Introduction

1.1.Motivation

The use of vapor compression systems, whether on the commercial or residential scale, is continuously increasing. This is because vapor compression systems comprise the majority of the HVACR systems. According to the US Department of Energy (2010) heating, ventilation, and air conditioning (HVAC) account for 40%, and 33% of primary energy use in residential and commercial buildings, respectively. Thus, there is a continuous need for improving the efficiency, and reducing the cost and environmental impact of these systems. In order to reach these targets, a large number of system designs need to be evaluated, either through simulation or building a prototype. The latter option is obviously expensive and time consuming. Hence, the development cost of vapor compression systems drops when using proper simulations tools as large number of prototypes can be evaluated without the need of manufacturing large number of prototypes (Negrão & Hermes, 2011).

There are two main categories of vapor compression system simulation tools: steady state, and transient. The steady state simulation time is typically much less than the transient simulation time. Also, vapor compression systems are commonly designed and rated using steady state conditions (Winkler, 2009). Along the same line, the US Department of Energy allows the use of Alternative Efficiency Determination Methods (AEDM) and Alternate Rating Methods (ARM) for covered products as alternatives to testing for the purpose of certifying compliance. These methods allow the certification of some equipment through using well validated models that are derived from

mathematical models and engineering principles that govern the energy efficiency and energy consumption characteristics of the system (U.S. Department of Energy, 2011). Moreover, vapor compression system design optimization involves using steady state simulations for system performance evaluation. This includes studying the effect of using small tube diameters in heat exchangers, and moving towards low GWP refrigerants. As a result of the aforementioned, the use of steady state simulation tools is more common than transient simulation tools.

A proper simulation tool should combine three main factors: robustness, speed, and accuracy (Ding, 2007). The solver robustness is important to simulate the system performance under different operating conditions and simulate new and potential energy efficient system configurations. The solver speed or computational efficiency plays an important role especially when performing a system level optimization or parametric analysis. However, improving one of these aspects usually negatively affects the other factors. Thus, research is still on going to develop a vapor compression system steady state simulation tool that has an acceptable level of these three factors and provides high level of flexibility in components and system modelling.

As mentioned previously, one of the main aims of the development and optimization of vapor compression systems is to reduce their environmental impact. Among the different environmental impact metrics, the LCCP (UNEP/TEAP, 1999), is the most comprehensive one. This urges the need to have a proper framework that can evaluate the LCCP of the vapor compression systems. Also, this framework need be capable of interacting with any vapor compression system steady state simulation tool to reflect the changes in the system design on the LCCP of the system.

1.2.Literature Review

A vapor compression system simulation tool comprises of two main parts; the component models, and the system solver. The component model can vary from empirical equations to detailed component equations. The 10 coefficient compressor map (ANSI/AHRI, 2004), and the constant efficiency compressor model (or finite volume heat exchangers model) are examples of the empirical equations, and detailed component equations, respectively. The system solver combines the component models together according to the relationship between component parameters. The aim is to obtain the steady state refrigerant state (e.g. pressure, enthalpy, temperature…etc.) while satisfying the energy and mass balance in the system. The accuracy at the system level depends mainly on the accuracy of the component models. Thus, the system solver should have acceptable speed and robustness (Qiao, et al., 2010).

1.2.1. Energy System Simulation Packages

There are many solvers that can be used for energy system simulation, such as vapor compression systems, that currently exists. These can be divided into two main categories with some solvers utilizing hybridizations of the two categories (Richardson, 2006). The first category is the general equation solvers. These tools allow the user to specify the system in terms of its governing equations and equations describing each of the component models. The solver then solves these set of equations. Although this category allows for the simulation of any system, it requires a lot of efforts from the designer. This is because the equation solver has no intellect about the specific problem and is extremely dependent on the user to formulate the model and properly specify it. The Engineering Equation Solver (EES) (F-Chart) is one example of such general

equation solvers. The second category of simulation packages is the advanced energy system solvers. These solvers are usually designed for a specific task (e.g. simulation of a heat pump model, solar power plant…etc.). This makes it easier for the user to perform the desired simulations. However, the user is usually limited with the specific system to which the tool is designed. This makes generalizations of the system very difficult if not impossible. Aspen Plus (Aspen Technologies) is one example of advanced energy system solvers. Hybridizations of the two categories provide fixed systems with user defined component models. An example of these hybridizations is Sinda/Fluint (C&R Technologies). In order to obtain a reliable vapor compression system simulation tool, the user should have the option to simulate user defined systems using user defined components. Although, such tool is highly required, it doesn't currently exist.

1.2.2. System Solution Techniques

The unknown variables in a vapor compression system solver are typically fluid-related state information (Qiao, et al., 2010). The system solvers can be divided in two main approaches in which the unknown variables are solved (Winkler, 2009): successive approach where a variable is solved before moving on to the next variable, and simultaneous approach which uses a non-linear equation solver to solve all the unknown variables simultaneously.

The successive approach (Davis & Scott, 1976; Hiller & Glicksman, 1976; Fukushima, et al., 1977; Ellison & Creswick, 1978; Tassou, et al., 1982; Domanski & Didion, 1983; Fischer & Rice, 1983; Domanski & McLinden, 1992; Stefanuk, et al., 1992; de Lemos & Zaparoli, 1996; Robinson & Groll, 2000; Koury, et al., 2001; Joudi & Namik, 2003;

Zhao, et al., 2003; Rigola, et al., 2005; Sarkar, et al., 2006; Winkler, et al., 2008; Blanco, et al., 2012; Santa & Garbai, 2013) is fast and robust. This is because the number of iterative variables for a certain system using this approach are less than the number of variables in the simultaneous approach. Another reason is that this approach is usually designed towards a certain system configuration which allows to optimize the solver code. Also, this approach works in an easier and more efficient way for simple system configurations. However, as the system configuration gets more complicated, this approach needs more than one nested loop to perform the system level iterations. Thus, this approach becomes less convenient (i.e. it gets more difficult to determine the proper and efficient solution scheme) to use as the system configuration becomes more complex (e.g. more components, more splits and merges, multi-stage cycles…etc.). Another major drawback of this solution scheme is that for a small modification to the system configuration (e.g. adding a suction line heat exchanger to a basic four component vapor compression system), major code changes, if not a new solution scheme, are required.

In the simultaneous approach (Parise, 1986; Almedia, et al., 1990; Jolly, et al., 1990; Herbas, et al., 1993; Bourdouxhe, et al., 1994; Paulus, et al., 1994; Rossi, 1995; Browne & Bansal, 1998; Hwang & Radermacher, 1998; Corberan, et al., 2000; Corberan, et al., 2002; Hui & Spitler, 2002; Richardson, et al., 2002; Richardson, et al., 2004; Sanaye & Malekmohammadi, 2004; Agrawal, et al., 2007; Shao, et al., 2008; Belman, et al., 2009) the number of unknown variables is higher than in the successive approach for the same system configuration. This is because all the unknown variables are independent and are solved for simultaneously. Although this approach provides higher

flexibility for the modeled system configuration, it has higher computational cost than the successive approach. Also, for this approach, unlike the successive approach, the sequence of running the different component models in the system is not important. It is clear that a new solver is required that combines the robustness and speed efficiency of the successive approach while maintaining the flexibility of the simultaneous approach.

1.2.3. Solver-Component Models Interaction

A third method of categorizing the system solvers is based on the relation between the system solver and component models. The relation between the system solver and component models is categorized into two main schemes: the global scheme and the component-based scheme (Winkler, 2009). In the global scheme, the equations of the component models are typically hard coded within the system solver. This helps improve the robustness of the solver since the solver is directly evaluating all the mathematical equations. However, the obvious drawback of this scheme is its inflexibility. Adding new components or changing part of the system configuration needs a lot of effort. This is because the set of equations and solution variables are not dynamically formulated based on the system configuration.

In the component-based solution scheme, the system solver is decoupled from the component models. In other words, the system solver treats the component models as black-box objects interacting with one another through a series of ports and junctions. The system solver only handles the connection information between the components to satisfy the mass, energy, and momentum balances. One major advantage of this scheme is that it can handle arbitrary system configurations. In order to benefit from this

advantage, a non-linear equation solver needs to be used. Amongst the different non-linear equation solvers, Newton-Raphson and quasi-Newton equation solvers (e.g. Broyden's method (1965) are the most prevalent ones because of their fast convergence ability (Qiao, et al., 2010). Also, using this approach, the system solver requires no specific details about the component model equations or data. This enables different users to use the same solver while developing their own component models which might contain proprietary data without the need to expose such data to the solver code developer. In 1971, Stoecker (1971) presented concepts with regards to a general component-based simulation tool capable of simulating any thermal system. Stoecker also discusses the advantages and disadvantages of solving a system successively or simultaneously. Moreover, the development of this solution scheme to handle different complex cycle configurations was presented in the area of absorption system simulation (Grossman & Michelson, 1985). The originally presented algorithm was later improved to model more complicated cycle configurations (Grossman & Gommed, 1987; Grossman & Zaltash, 2001). In order to create a generic vapor compression system simulation tool that can handle arbitrary system configurations, a component-based solution scheme is needed. However, only very few vapor compression system simulation packages implement this solution scheme.

1.2.4. Existing Vapor Compression System Simulation Packages

There currently exists many vapor compression system steady state simulation tools. The Oak Ridge National Laboratory (ORNL) Heat Pump Design Model (HPDM) (Fischer & Rice, 1983) is the first simulation tool developed to help in designing the vapor compression systems. The tool has experienced a lot of improvements and is still

in use today. This tool has the benefit of implementing a component-based solution scheme. The tool was upgraded in 2006 to Mark VII version (DOE/ORNL, n.d.) and later in 2014 to a newer and more comprehensive version (Shen & Rice, 2014).

The National Institute of Standards and Technology (NIST) offers a vapor compression cycle design program called CYCLE_D (Domanski, et al., 2003). This tool is not developed to perform detailed cycle analysis but rather to provide information on the performance of pure and mixed refrigerants. Thus, it is only capable of simulating simple cycles.

The Department of Mechanical Engineering (MEK), Section of Energy Engineering (ET) at the Technical University of Denmark (DTU) offers a collection of simulation models for refrigeration systems CoolPack (Technical University of Denmark (DTU), n.d.). CoolPack covers different simulation purposes including cycle analysis, system dimensioning, system simulation, component calculations, analysis of operating conditions, transient simulation (cooling of an object/room), refrigerant calculations, and life cycle cost (LCC). The steady state simulation in this tool is coded using EES. The cycle analysis part of the tool has 11 different system configurations varying from single stage to two stage cycles as well as a combination of both. However, the tool is not component based, and limited to these predefined component models and system configurations. Also, this part of the cycle analysis section doesn't allow for detailed inputs and sizing of the different component models. Thus, the tool has a design section in order to allow for detailed component models. However, it is limited to a single stage cycle with suction line heat exchanger.

The Center for Environmental Energy Engineering (CEEE) Modeling and Optimization Consortium (MOC) at the University of Maryland College Park offers a Thermodynamic Cycle Model (TCM) (University of Maryland, College Park, n.d.). This tool allows for simple analysis of 11 different system configurations varying from single stage to two stage cycles as well as ejector cycle and fuel cells. Also, it allows for the addition of user defined cycles.

Along the same line, SysMo Ltd presents an open computational platform SmoWeb (SysMo Ltd, n.d.). This web tool provides system analysis for different system configurations. However, it is limited to predefined cycles and doesn't allow for detailed sizing of the component models.

Rossi (1995) presented a modular vapor compression system simulation tool, ACMODEL, to analyze and evaluate fault detection and diagnostics of vapor compression systems. Although the tool was improved since its first version, it still suffers from a limited component library. Also, ACMODEL requires all the input parameters to be provided by using batch files, hence, suffering from lack of a user friendly interface.

FKW Research Center for Refrigeration and Heat Pumps offers a Cycle Calculation Program KMKreis (FKW Research Center for Refrigeration and Heat Pumps, 2013). This program is simple and has a number of predefined often used basic types of refrigeration cycles. However, similar to CYCLE_D, it is not aimed to be used as a detailed vapor compression system simulation and design tool. It doesn't allow for the detailed specification of the component model inputs.

Corberan et al. (2000) presented a modular water-to-air heat pumps simulation model. The model was later enhanced and presented as a commercially available software, Investigación y Modelado de Sistemas Térmicos Advance Refrigeration Technologies (IMST-ART), for the design of vapor compression systems. The tool uses sub-models to model the components within the cycle while the system solver uses the Hybrid method to solve for the unknown variables simultaneously. This software, however, is limited to the simulation of the basic four component cycle with the possibility of adding some accessories (pipes, liquid to suction heat exchanger, and 4-ways valve), and a two stage cycle with intercooler.

Some vapor compression system manufacturers also develop their own system simulation tools. Emerson Climate Technologies offers System Design Simulator (SDS) (Emerson Climate Technologies, 2015) which is based on the ORNL HPDM. This simulator is available for purchase by customers interested in Emerson products and it allows the user to directly include Emerson products into the simulation.

Richardson (Richardson, et al., 2002; Richardson, 2006) presented a generic component-based steady-state simulation tool, VapCyc. This tool allows for the simulation of four different cycle types (basic cycle with four components, basic cycle with suction line heat exchanger, two stage flash cycle and two-stage split cycle) with additional components. A multi-objective genetic algorithm (Aute & Radermacher, 2014) was integrated into this tool for system level optimization which is an important feature in this tool. Richardson used the simultaneous approach to solve the system level unknowns to provide complete flexibility in designing vapor compression system configurations. However, this approach requires heat exchanger models implementing

the inlet/outlet pressure boundary condition. This boundary condition requires additional iterations in the heat exchanger model to determine the refrigerant mass flow rate. These additional iterations, in addition to the high number of unknowns of the simultaneous approach causes a decrease in the computational efficiency and the solver robustness. Winkler et al. (2008) added another solver to the tool called Enthalpy Marching Solver (EMS). The EMS implements the successive solution scheme which requires fewer unknown variables and therefore is faster and more robust than the Junction Solver. However the EMS has great difficulty of handling the refrigerant merging and splitting, and the arbitrary system configurations.

1.2.5. Summary

There are many steady state simulation tools that exist in literature. However, these tools either implement the fast and robust successive approach which has limited flexibility to system configuration, or the flexible simultaneous approach which suffers from speed and robustness problems. Also, most of these tools require the equations used in the component models to be hardcoded and/or exposed to the system solver. This limits the widespread use of these tools among the vapor compression system manufacturers due to the propitiatory equations and data used in the different components. Thus, some of the existing tools use the component-based solution scheme where the different components are defined as refrigeration system components, and are modeled as black box objects interacting with one another through a series of ports and junctions (DOE/ORNL, n.d.; Winkler, et al., 2006). However, these tools lack one or more of the key features: a user friendly interface, the ease of incorporating new component models in the system, the flexibility to create new

arbitrary cycles, and the capability to perform further analysis on the system (e.g. optimization, sensitivity, or parametric analysis).

1.3.Research Objectives

It is clear from the literature that although the research field of steady state simulation of vapor compression systems is mature, there still exist many opportunities for further development. The main challenge in this field is the development of a reliable steady state system simulation tool with high levels of robustness, computational efficiency, and flexibility. Also, the tool needs to allow for a detailed level of component models inputs.

One of the main aims of the study of the performance of the vapor compression systems is to improve their energy efficiency, and reduce their negative environmental impact. The energy efficiency of the system can be evaluated by looking at the system's coefficient of performance (COP), energy efficiency ratio (EER), or seasonal energy efficiency ratio (SEER). However, this doesn't provide a global image of the environmental impact of the system. Therefore, one of the comprehensive metrics for determining the environmental impact of vapor compression systems on the environment needs to be used. In fact, a user friendly tool needs to be developed to take into account the vapor compression system performance from the system simulation tool when evaluating the environmental impact of the system.

In the light of these challenges, this research has the following objectives:

1. Develop a comprehensive component-based vapor compression system steady state solver that can handle arbitrary system configurations and arbitrary primary and secondary refrigerant flow circuits, and user-defined convergence

criteria. This objective also includes comprehensive testing and validation of the solver.

2. Use the comprehensive solver to design and optimize vapor compression systems using next generation components. This includes using lower GWP refrigerants and heat exchangers with small diameter tubes.
3. Develop an open source modular LCCP evaluation and design based tool for vapor compression systems. The tool can be coupled with any vapor compression system simulation tool.

The development of the new solver helps evaluate the performance any newly proposed arbitrary system configuration. This reduces the engineering time of developing advanced heat pump technology that is capable of getting the maximum efficiency out of the system.

Optimizing vapor compression systems using small diameter tubes and lower GWP refrigerants helps study the potential designs of next generation vapor compression systems. These systems would have significant material, charge, emissions, and cost reduction while maintaining the same system COP. This optimization also helps in designing and manufacturing systems with higher COP and/or SEER without the need to increase the size of the baseline systems.

Moreover, developing the LCCP framework allows for designing of vapor compression systems while primarily considering their environmental impact. It also enables performing multi objective optimization, sensitivity, and parametric studies on the systems to determine the effect of changing the system design on its LCCP.

2. Comprehensive VapCyc Solver

This chapter describes the outline for the comprehensive VapCyc solver. The first section explains the different definitions and assumptions that are used in the comprehensive solver. These definitions are explained on a simple four component vapor compression cycle. The second section describes the outline of the single fluid arbitrary cycle solver. This solver can handle any user defined cycle that comprises one working fluid. This solver acts as the core solver of the comprehensive VapCyc solver. This solver supports user defined convergence criteria. It also allows for disabling/enabling any of the components in the cycle if it is connected in parallel with other components. The third section shows the multi-fluid solver that can handle any user defined cycle with multiple working refrigerants (each refrigerant forms a refrigerant loop). This solver allows for disabling/enabling any of the refrigerant loops in the cycle. The fourth section of this chapter describes how the comprehensive solver handles open refrigerant streams. The last section of this chapter presents the validations completed using the comprehensive solver.

2.1.Definitions and Assumptions

2.1.1. Component

The cycle shown in Figure 2.1 has four components (compressor, condenser, expansion device, and evaporator). The component (or component model) contains all the necessary equations to satisfy the conservation laws of mass, energy, and momentum. The component model can vary from empirical equations to detailed component equations. The 10 coefficient compressor map (ANSI/AHRI, 2004), and the constant

efficiency compressor model (or finite volume heat exchangers model) are examples of the empirical equations, and detailed component equations, respectively.

In the component-based solution scheme, the system solver deals with the different components as black boxes. The solver only knows the component type (e.g. compressor, condenser). However, it doesn't know the details of the component model (e.g. type of heat exchanger, equations). The solver communicates with each component model through its inlet and outlet ports. Every component in the cycle has a component ID with the first two digits reflecting the component type and the other two digits representing the component number (e.g. first compressor is 1001, second compressor is 1002, and first condenser is 2001). Thus, the solver can theoretically handle up to 99 components for each component type. Each component in the new solver implements a component standard that is described in Appendix A.

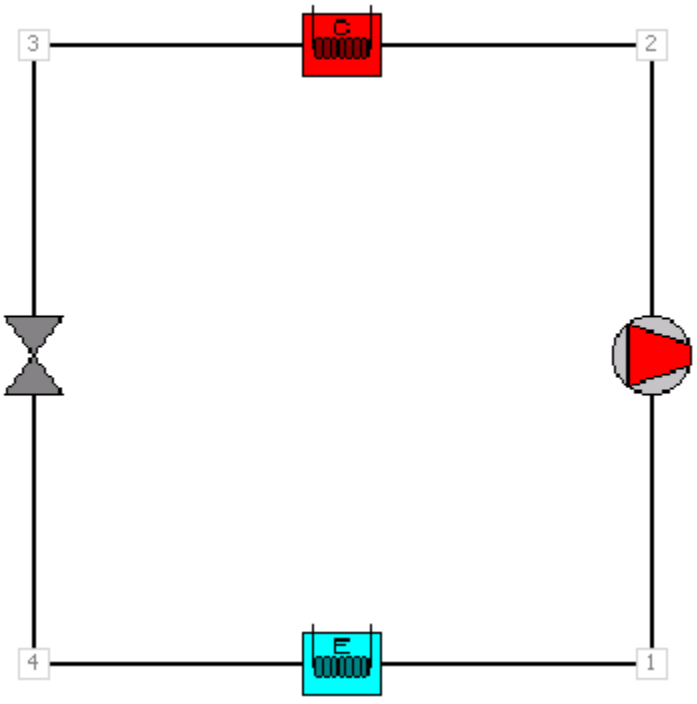

Figure 2.1: Basic vapor compression cycle

2.1.2. Port

As mentioned in the previous section, the solver communicates with the component through its ports. The solver uses the ports of the component to pass the inlet fluid state (e.g. pressure, enthalpy) and obtain the outlet fluid state upon successful execution of the component model. Each component model can have any number of inlet and outlet ports. In the comprehensive solver, inlet port states have odd numbers (1, 3, etc.) while outlet port states have even numbers. Each of the components shown in Figure 2.1 has two ports (one inlet and one outlet). However, a suction line heat exchanger would have 4 ports (two inlets and two outlets). The fluid port state can have any of the following information passed from and to the solver: pressure, enthalpy, temperature, quality, mass flow rate, mass fraction.

2.1.3. Fluid Group

As mentioned in the previous section, each component can have any number of ports. A single component can also utilize any number of refrigerants (e.g. the cascade heat exchanger has two different refrigerants passing through it). In order to differentiate the refrigerant paths in a component, a fluid group is defined. A single component can have more than one fluid group. The fluid group carries information including the refrigerant, port states (each fluid group has its own number of inlet and outlet ports), charge, work, heat, and power consumption. Every port through which the solver interacts with a component has a port ID which identifies the component ID, fluid group number, and port number (e.g. port ID 10010102 reflects the second port in the first fluid group in the first compressor).

2.1.4. Refrigerant

The refrigerant flowing in each fluid group can be any fluid from any of the following:

- Built in refrigerant (e.g. R-410A)
- User-defined refrigerant
- Air (both dry air and moist air)
- Glycol
- Ammonia water

Depending on the refrigerant in the port, the port state is determined to be known (e.g. for the built in refrigerants, the pressure, enthalpy, and mass flow rate are required)

2.1.5. Component Boundary Condition

The component boundary condition determines which parameters from the inlet/outlet port states that the component model requires as an input to execute successfully. It also determines the manner in which the system to component communication takes place. The comprehensive solver interacts with components that utilize two types of boundary conditions: mass flow based, and pressure based.

For the pressure based components, the inlet pressure and enthalpy, and outlet pressure are required as inputs for the models to execute. These parameters will be passed from the solver to the component prior to execution of the component model. After the component model runs successfully, it passes the inlet and outlet mass flow rates, and the outlet enthalpy to the system solver. The main pressure based components in the comprehensive solver are the compressor, and pump.

For the mass flow based components, the inlet pressure, enthalpy, and mass flow rate are required as inputs for the models to execute. These parameters will be passed from

the solver to the component prior to execution of the component model. After the component model runs successfully, it passes the outlet pressure, enthalpy, and mass flow rate to the system solver. The mass flow based components in the comprehensive solver include the heat exchangers, tubes, and flash tank. Although the expansion device is typically a pressure based component, in the comprehensive solver it is modeled as an isenthalpic mass flow based device (i.e. $h_{out} = h_{in}$) with the outlet pressure determined by the solver (one of the iterative unknown values).

2.1.6. Junction

A junction is a point in the cycle in which component ports are connected. The cycle in Figure 2.1 has four junctions with two ports connected to each of these junctions. For a merge occurring at a junction (e.g. outlet of multiple condensers connected to a junction), the junction enthalpy is calculated based on the mass and energy balance of the different inlet ports to the junction.

2.1.7. Pressure Level

A pressure level is a pressure at which one or more components are operating. The condenser (or multiple condensers in series) operates at one pressure level despite the pressure drops. On the other hand, a compressor operates between two different pressure levels. The cycle shown in Figure 2.1 has two pressure levels: the low side (evaporator and compressor suction) and high side (compressor discharge and condenser). For each cycle in the system, the solver initially assumes it operates at two pressure levels similar to the basic vapor compression cycle. Thus, the solver assumes that all the compressors initially have the same suction and discharge pressures.

2.2.Arbitrary Cycle Solver Outline

The new solver falls under the successive solution scheme category of solvers. However, the solver uses highly flexible data structures to overcome the flexibility problem associated with this type of system solvers. The solver outline consists of four main steps:

1. Determining the unknown variables and formulating the residual equations
2. Determining the number of required initial guess values and convergence criteria
3. Running the non-linear equation solver

The most challenging steps in this outline are the first two steps. These steps makes the solver gain its flexibility to simulate arbitrary system configurations. Thus, these two steps are the main focus in the new solver. In this section, the comprehensive solver simulates the performance of a basic vapor compression cycle with two condensers, shown in Figure 2.2, to demonstrate the main concept of the solver.

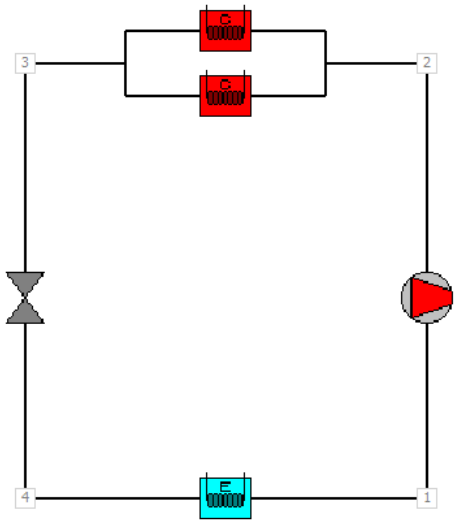

Figure 2.2: Basic vapor compression cycle with two condensers

The unknown variables for this cycle are the pressure and enthalpy at each junction and the refrigerant mass flow rate fraction in the condensers. This makes a vector of a total of 9 unknown variables [P_1 P_2 P_3 P_4 h_1 h_2 h_3 h_4 m_x]. The heat exchanger in this solver have mass flow rate boundary conditions. This means that the heat exchangers require the inlet pressure, inlet enthalpy, and inlet mass flow rate to execute and return the pressure and enthalpy for each outlet. Thus, the pressure at junction 3 is calculated based on the pressure at junction 2 and the runs of the condenser component model. Also, based on the enthalpy marching solver (Winkler, et al., 2008), the enthalpy can be propagated from one component to the next (e.g. the enthalpy outlet of the compressor in the enthalpy inlet to the condenser). Therefore, the only unknown enthalpy is at the compressor inlet. These two considerations reduce the number of unknown variables to 5 variables [P_1 P_2 P_4 h_1 m_x]. Before moving on to the solving scheme, we need to derive a general method to be used by the solver to determine the unknown variables in any arbitrary system configuration. The solver applies the following rules to determine the number of unknown variables:

1. For every pressure based component (compressor, pump …etc.), the inlet pressure and enthalpy, and the outlet pressure are unknown.
2. For each refrigerant flow split, the solver adds a number of unknown variables equal to the number of additional split branches (i.e. number of additional unknowns = number of branches -1).
3. For each expansion device, the outlet pressure is an unknown.

Then, a non-linear equation solver is used to solve the residual equations to obtain the value of the unknown variables. Hence, we need a set of residual equations

corresponding to the number of unknown variables. The solver uses the following rules in the first step to formulate the residual equations:

1. For the high side (i.e. discharge) pressure, the residual equation is based on an input system constraint (e.g. system subcooling at condenser outlet, or discharge pressure for a transcritical system). In this example, it is h_i-$h_{input,sc}$=0 where h_i is the calculated enthalpy during the system iterations and $h_{input,sc}$ is the desired enthalpy value (based on specified subcooling) at that point. This provides one residual equation.
2. For every refrigerant flow merge, the pressure levels from each branch are equal to one another. This provides a number of residual equations equal to the number of additional split branches (i.e. number of residual equations = number of branches -1). This will provide another residual equation in the current example ($P_{cond2,out}$-$P_{cond1,out}$=0).
3. For every pressure based component, the solver formulates two residual equations at the component inlet. These two equations ($P_{1,i}$-$P_{1,guess,i}$=0, $h_{1,i}$-$h_{1,guess,i}$=0) compare the calculated pressure based component inlet (guess) pressure and enthalpy values after each iteration with the calculated values from the outlet of the upstream component (i.e. junction pressure based on the outlet of the upstream components). The solver uses inlet pressure guess value as the reference pressure at the first iteration. In this example, the initial suction enthalpy is based on the suction pressure guess value and the desired superheat However, it can also be set initially equal to the saturated enthalpy at the suction pressure guess value.

4. For every expansion device, the solver compares the enthalpy calculated based on the specified convergence criteria (e.g. superheat value) with the enthalpy calculated at the specified port at each iteration. This provides a number of residual equations equal to the number of unknown outlet pressures for each of the expansion devices in the cycle.

Also, the non-linear equation solver needs initial guess values as a starting point for some of the unknown variables. The solver uses the following rules to determine the number of required guess values, and convergence criteria in the second step:

1. For each pressure level containing a condenser (e.g. in the example cycle = 1), one convergence criteria (e.g. subcooling at any condenser outlet for subcritical cycle, gas cooler outlet pressure for transcritical cycle) is a required input to the solver.
2. For every compressor, the inlet and outlet pressures are two input guess values to the solver.
3. For every expansion device, a corresponding convergence criteria along the same refrigerant path of the expansion device (e.g. evaporator outlet superheat) is an input to the solver.

Table 2.1 summarizes the unknown variables and the residual equations for the example system. The system requires four input values: P_1 (initially we assume $P_4=P_1$), P_2, subcooling, and superheat. Applying the previous steps to any system configuration, the solver determines the number of required guess values, and formulates the residual equations. The solver then assigns the default residual equations based on the input

convergence criteria. Finally, the solver might require additional (i.e. missing or unspecified) residual equations.

Table 2.1: Unknowns and residual equations of example cycle

Unknown Variables	Residual Equations
P_1	$P_{1,i}-P_{1,guess,i}=0$
P_2	$h_{3,i}-h_{input,sc}=0$
P_4	$h_{1,i}-h_{input,sh}=0$
m_x	$P_{cond2,out}-P_{cond1,out}=0$
h_1	$h_{1,i}-h_{1,guess,i}=0$

At every iteration, we need to run all the component models. As mentioned previously, at this point many of the existing tools are not flexible enough as the sequence of executing the components is important and typically hardcoded. In the comprehensive solver, one of the key steps is to run all the pressure based components (e.g. compressors) at the beginning of each iteration. This is because for all the pressure based components, the suction and discharge pressures are known (either from the guess values or the previous iteration) and the inlet enthalpy is calculated (based on the input suction superheat, or the previous iteration). Once the solver runs all the pressure based components, it loops through all the other components in the components list to run them one by one by. For each component in the list, if the upstream refrigerant state (i.e. inlet port state) is known, the solver runs the component model. The solver then checks this component as run. However, if the inlet port state has not been calculated yet, the solver moves to the following component. As an example, in Figure 2.2, after

running the compressor, if the solver checks the evaporator, it will not run it as h_4 is not calculated yet. The solver will only be able to run the condensers since the refrigerant state at junction 2 is already calculated. The solver keeps repeating the same loop until it runs all the component models. It then calculates the residuals and passes the values to the non-linear equation solver to proceed to the following iteration. This keeps going until convergence occurs within the specified tolerance. Figure 2.3 shows the solver flowchart.

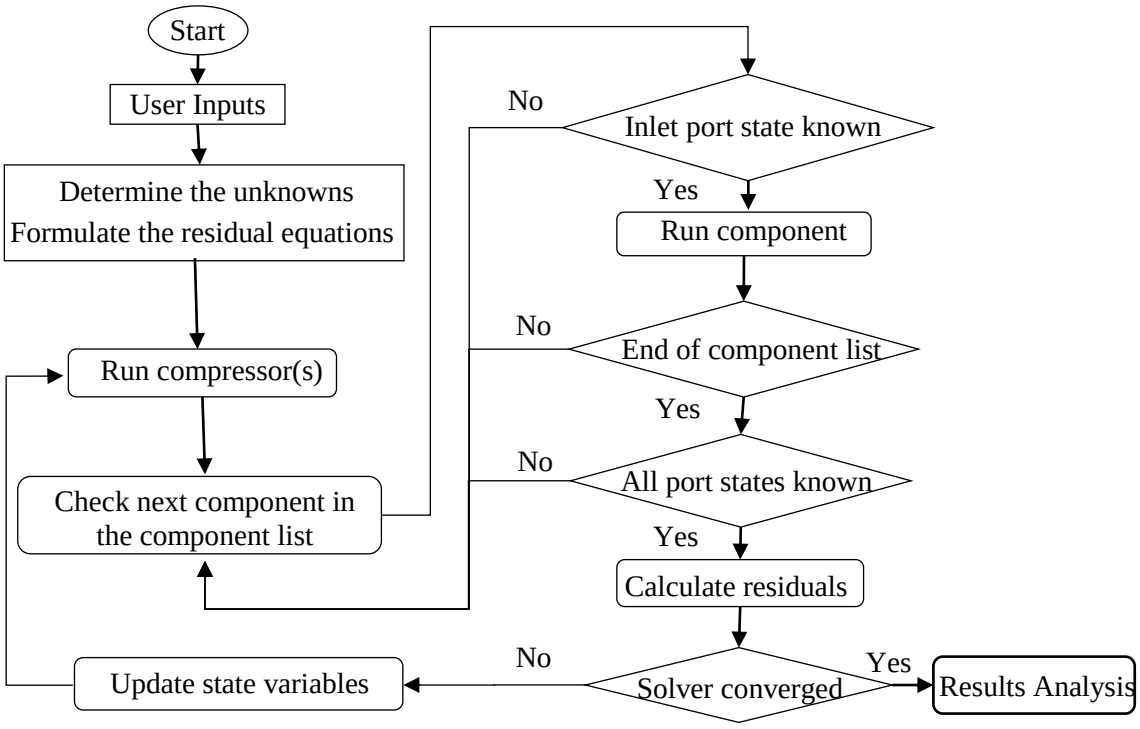

Figure 2.3: Solver flowchart

A random cycle generator is also developed using this solver. This cycle generator generates a basic four component cycle with additional pipes and components in series and parallel. This cycle generator confirms that the solver can successfully solve cycles with more than 500 components including up to 99 compressors (the maximum limit for each component type).

It is worth noting that the solver assigns the unknown variables and residual equations based on the ports of the components rather than the junctions in the cycle. The reason for that is demonstrated in section 2.2.1. The following sections show some sample cycles and the corresponding unknown variables and residual equations. These cycles will cover the different additional assumption used in the solver to determine the unknowns and residuals.

2.2.1. Variable Refrigerant Flow (VRF) System

The VRF system (Goetzler, 2007), shown in Figure 2.4, has multiple branches with expansion devices. For each branch, the mass flow rate fraction is an unknown with a corresponding pressure equation as a residual. Also, for each expansion device the superheat at the exit/last port in the branch is specified as a convergence criteria. As mentioned previously, the solver assigns the unknown variables and residual equations based on the ports of the components rather than the junctions in the cycle. The VRF system demonstrates the importance of this structure. Assigning the superheat to the junction rather than the port means that both evaporators must have the same superheat value, or even both branches must have superheat as the convergence criteria. On the other hand, assigning the residual equations to ports allows for flexibility when simulating the system (i.e. each evaporator can have a different outlet port superheat value).

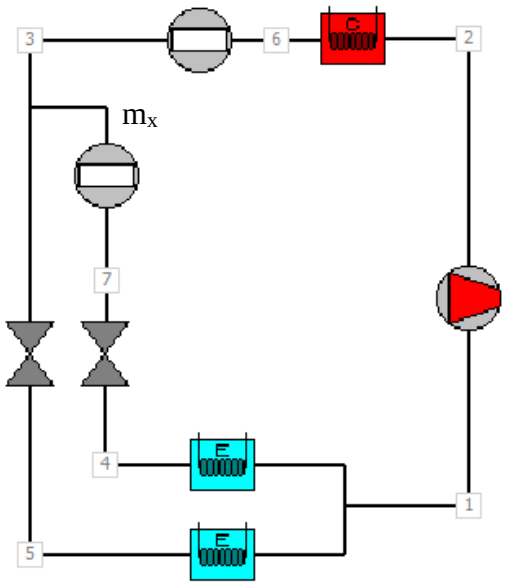

Figure 2.4: VRF System

Table 2.2: Unknowns and residual equations for VRF system

Unknown Variables	Residual Equations
P_1	$P_{1,i}-P_{1,guess,i}=0$
P_2	$h_{3,i}-h_{input,sc}=0$
P_4	$h_{evap1,i}-h_{input,sh1}=0$
P_5	$h_{evap2,i}-h_{input,sh2}=0$
m_x	$P_{evap2,out}-P_{evap1,out}=0$
h_1	$h_{1,i}-h_{1,guess,i}=0$

2.2.2. Simple Cycle with Additional Compressors in Parallel

Although this cycle, shown in Figure 2.5, has a split at the inlets of the compressors, the mass flow rate fraction is not an unknown as shown in Table 2.3. This is because the compressor is a pressure based device that runs at the beginning of each of the solver iterations. Thus, for each branch which contains a pressure based device, the

mass flow rate is known. In order to determine a branch which contains a pressure based component, the solver checks the first three components in the branch searching for the pressure based component. If the solver finds another split after any of the first three downstream components (i.e. before finding a pressure based component), or any of these downstream components (i.e. before the pressure based component is found) is not a tube, the mass flow rate for this branch becomes an unknown. Thus, adding a tube before any of the compressor doesn't add a mass flow rate unknown for this system. In that case with additional tube, once the compressor run is complete, the mass flow rate of the compressor is assigned to both ports of the tube. This mass flow rate assignment applies to any two port component in series directly before a pressure based device. Also, the pressure equality residual equation at the outlets of the condensers corresponds to the additional unknown outlet pressure (P_2 and P_3 are unknown). Thus, only one high side convergence criteria (e.g. subcooling at condenser outlet port) is still required for this cycle.

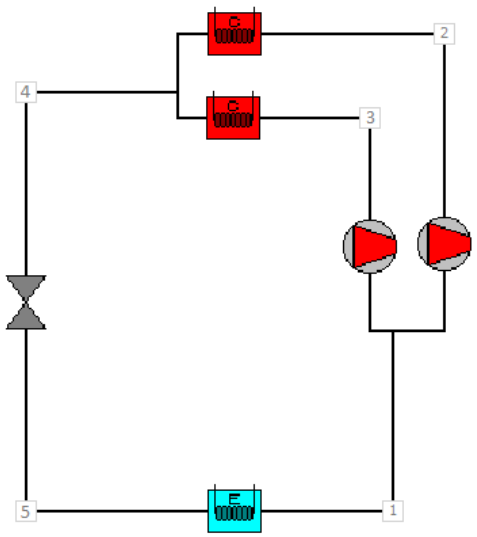

Figure 2.5: Simple cycle with additional compressors in parallel

Table 2.3: Unknowns and residual equations of cycle with additional compressors in parallel

Unknown Variables	Residual Equations
P_1	$P_{1,i}-P_{1,guess,i}=0$
P_2	$h_{4,i}-h_{input,sc}=0$
P_3	$P_{cond2,out}-P_{cond1,out}=0$
P_5	$h_{1,i}-h_{input,sh}=0$
h_1	$h_{1,i}-h_{1,guess,i}=0$

Although adding a tube before the compressor in this cycle, as shown in Figure 2.6, doesn't impose additional mass flow rate unknown, it adds additional pressure and enthalpy unknowns and residual equations for the compressor, as shown in Table 2.4. This is because in order to run the compressors at the beginning of the solver, the inlet pressure and enthalpy for each compressor needs to be defined. In the case of a split with no additional components before the compressor, the compressor branches share the same inlet conditions. This reduces the number of unknowns for each branch where the compressor is the first component after the split.

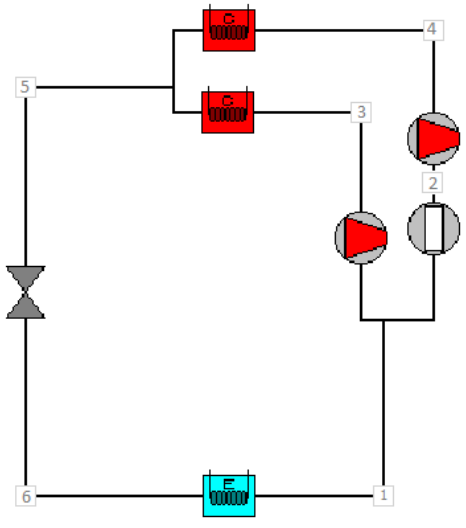

Figure 2.6: Simple cycle with additional compressors and a tube in parallel

Table 2.4: Unknowns and residual equations of cycle with additional compressors and a tube

Unknown Variables	Residual Equations
P_1	$P_{1,i}-P_{1,guess,i}=0$
P_2	$P_{2,i}-P_{2,guess,i}=0$
P_3	$h_{5,i}-h_{input,sc}=0$
P_4	$P_{cond2,out}-P_{cond1,out}=0$
P_6	$h_{1,i}-h_{input,sh}=0$
h_1	$h_{1,i}-h_{1,guess,i}=0$
h_2	$h_{2,i}-h_{2,guess,i}=0$

2.2.3. Simple Cycle with Suction Line Heat Exchanger (SLHX)

The SLHX cycle, shown in Figure 2.7, has two additional unknowns compared to the simple four component cycle, as shown in Table 2.5. These unknowns are the inlet pressure and enthalpy to the low side of the SLHX.

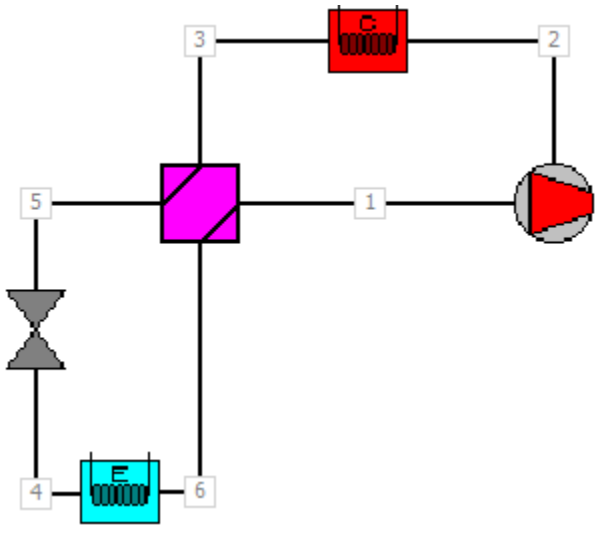

Figure 2.7: Simple cycle with suction line heat exchanger

Table 2.5: Unknown variables and residual equations of cycle with suction line heat exchanger

Unknown Variables	Residual Equations
P_1	$P_{1,i}-P_{1,guess,i}=0$
P_2	$h_{3,i}-h_{input,sc}=0$
P_4	$h_{1,i}-h_{input,sh}=0$
h_1	$h_{1,i}-h_{1,guess,i}=0$
P_6	$P_{6,i}-P_{6,guess,i}=0$
h_6	$h_{6,i}-h_{6,guess,i}=0$

2.2.4. Vapor Injection Heat Pump System with a Flash Tank

The 3 port vapor injection compressor, shown in Figure 2.8, requires additional inlet pressure and enthalpy inputs, as shown in Table 2.6. The additional intermediate pressure unknown variable requires an additional residual equation. This equation comes from the mass balance where the liquid refrigerant mass flow rate at 5 needs to be equal to the refrigerant mass flow rate at port 1 of the compressor.

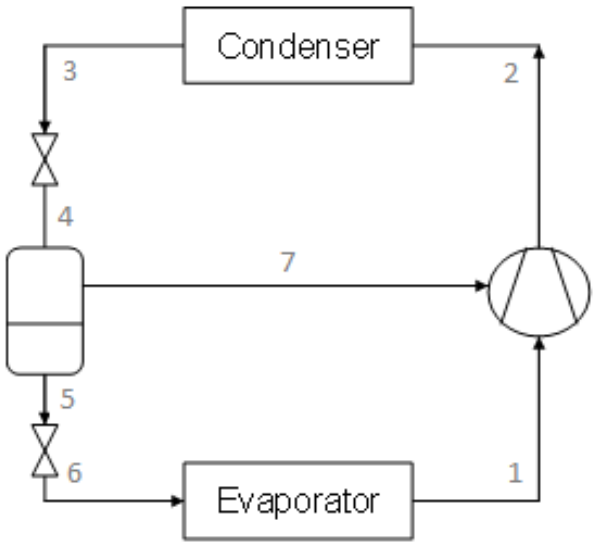

Figure 2.8: Vapor injection heat pump system with a flash tank

Table 2.6: Unknown variables and residual equations of system with a flash tank

Unknown Variables	Residual Equations
P_1	$P_{1,i}-P_{1,guess,i}=0$
P_7	$P_{7,i}-P_{7,guess,i}=0$
P_2	$h_{3,i}-h_{input,sc}=0$
P_6	$h_{1,i}-h_{input,sh}=0$
P_4	$m_5-m_1=0$
h_1	$h_{1,i}-h_{1,guess,i}=0$
h_7	$h_{7,i}-h_{7,guess,i}=0$

2.3.Multi-fluid Solver

The solver outlined in section 2.2 can handle user defined cycles with one fluid in the system. However, many vapor compression systems, such as the cascade system shown in Figure 2.9, utilize more than one refrigerant. Thus, the multi-fluid solver can handle more than one refrigerant in the system. This solver is based on the arbitrary cycle solver. The solver determines the unknown variables, and residual equations for each of the refrigerant loops (e.g. junctions 1, 2, 3 and 4 for one refrigerant loop in Figure 2.9) similar to the arbitrary cycle solver. That is, the cascade cycle has 8 unknown variables and corresponding residual equations with 2 high side and 2 low side convergence criteria (the equations for the high temperature cycle is shown in Table 2.7). However, when running the non-linear equation solver and the component models, the same outline as the one shown in Figure 2.3 is used. That is, for the cascade cycle shown, the two compressors are run at the beginning of the solver runs. The

cascade heat exchanger (HX) runs as the last component in the cycle since it requires that junctions 4 and 8 are determined beforehand.

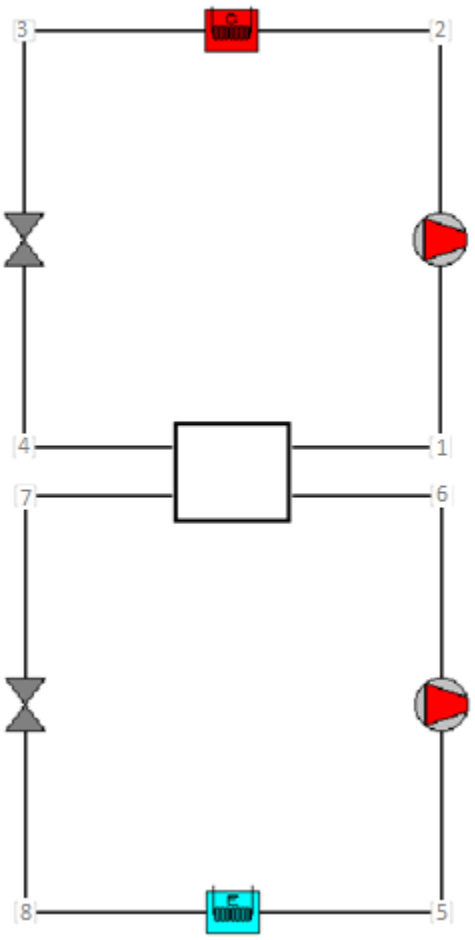

Figure 2.9: Cascade cycle

Table 2.7: Unknown variables and residual equations of example cycle

Unknown Variables	Residual Equations
P_1	$P_{1,i}-P_{1,guess,i}=0$
P_2	$h_{3,i}-h_{input,sc}=0$
P_4	$h_{1,i}-h_{input,sh}=0$
h_1	$h_{1,i}-h_{1,guesss,i}=0$

2.4.Open Fluid Stream Solver

Some vapor compression systems have multiple refrigerant circuits with one or more of these circuits being open. In order to have a comprehensive steady state vapor compression system solver, it needs to supports open refrigerant streams as well as closed ones. The open fluid stream solver is based on the multi-fluid solver. For each of the open refrigerant streams, the inlet port state to the stream is an input to the solver. The outline for the comprehensive solver handling the open refrigerant streams is shown in Figure 2.10. The solver initially assumes all the port states in the open refrigerant stream to be equal to the inlet port state. The solver then starts the non-linear equation solver for the closed refrigerant loops. After a specified number of iterations (e.g. 3) iterations of the closed loops non-linear equation solver or if it converges to the specified convergence criteria before the specified number of iterations, the closed loops solver exits. The open fluid stream solver then runs the open streams starting with the inlet components and iterating until all the component models in the open streams are run. At that point, all the component models in the system are run. The open fluid stream solver then checks if all the fluid port states in the open streams are within the desired tolerance of the fluid port states of the previous iteration (the initial conditions for all ports for the first iteration). If the closed loops non-linear solver converged and all the port states of the open streams are within the specified tolerance, this means that the open fluid stream solver converged successfully satisfying the mass and energy balances in the system. Otherwise, it keeps alternating between the closed loops and the open streams.

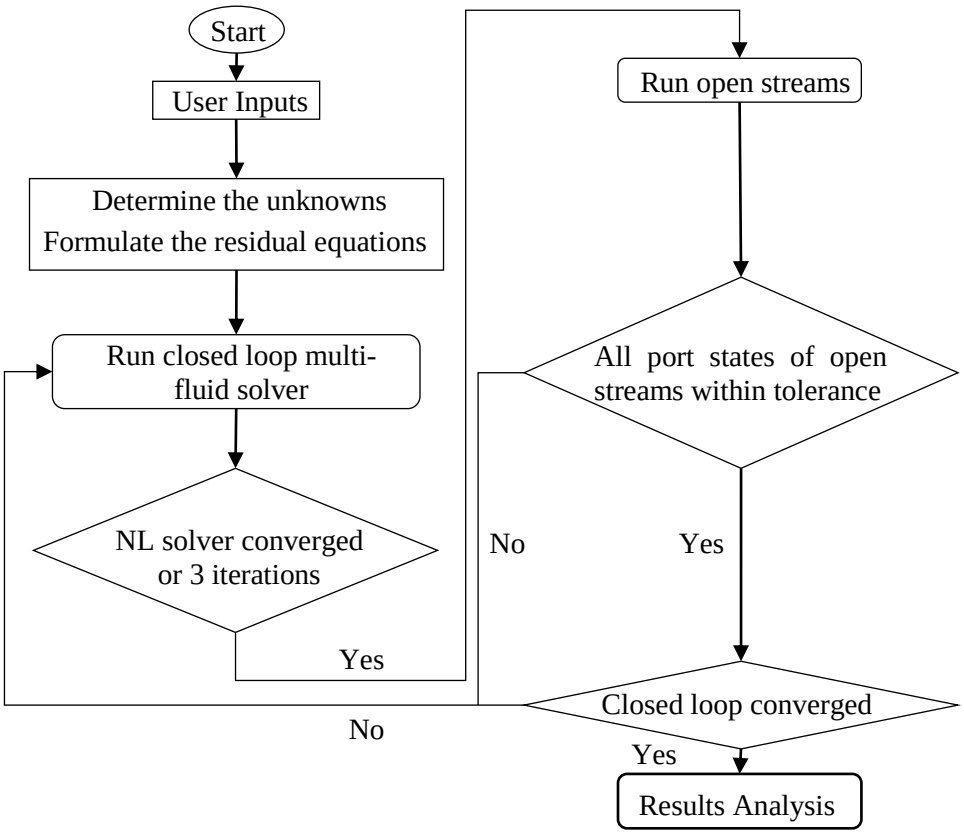

Figure 2.10: Open fluid stream solver outline

2.5.Solver Validations

In the previous sections, the outline of the novel comprehensive solver was explained using some sample cycle configurations. This section presents validations for the comprehensive solver.

2.5.1. Residential Air Source Heat Pump (ASHP) System

In this section, a residential ASHP system is validated against experimental data in the AHRI low GWP AREP report by Alabdulkarem et al. (2013). The compressor model is a ten-coefficient (AHRI-540-2004 Standard (ANSI/AHRI, 2004)) model with power and mass flow rate adjustment factors. The condenser and evaporator are based on a

finite volume heat exchanger model (Jiang, et al., 2006). This cycle has 4 unknown variables. The expansion device's inlet subcooling and suction superheat are the convergence criteria. These criteria values are set to be equal to the experimental values for the corresponding testing conditions and refrigerant. The modeling results match the experimental results within 5% accuracy as shown in Figure 2.11.

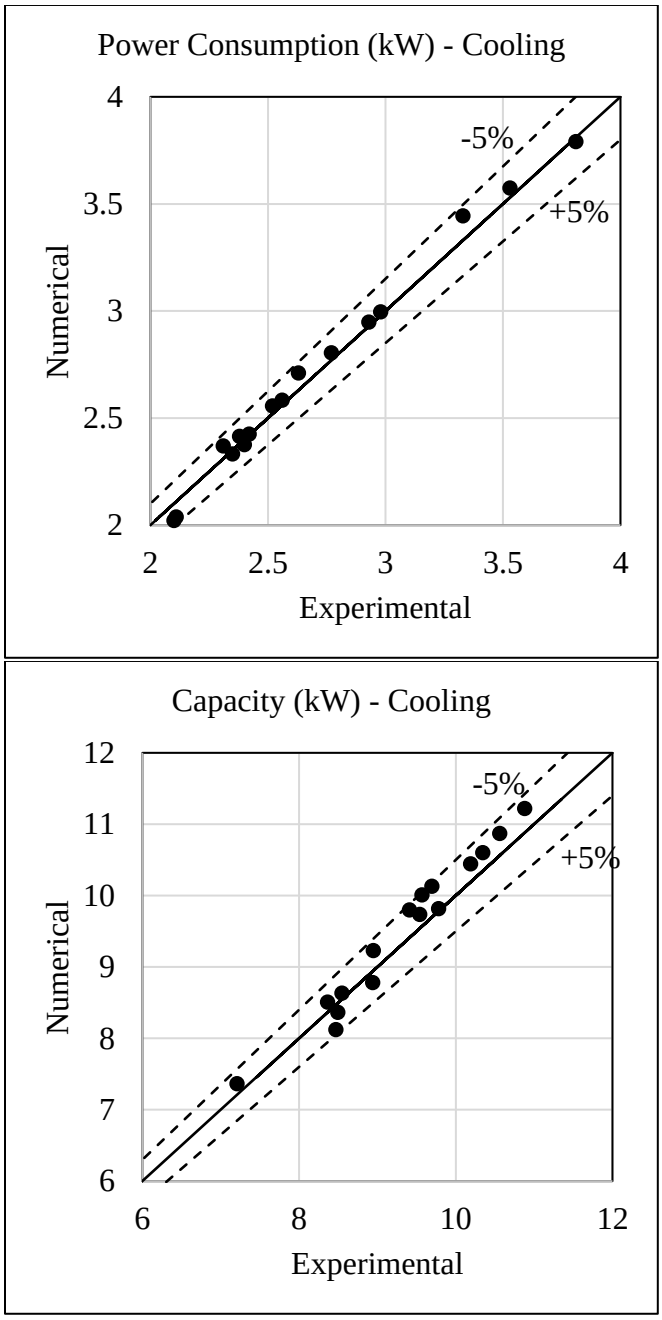

Figure 2.11: ASHP validation

It is worth noting that the same validation study was previously done using the enthalpy marching solver and results showed the same agreement (Alabdulkarem, et al., 2015).

2.5.2. Vapor Injection Heat Pump System with a Flash Tank

In this section, a vapor injection heat pump system with a flash tank, shown in Figure 2.12, is validated against experimental data by Xu et al (2013). The compressor model is a two stage compressor with an intermediate suction port. The condenser and evaporator component models use a finite volume heat exchanger simulation tool (Jiang, et al., 2006). This cycle has 7 unknown variables and corresponding residual equations, as previously shown in section 2.2.4. The expansion device's inlet subcooling and suction superheat are the convergence criteria. These criteria values are set to be equal to the experimental values for the corresponding testing conditions and refrigerant. The modeling results match the experimental results within 10% accuracy as shown in Figure 2.13.

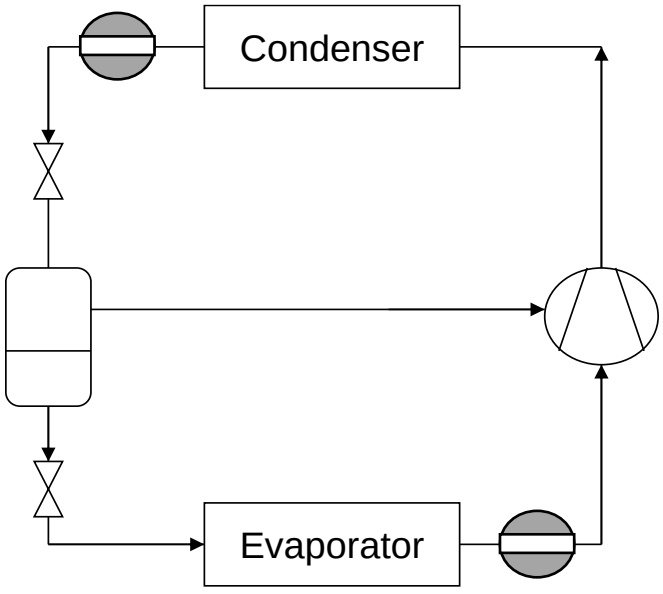

Figure 2.12: Vapor injection cycle schematic

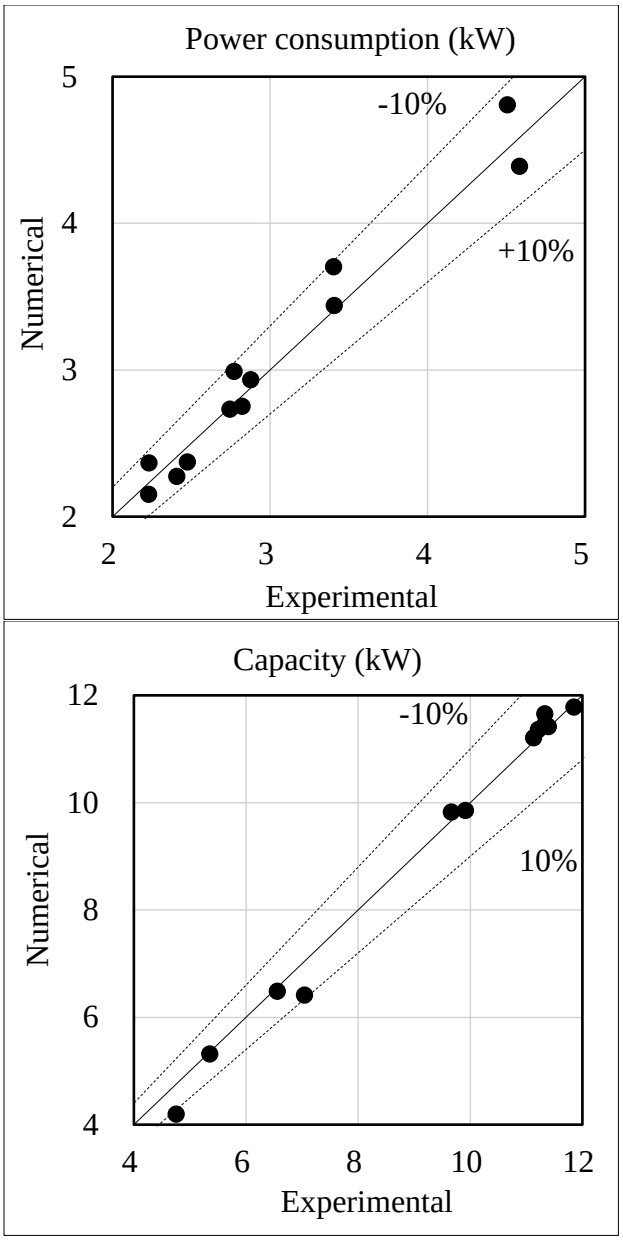

Figure 2.13: Flash tank cycle validation

2.5.3. CO_2 Two-Stage Refrigeration System with Mechanical Subcooler

In this section, a CO_2 two-stage refrigeration system with mechanical subcooler, shown in Figure 2.14, is validated against experimental data (Beshr, et al., 2016).

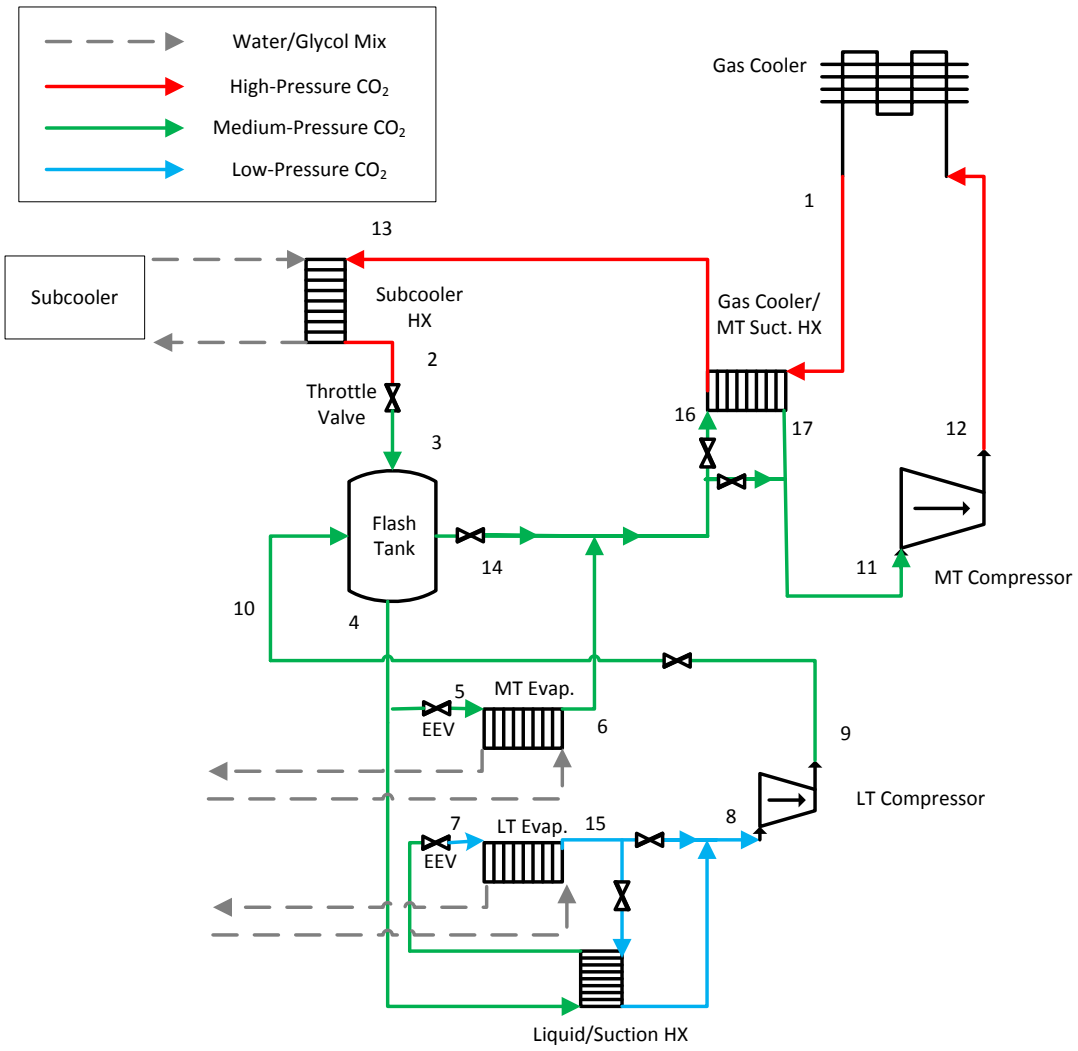

Figure 2.14: Supermarket refrigeration system schematic (Beshr, et al., 2016)

The CO_2 gas cooler component model is based on a finite volume HX model (Jiang, et al., 2006) while the subcooler HX, medium temperature (MT) and low temperature (LT) evaporators use a finite volume plate HX model (Qiao, et al., 2013; Eldeeb, et al., 2016). The R134a subcooler is not simulated in the system model and the inlet glycol operating condition is based on the experimental data. The LT compressor model is a ten-coefficient (AHRI-540-2004 Standard (ANSI/AHRI, 2004)) model with a power adjustment factor of 0.87 while the MT compressor is defined using the volumetric and

isentropic efficiencies, the displacement volume and RPM. This system has 11 unknown variables and corresponding residual equations. This system requires setting 4 different convergence criteria in the system. The selected criteria are the discharge pressure for transcritical operating conditions (outlet GC/condenser quality for subcritical operating conditions) at point 1, expansion valve outlet quality at point 14, and superheat at the outlet of each of the two evaporators. These convergence criteria values are set to be equal to the experimental values for the corresponding testing conditions. The validation results for the COP, power consumption and total system capacity are shown in Figure 2.15. The predictions are within 3% of the experimental data.

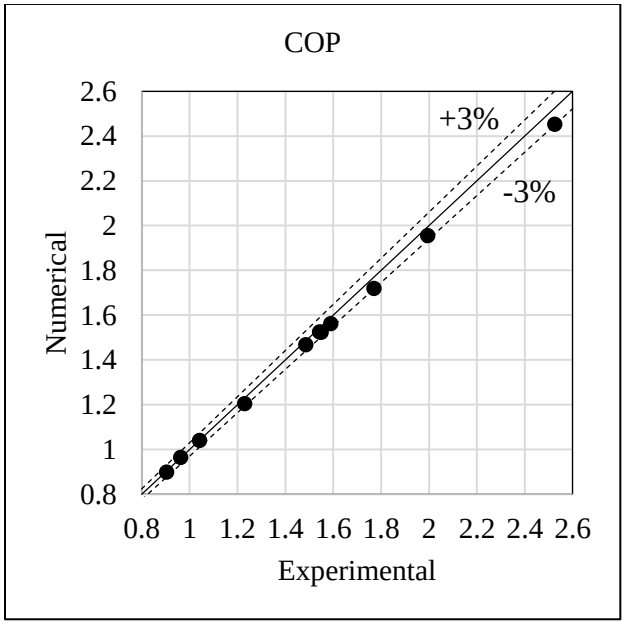

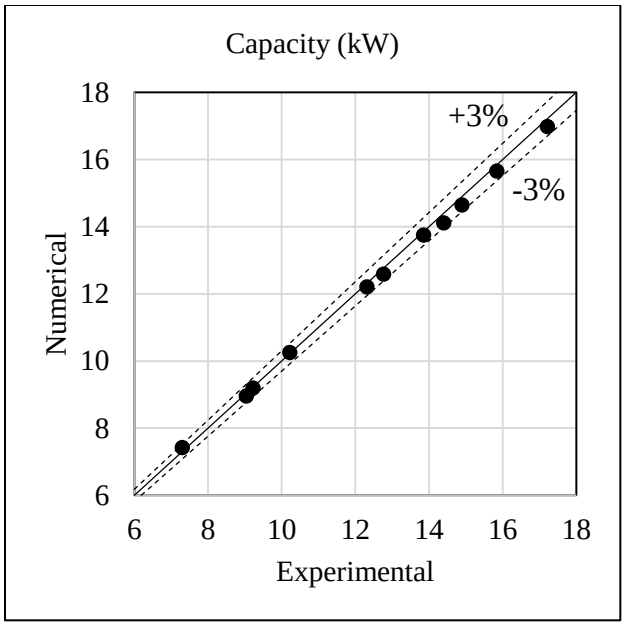

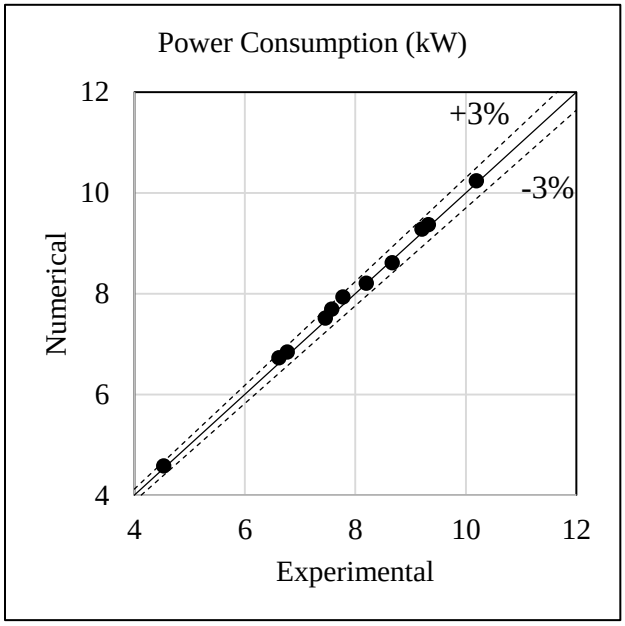

Figure 2.15. Validation results

3. System Optimization

In the previous chapter, the outline of the novel comprehensive solver was explained using some sample cycle configurations. This chapter presents optimization studies performed using the new solver. The optimization study presented in this section is published in the International Journal of Refrigeration (Beshr, et al., 2015).

3.1.Motivation

One of the key components in the HVAC system that plays an important role in the design process is the air-to-refrigerant HX. Thus, many efforts focus on the design and optimization of the HXs in order to maximize the HX effectiveness while minimizing the system power consumption and refrigerant charge (Webb & Kim, 2005). In order to meet the aforementioned goals, plate fin HXs with tube diameters smaller than 5 mm began to replace the 7 mm and larger diameter tubes (Pettersen, et al., 1986; Paitoonsurikarn, et al., 2000; Saji, et al., 2001; Kasagi, et al., 2003; Kasagi, et al., 2003; Choi, et al., 2004; Foli, et al., 2006; Shikazono, et al., 2007; Gholap & Khan, 2007; Abdelaziz, et al., 2010; Sanaye & Hajabdollahi, 2010; Dang, et al., 2011; Ding, et al., 2011; Najafi, et al., 2011; Wu, et al., 2012; Bacellar, et al., 2015). Shifting towards designs with diameters smaller than 5 mm requires thorough analysis and optimization of numerous HX design parameters. In order to do so, a comprehensive understanding of the heat transfer and pressure drop on the air and refrigerant sides is required. On the refrigerant side, the heat transfer and pressure correlations in literature are validated and found acceptable for small diameter tubes. However, very few correlations exist in the literature for the prediction of the air side performance of small diameter HX

designs (Bacellar, et al., 2014; Bacellar, et al., 2015). This lack of correlations in the 2-5 mm diameter range along with the research focus on the current most advanced finned micro-channel HX (MCHX) prompted few studies (Pettersen, et al., 1986; Ding, et al., 2012; Wu, et al., 2012; Bacellar, et al., 2014; Bacellar, et al., 2015; Bacellar, et al., 2015) in literature to study the 3-5 mm tube diameter HXs. Except for the work by Ding et al. (2012) which focuses only on 5 mm tube diameter HXs, there are no significant studies that investigate the design and optimization of small diameter tube-fin HXs and their effect on HVAC performance and environmental impact of the systems. Thus, this study focuses on the design optimization of 3-5 mm tube plate fin HXs and compares the benefits to a baseline design of 9.5 mm tube heat exchangers. The baseline design was chosen because it was readily available.

In an effort to reduce the environmental impact of HVAC systems by shifting towards low or zero GWP refrigerants, the Air Conditioning, Heating, and Refrigeration Institute (AHRI) started an industry wide collaborative effort known as the low GWP Alternative Refrigerants Evaluation Program (AREP). This program aims to gather industry resources in the hopes of finding and assessing promising alternative refrigerants (The Air Conditioning, Heating and Refrigeration Institute, n.d.). The studied refrigerants are either pure R-32, or blends comprised of R-32, R-1234yf, or R-1234ze in an effort to obtain a balance between low GWP, cost, safety, and system efficiency (Pham & Rajendran, 2012). Pure R-32 seems to be one among several potential candidates for the replacement of R-410A in ASHP systems (Wang, et al., 2012). This is due to its comparable performance with the baseline R-410A (Wang, et al., 2012; Alabdulkarem, et al., 2013; Burns, et al., 2013; Lei & Yanting, 2013). Thus,

this study presents the optimization results for the baseline R-410A and the alternative low GWP refrigerant R-32. The aforementioned AREP reports focus on a drop-in test; using the baseline R-410A system to determine the performance of R-32 as a replacement refrigerant. In that case, the system is not optimized to provide the optimal performance when utilizing R-32. Also, some of these reports show soft optimization to the R-32 system (Li & By, 2012). This means performing a further analysis to determine the effect of making slight changes to the system, such as changing the system charge, compressor sizing, and using a suction line HX on the system performance. Nevertheless, this soft optimization is limited in its results because it focuses on a limited number of parameters, and is performed in a discrete simulation or retesting mode rather than continuous optimization mode. In order to explore a larger and comprehensive design space with mixed-discrete design variables, we use a multi-objective genetic algorithm (MOGA) in the optimization of the HXs.

To sum up, this study presents the optimization of a residential ASHP system (Alabdulkarem, et al., 2013) with the objective of minimizing the HX cost (based on minimizing the required HX materials) and maximizing the system COP. The optimization is carried out for both R-410A and its alternative R-32. Both the condenser and evaporator geometry parameters are used as design variables during optimization. This study shows the potential system performance improvement and cost reduction when using small diameter HXs. The aim of this study is to show the benefits of comprehensive optimization as opposed to soft optimization and component-only optimization.

3.2.System Model

The ASHP system simulated in this study is similar to the system tested experimentally in the AHRI low GWP AREP report by Alabdulkarem et al. (2013) validated in section 2.5.1. The schematic of the HXs is shown in Figure 3.1.

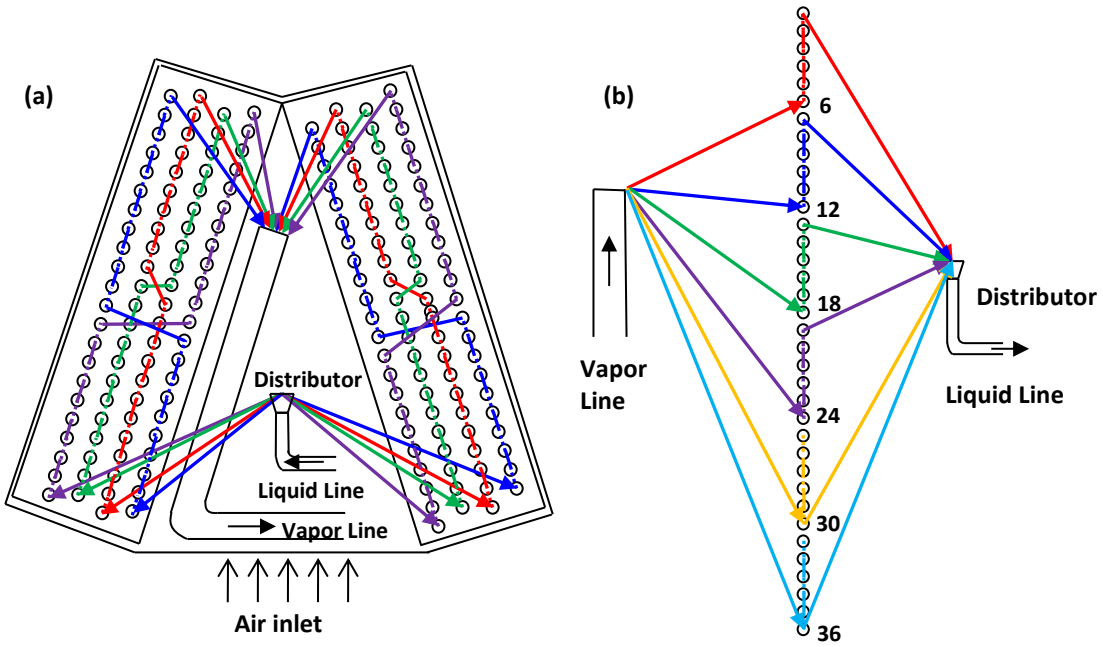

Figure 3.1: Schematic of baseline HXs: a) evaporator, b) condenser

Table 3.1 shows the correlations used for the air and refrigerant sides in both HXs. The energy consumption of the system used in the COP calculation is based on the compressor power and the actual fan power delivered to the air flowing through the HXs. In this study, a MOGA (Deb, 2001; Aute & Radermacher, 2014) is used for the system optimization.

Table 3.1: Correlations used in HX Modeling

HX	Type	Phase	Correlation
Evaporator	Heat transfer	Refrigerant - Two Phase	Jung et al. (1989)
		Refrigerant - Vapor Phase	Dittus & Boelter (1985)
		Air (2-5 mm tube diameter)	Bacellar et al. (2014)
		Air (9.5 mm tube diameter)	Wang et al. (1998)
	Pressure Drop	Refrigerant - Two Phase	Jung & Radermacher (1989)
		Refrigerant - Vapor Phase	Blasius (Incropera & DeWitt, 1996)
		Air (2-5 mm tube diameter)	Bacellar et al. (2014)
		Air (9.5 mm tube diameter)	Wang et al. (1998)
	Void Fraction	Two Phase	Koyama et al. (2004)
Condenser	Heat transfer	Refrigerant - Liquid Phase	Dittus & Boelter (1985)
		Refrigerant - Two Phase	Cavallini et al. (2003)
		Refrigerant - Vapor Phase	Dittus & Boelter (1985)
		Air (2-5 mm tube diameter)	Bacellar et al. (2014)
		Air (9.5 mm tube diameter)	Wang et al. (1998)

Condenser	Pressure Drop	Refrigerant - Liquid Phase	Bhatti & Shah (1987)
		Refrigerant - Two Phase	Lockhart & Martinelli (1949)
		Refrigerant - Vapor Phase	Churchill (1977)
		Air (2-5 mm tube diameter)	Bacellar et al. (2014)
		Air (9.5 mm tube diameter)	Wang et al. (1998)
	Void Fraction	Two Phase	Koyama et al. (2004)

Also, the optimization is repeated for both R-410A and R-32, each for ASHRAE (1995) cooling tests A B, and C operating conditions. However, this chapter focuses on the A and C test conditions because these are the two extreme test conditions in the ASHRAE cooling test matrix.

3.2.1. Optimization Problem

The two objectives in this optimization study are to maximize the COP of the system while minimizing the cost. Equation 3.1 describes the optimization problems, and Table 3.2 shows the design space. The system capacity, HX refrigerant, and the values of the air side pressure drops for the baseline are different from one test to the other. Also, the condenser face area constraint is based on the range of testing and the applicable range of the air velocity in the correlation used, and the baseline air volume flow rate.

There are some additional assumptions and design considerations when generating the new HXs for each iteration. The total refrigerant flow cross sectional area in the HX is the same as the baseline case. Hence, the total number of tubes for the 3 mm diameter

is almost 10 times ($(9.5/3)^2$) the number of tubes of the baseline 9.5 mm tube diameter. This assumption is used to calculate the total number of tubes in the new design. The total number of tubes is divided by the number of tube banks, which is a design variable, to determine the number of tubes per row. Moreover, the generated HX for each iteration has counter flow configuration, as opposed to the cross flow baseline design. This is because the counter flow configuration is the most efficient in terms of heat transfer rate per unit surface area. Furthermore, the HX material cost is used as the representative cost, and is calculated from Equation 3.2. Finally, in Equation 3.2, the tube material cost per unit mass is assumed to be 1.5 times the fin material cost per unit mass.

Table 3.2: Design space

HX	Design Variable	Unit	Baseline	Range	Variable Type
Condenser	Tube Outer Diameter	mm	9.5	3-5	Discrete
	Fins per inch	in^{-1}	21	20-40	Discrete
	Fin Type	-	Wavy Louver	Flat Plate, Bare Tube	Discrete
	Tube Length	m	2.16	1.5-3.5	Continuous
	Vertical Spacing Ratio	-	2.632	1.5-3	Continuous
	Horizontal Spacing Ratio	-	2.632	1.5-3	Continuous
	Number of Tube Banks	-	1	1-2	Discrete
	Circuits per bank	-	6	6-125	Discrete

Evaporator	Tube Outer Diameter	mm	9.5	3-5	Discrete
	Fins per inch	in^{-1}	15	20-40	Discrete
	Fin Type	-	Wavy Louver	Flat Plate, Bare Tube	Discrete
	Tube Length	m	0.503	0.15-1	Continuous
	Vertical Spacing Ratio	-	2.105	1.5-3	Continuous
	Horizontal Spacing Ratio	-	2.632	1.5-3	Continuous
	Number of Tube Banks	-	4	2-9	Discrete
	Circuits per bank	-	1	4-125	Discrete

$$
\begin{aligned}
&Minimize: HX\ Cost \\
&Maximize: COP \\
&Subject\ to: \\
&\quad Capacity > Baseline\ [W] \\
&\quad FA_{evap} < Baseline * 1.25\ [m^2]\ (Baseline = 0.22 m^2) \\
&\quad \Delta P_{ref,evap} < 20000\ [Pa] \\
&\quad \Delta P_{air,evap} < Baseline * 2\ [Pa] \\
&\quad FA_{cond} < 3.6\ [m^2]\ (Baseline = 1.94 m^2) \\
&\quad \Delta P_{ref,cond} < 40000\ [Pa] \\
&\quad \Delta P_{air,cond} < Baseline * 2\ [Pa]
\end{aligned}
\qquad \text{Equation 3.1}
$$

$$
C = (MC * \rho * V)_{tube} + (MC * \rho * V)_{fin} \qquad \text{Equation 3.2}
$$

3.2.2. Results and discussion

Figure 3.2 and Figure 3.3 show the Pareto sets for R-410A and R-32, respectively. The shading of the symbols indicates the relative evaporator face areas between the designs.

The size of the symbols represents the relative condenser face area. The cost reduction is 45%, and 44% for R-410A systems designed and optimized for tests A and C operating conditions, respectively. Also, the cost reduction is 50%, and 47% for R-32 systems designed and optimized for tests A and test C operating conditions, respectively.

For the designs in the Pareto set, i.e., for the optimal designs, the evaporator tube diameter is either 3, 4, or 5 mm, while the condenser tube diameter is either 3 or 4 mm. The 5 mm tube diameter condenser designs show a better performance and lower costs than the baseline design. However, the 3 and 4 mm condenser tubes show better performance and lower cost than that of the 5 mm tubes. That is because for the same material volume, the 3 and 4 mm tubes show lower air and refrigerant sides thermal resistance. Thus, the 5 mm tubes do not show in the condenser Pareto set designs.

For the small diameter tubes, the required number of tubes to maintain the total refrigerant flow cross sectional area in the HX is much larger (5.6 times for 4 mm tubes, and 10 for 3 mm tubes) than the number of tubes in baseline design. However, for many of the Pareto designs, the evaporator and condenser face areas are smaller than the baseline face areas. This is because there are many other design parameters which affect the face area, such as the tube spacing, number of tube banks, and tube length. Increasing the number of tube banks helps to accommodate the increase in the number of tubes without increasing the face area. Nevertheless, this leads to an increase in the air side pressure drop, which is one of the constraints. Thus, for all evaporator Pareto designs, the number of tube banks is in the range of 4 to 7 (although the design space ranges from 2 to 9), as compared to the baseline design of 4 tube banks.

Also, all the condenser Pareto designs with a smaller face area than the baseline has 2 tube banks as compared to the 1 tube bank design. Reducing the vertical tube spacing helps reduce the face area because it allows more tubes to fit in the same HX height. It also helps in air flow acceleration and mixing, which improves the heat transfer performance. However, as the tubes get closer, the air side pressure drop increases, which can exceed the constraint level, especially as the number of tube banks increases. Hence, only for some R-32 Pareto evaporator designs with 4 tube banks, the tubes' vertical spacing ratio was 1.5 (which is the minimum value in the design range).

For finned tubes, as the fins per inch increases, effects similar to the effects of reducing the tube vertical spacing are seen. Therefore, having higher fins per inch for the small tube diameters helps improve the fin effectiveness by up to 25% of the baseline effectiveness. Furthermore, shorter HX tubes cause a decrease in the HX face area. In order to obtain the same heat load as the baseline designs, shorter tubes are only possible if the heat transfer in the small diameter tubes is improved. This is dependent on the air and refrigerant side thermal resistances and the tube circuitry.

For all of the Pareto designs, the number of refrigerant tube inlets is equal to the maximum number allowed in the design problem (i.e. the maximum number of circuits is half the number of tubes per tube bank). Also, this high number of refrigerant inlets and the use of shorter tubes, especially for the low cost (lower than 65% of the baseline cost) designs, lead to a significantly lower (up to 80% reduction) refrigerant pressure drop. However, one of the main causes of refrigerant flow mal-distribution in HXs is the mechanical design of headers and feeder tubes (Muller & Chiou, 1988). In this study, for air or refrigerant flow mal-distribution is not taken in consideration. Thus,

from a practical point of view, the aforementioned high number of refrigerant feeder tubes is expected to cause or increase the refrigerant mal-distribution, which in turn might negatively affect the performance of the HXs. Furthermore, one manufacturing aspect of the optimized designs that needs to be considered is the need for two different sizes of U-bends in each HX. This is because of the different values for vertical and horizontal tube spacing in each HX.

The COP improvement for optimized designs is roughly 17%, and 15% for R-410A and R32, respectively. Although some studies in the literature show that bare tubes with diameters smaller than 2 mm have the potential for HX performance to be better than MCHX and finned tubes (Choi, et al., 2004; Gholap & Khan, 2007), all of the Pareto designs have flat plate fins (i.e. no bare tube designs) for both HX. This shows that at the studied diameter range (3-5 mm), the role of the extended surfaces is still important and more dominant than the effect of the high flow acceleration and mixing caused by turbulence within the tubes.

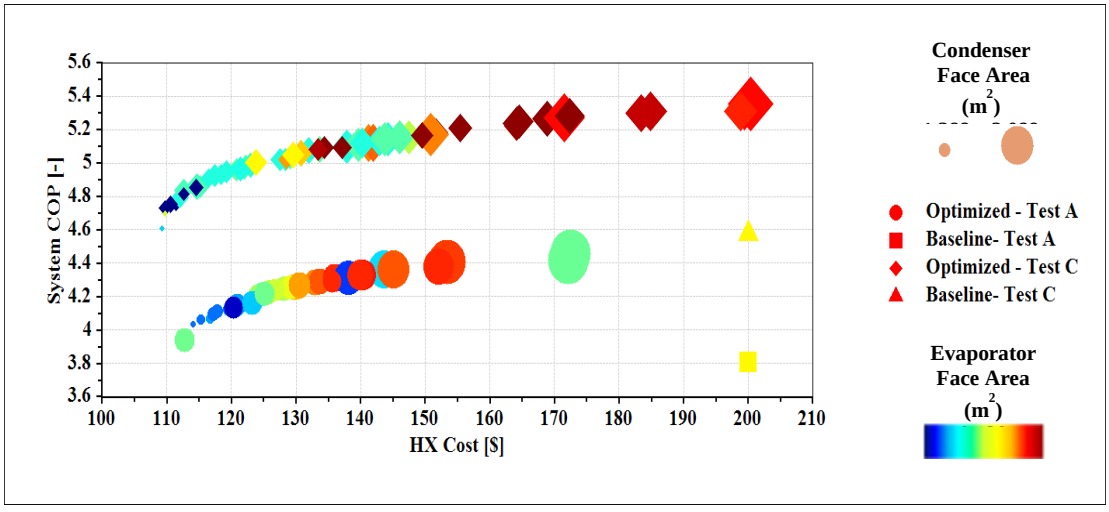

Figure 3.2: R-410A Pareto set

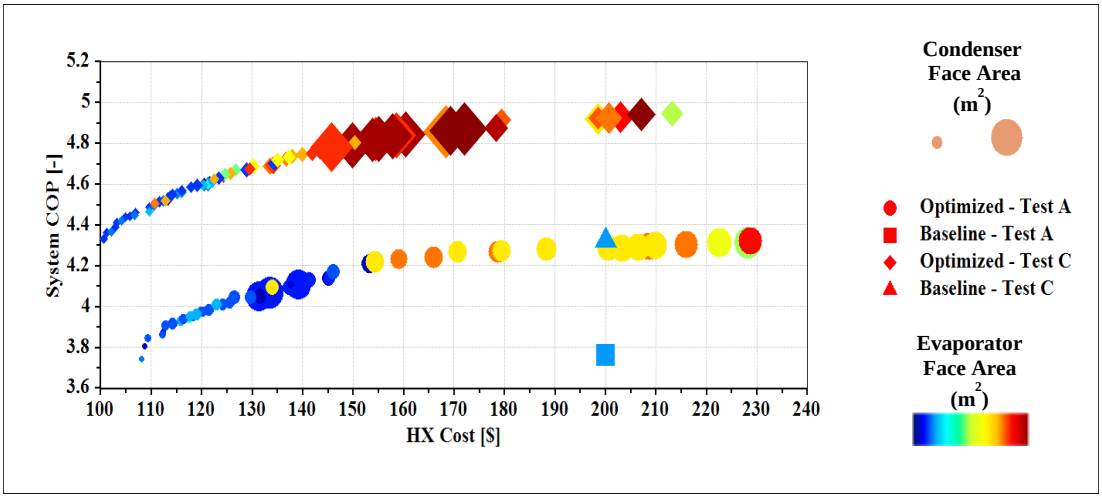

Figure 3.3: R-32 Pareto set

Figure 3.4 shows the refrigerant charge of the optimum designs compared to the baseline system. The charge of the baseline system can be reduced by 33% by shifting towards the optimized low cost small tube diameter HX designs for both refrigerants. It is worth mentioning that the system charge is calculated based on the internal volume of the HXs and the void fraction correlation (Koyama, et al., 2004). Also, the accuracy of the charge calculation is dependent on the void fraction correlation. Table 3.3 also compares some parameters of two sample Pareto designs, with low cost at the same COP and high COP at the same HXs cost, with the baseline design.

It is clear from Table 3.3 that the tube material volume for the small tube designs is less than the baseline design, however, the fin material volume is higher than the baseline for the high COP designs. This shows that for the high performance small tube designs, fins start to play a more important role in the HXs and system performance. As mentioned in the assumptions section, the tube material cost per unit mass to be 1.5 times the fin material cost per unit mass. This assumption affects the representative cost of the system, however, the overall trends and benefits from shifting towards small

diameter tubes is not affected. In order to inspect this assumption, the tube to fin cost ratio is changed to 3 and the effect on the designs is shown in Table 3.3. The last row in Table 3.3 shows the updated representative cost of the system. It is clear from the results, that the cost reduction of the low cost doesn't change compared to the baseline system. The high COP system has 10% lower cost than the baseline system when using the new assumption.

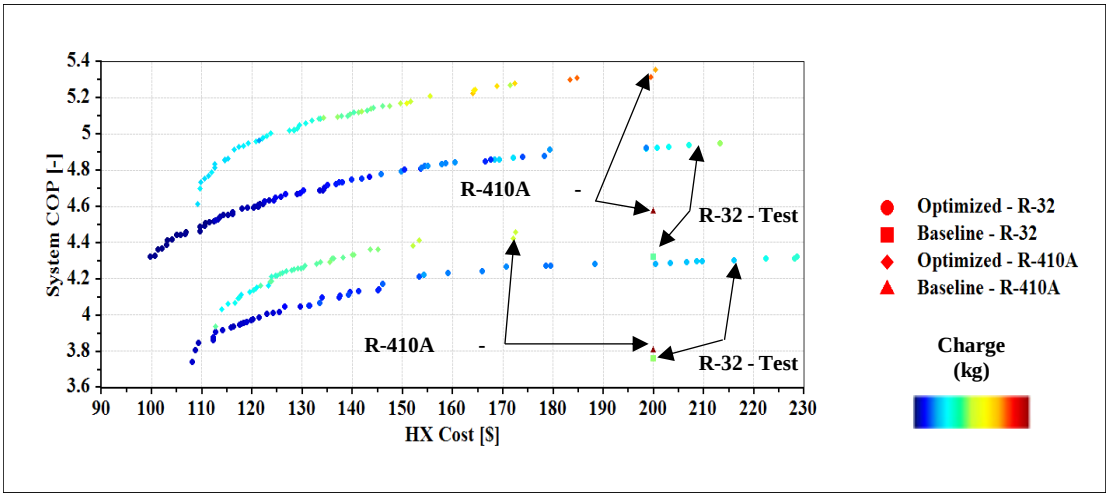

Figure 3.4: Variation of system charge among Pareto designs

Table 3.3: Comparison of optimal designs

		Condenser					
		R-410A			R-32		
		Baseline	High COP	Low Cost	Baseline	High COP	Low Cost
Tube Diameter [mm]		9.5	3	5	9.5	4	4
Face Area	[m^2]	1.944	3.089	1.450	1.944	1.922	1.258
	[%]	100	158.90	74.59	100	98.87	64.71
Tube Material Volume	[m^3]	0.0017	0.0016	0.0010	0.0017	0.0013	0.0008
	[%]	100	94.12	58.82	100	76.47	47.06
Fin Material Volume	[m^3]	0.0040	0.0068	0.0017	0.0040	0.0061	0.0017
	[%]	100	170.00	42.50	100	152.50	42.50
Air side pressure drop	[Pa]	13.9	4.92	12.12	12.58	10.72	15.40
	[%]	100	35.40	87.19	100	85.21	122.42
Refrigerant Charge	[kg]	1.09	0.953	0.563	0.712	0.414	0.306
	[%]	100	87.43	51.65	100	58.15	42.98
HX Internal Volume	[m^3]	0.0038	0.0036	0.0022	0.0038	0.0029	0.0019
	[%]	100	94.74	57.89	100	76.32	50.00
Cost	[$]	134.2	158.9	72.0	134.2	135.0	62.9
	[%]	100	118.41	53.65	100	100.60	46.87

		Evaporator					
		R-410A			**R-32**		
		Baseline	High COP	Low Cost	Baseline	High COP	Low Cost
Tube Diameter [mm]		9.5	3	4	9.5	4	4
Face Area	[m^2]	0.221	0.257	0.176	0.221	0.261	0.213
	[%]	100	116.29	79.64	100	118.10	96.38
Tube Material Volume	[m^3]	0.0010	0.0005	0.0004	0.0010	0.0007	0.0005
	[%]	100	50.00	40.00	100	70.00	50.00
Fin Material Volume	[m^3]	0.0013	0.0014	0.0013	0.0013	0.0026	0.0009
	[%]	100	107.69	100.00	100	200.00	69.23
Air side pressure drop	[Pa]	73.26	44.66	66.87	73.99	48.08	62.24
	[%]	100	60.96	91.28	100	64.98	84.12
Refrigerant Charge	[kg]	0.409	0.32	0.232	0.307	0.361	0.211
	[%]	100	78.24	56.72	100	117.59	68.73
HX Internal Volume	[m^3]	0.0022	0.0011	0.0010	0.0022	0.0015	0.0012
	[%]	100	50.00	45.45	100	68.18	54.55
Cost	[$]	65.8	41.5	37.2	65.8	63.6	36.9
	[%]	100	63.07	56.53	100	96.66	56.08

		System					
		R-410A			R-32		
Representative Cost	[$]	200	200.4	109.2	200	198.6	99.8
	[%]	100	100.20	54.60	100	99.30	49.90
Updated Representative Cost	[$]	345.6	312.8	181.9	345.6	307.6	166.9
	[%]	100	90.51	52.63	100	89.00	48.29

Figure 3.4 shows that the charge for the R-32 systems, whether baseline or optimized, is much lower than the R-410A systems. This is due to the density of R-32 being much smaller than R-410A. This is another benefit to the R-32 system on top of its lower GWP, making it more promising as a replacement for R-410A. Also, the improvements for each refrigerant for the systems designed and optimized for tests A and C operating conditions are comparable. Thus, the optimization runs for each operating conditions and each refrigerant is repeated twice. However, when running an individual Pareto design that shows higher cost reduction at one operating conditions (e.g. test C) at the other operating conditions (e.g. test A), it might not meet the capacity constraint or COP at the latter conditions (test A). Thus, it is important when designing and optimizing an ASHP system to make sure that it satisfies all the constraints at different testing and operating conditions. Moreover, although HX circuiting optimization might help to improve the HX performance and cause further material reduction, this study focused on simple refrigerant circuiting rather than optimized or complex circuits. This is mainly for two reasons. The first is that, given the current optimized designs, the

potential additional improvements are expected to be small. The second reason is that with the large number of HX tubes and feeder tubes, further circuiting is expected to impose higher flow maldistribution and HX manufacturing difficulties. Finally, this study does not include the effect of fin or internal tube enhancements. Using enhanced fins and tubes would potentially increase the air and refrigerant heat transfer coefficients. However, these enhancements potentially lead to an increase in the pressure drop causing these enhanced tube HXs to be infeasible deigns.

3.2.3. Conclusion

This study presents the multi-objective optimization of an ASHP system to determine the potential system performance improvements and material savings from using small diameter tubes in the HXs. The goal is to minimize the system cost and maximize the system COP while using a conventional refrigerant R410A and an alternative lower GWP refrigerant, R32. The HXs cost is the representative cost of the system cost, and the HXs geometry and circuity are the design variables. The optimal designs have evaporator tube diameters of either 3, 4, or 5 mm, and a condenser tube diameters of either 3 or 4 mm. The HXs cost can be reduced by 44% and 47% for R-410A, and R-32, respectively. Also, the COP improvement for the same HXs cost is 17%, and 15% for R-410A, and R-32, respectively. Furthermore, a charge reduction of 33% is possible in the optimized ASHP system for both refrigerants. These material and charge reduction help in reducing the environmental impacts of the vapor compression systems while maintaining the same system COP. It also helps in designing and manufacturing systems with higher seasonal energy efficiency ratio without the need to increase the size or material used in the baseline HXs.

4. LCCP Framework

4.1.Introduction

The quantification of the environmental impact of vapor compression systems is becoming more important as we strive to minimize our emissions footprint. The Montreal Protocol on Substances that Deplete the Ozone Layer (United nations environment programme ozone secretariat, 1989) limited the production and use of chlorofluorocarbons (CFCs), and hydrochlorofluorocarbons (HCFCs) which were commonly used in the air conditioning systems. Later on, the Kyoto protocol (United Nations, 1998) placed restrictions on greenhouse gas (GHG) emissions including high GWP refrigerants commonly used in vapor compression systems servicing HVAC&R needs. One method to reduce the negative environmental impact of such systems is to design them with environmental impact as one of the primary performance criterion. Several metrics have been proposed and used in public literature for quantification of this environmental impact.

The system's LCCP was introduced as an inclusive metric in the 1999 report of the Montreal Protocol Technology and Economic Assessment Panel (TEAP) (UNEP/TEAP, 1999). The LCCP analysis aim is to calculate the equivalent mass of carbon dioxide (CO_2) released into the atmosphere due to the operation of a system, throughout its lifetime, from construction to operation and destruction.

The CO_2 emissions from a vapor compression system are divided into direct and indirect emissions. Direct emissions include the environmental impact of leakage of refrigerant which occurs during system operation, servicing, and at the end of life as well as during the refrigerant production and transportation. Indirect emissions include

the environmental impact associated with the production and distribution of the energy required to operate the refrigeration system as well energy associated with production and transportation of the different system components. The LCCP methodology can be used to compare the environmental performance of different refrigerants and technologies in applications such as automobile air conditioning, residential and commercial refrigeration, unitary air conditioning, and HVAC chillers (Arthur D. Little Inc., 2002). Papasavva et al. (2010) developed a comprehensive life cycle analysis tool limited to mobile air conditioners (GREEN-MAC LCCP). The LCCP tool presented in (Zhang, et al., 2011) focused on residential air source heat pumps (ASHP). However, this tool cannot be extended to other systems and it can only be used for evaluating the LCCP of an existing ASHP system rather than designing the system based on LCCP.

This section presents an open-source and modular framework for LCCP based design of vapor compression systems servicing HVACR needs. The presented framework is generic and can be applied universally to any vapor compression system (e.g. air conditioning, residential ASHP, supermarket refrigeration…etc.).

4.2.LCCP Framework

Figure 4.1 shows the proposed LCCP framework (Oak Ridge National Laboratory, and the University of Maryland College Park, 2013). The core module in this framework is the open-source LCCP calculation methodology. This module is connected with three input modules: the system performance model, the load model, and the standardized reference data sets for emissions and weather. These modules interact with each other via standardized communication interfaces that describe the data input-output interfaces. Due to the modular nature of the framework, any individual module can be

replaced with a user-defined module. Hence, the framework is extensible and suitable for the analyses of a variety of systems.

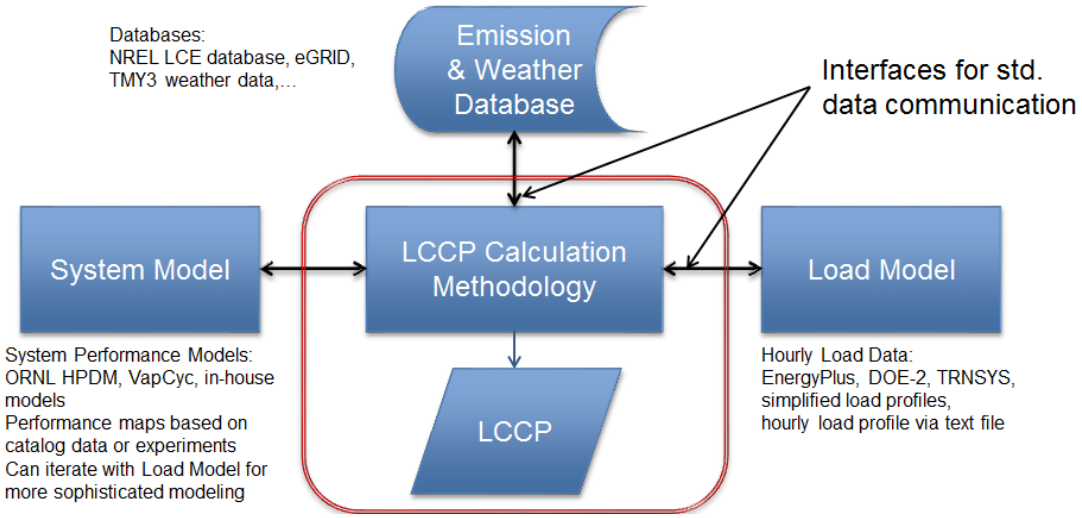

Figure 4.1: LCCP Framework

The system performance model uses the weather data and calculates the hourly power consumption of the system at rated capacity. In turn, the load model provides the hourly load values. These hourly load and rated power consumption values are then used to calculate the actual hourly energy consumption of the system. The hourly energy consumption is then multiplied by the hourly emission rate for electricity production, obtained from location-specific standardized reference datasets for emissions, Deru and Torcellini (2007) was used for hourly emission rate within the USA. Different building energy modeling tools such EnergyPlus (U.S. Department of Energy, 2012) can be used in the load module to determine the hourly load profile only, or both the hourly load and the system energy consumption. In the latter case, a separate system performance model is not required.

The Typical Meteorological Year (TMY) data from the National Solar Radiation Data Base (National Renewable Energy Laboratory, 2012) is used as default weather data. These datasets include hourly values for dry-bulb temperature, dew-point temperature, and relative humidity. Finally, the default GWP values used in the tool are based on a 100 year time horizon (GWP_{100}) and are obtained from the IPCC Fifth Assessment Report (AR5) (2013). The GWP values of other refrigerants which are not listed in AR5 were obtained from the AHRTI report (Zhang, et al., 2011), based on values provided by manufacturers, or compiled from publicly available information.

4.3.Emission Calculations

4.3.1. Direct Emissions

The six contributors to the direct emissions may be combined to yield the total direct emissions, Em_{direct}, as shown in Equations (4.1-4.6) where $Em_{ref,leak}$ are due to refrigerant leakage, Em_{acc} are due to accidents, Em_{serv} are due to servicing, $Em_{ref,EOL}$ are due to refrigerant leakage at end-of-life, $Em_{ref,prod}$ are due refrigerant production and transportation, $Em_{reaction}$ is the reaction byproduct of the atmospheric breakdown of the refrigerant emissions. The latter term is a user-input value with the default value being zero.

$$Em_{direct} = Em_{ref,leak} + Em_{acc} + Em_{serv} + Em_{ref,EOL} + Em_{ref,prod} + Em_{reaction} \quad \text{Equation 4.1}$$

$$Em_{ref,leak} = m_{ref} \times Life_{sys} \times LR_{annual} \times GWP \quad \text{Equation 4.2}$$

$$Em_{acc} = m_{ref} \times Life_{sys} \times LR_{acc} \times GWP \quad \text{Equation 4.3}$$

$$Em_{serv} = N_{serv} \times m_{ref} \times LR_{serv} \times GWP \quad \text{Equation 4.4}$$

$$Em_{ref,EOL} = LR_{ref,EOL} \times m_{ref} \times GWP \quad \text{Equation 4.5}$$

$$Em_{ref,prod} = LR_{ref,prod} \times m_{ref} \times GWP$$ Equation 4.6

4.3.2. Indirect Emissions

The total indirect emissions, $Em_{indirect}$, can be calculated as shown in Equations (4.7-4.11). There are six contributors to the indirect emissions: emissions due to energy required to manufacture the system, $Em_{sys,man}$, emissions due to energy used to manufacture the refrigerant, $Em_{ref,man}$, emissions due to energy required to recycle the system, $Em_{sys,EOL}$, lifetime emissions due to electric energy consumption, Em_{elec}, emissions due to refrigerant recycling and disposal at end-of-life, $Em_{ref,disp}$, and emissions due to energy used to transport the system, $Em_{sys,trans}$. The latter two terms are user-input values with the default values being zero.

$$Em_{indirect} = Em_{sys,man} + Em_{ref,man} + Em_{sys,EOL} + Em_{elec} + Em_{ref,disp} + Em_{sys,trans}$$ Equation 4.7

$$Em_{sys,man} = \sum_{mat} m_{mat} \times CO_{2eq,mat}$$ Equation 4.8

$$Em_{ref,man} = m_{ref} \times (1 + Life_{sys} \times LR_{annual} - R) \times CO_{2eq,ref}$$ Equation 4.9

$$Em_{sys,EOL} = \sum_{mat} E_{recyc,mat} \times m_{mat} \times CO_{2eq,mat}$$ Equation 4.10

$$Em_{sys,elec} = Life_{sys} \times \sum_{n=0}^{8760} E_{h,con} \times Em_{R}$$ Equation 4.11

4.3.3. Total Emissions

Finally, the total emissions (Em_{total}), representing the LCCP and including the contributions from direct and indirect emissions, is calculated as shown in Equation 4.12.

$$Em_{total} = Em_{direct} + Em_{indirect}$$ Equation 4.12

4.4.LCCP Case Studies

This section presents some of the case studies that were performed using the developed LCCP framework described in the previous chapter. The study in the first section is published in the International Journal of Refrigeration (Beshr, et al., 2015). Moreover, the study in the second section is published in the International Journal of Life Cycle Assessment (Beshr, et al., 2015).

4.4.1. Supermarket Refrigeration

4.4.1.1. Introduction

Commercial refrigeration systems have a major negative environmental impact. This is mainly due to their high refrigerant charge leakage, and high electricity consumption. A typical 3300 m^2 store in the USA consumes 2-3 GWh of energy which results in significant indirect carbon dioxide equivalent (CO_{2eq}) emissions. Furthermore, a typical supermarket using multiplex direct expansion (DX) refrigeration system requires 1400-2300 kg of refrigerant, and has an average annual charge loss of 30% (Southern California Edison, 2004). Using high or moderate GWP refrigerants together with these high refrigerant leak rates contributes to significant direct CO_{2eq} emissions. Methods for reducing the negative environmental impact of commercial refrigeration systems include using low GWP refrigerants, improving the efficiency of the systems, and designing systems (component sizing, refrigerant selection, etc.) with environmental impact as one of the primary performance criterion.

Natural refrigerants tend to have very low GWP, however, the efficiency and overall environmental impact of systems utilizing natural refrigerants need to be evaluated. Many ongoing efforts are pursued to develop suitable low GWP alternative refrigerants

for use in commercial refrigeration with a tradeoff between low GWP, affordability, safety, and system efficiency. One of the promising refrigerants for commercial systems studied in the AHRI AREP program is the blend N-40, which shows competitive performance with significantly lower GWP than R-404A (Motta, 2011).

Moreover, designing a system while primarily considering its environmental impact requires an evaluation of the system's overall environmental impact as a function of its design parameters. The most comprehensive metric proposed for this evaluation is the system's LCCP.

A computational tool (computer program) based on the framework developed LCCP framework (presented in chapter 4) is used to compare the LCCP of four supermarket refrigeration systems, in six US cities representing different climate zones. Leak tight and energy efficient systems using CO_2 have been investigated in literature. Among these systems, the transcritical CO_2 booster system, and the cascade system show good potential for having lower total emissions (Abdelaziz, et al., 2012; Rajendran, 2013). Also, the secondary circuit system shows promising energy savings (Southern California Edison, 2004). Thus, in this study, the N-40/L-40 secondary circuit system is compared with the transcritical CO_2 booster system, the cascade CO_2/N-40 system, and the multiplex DX utilizing R-404A and N-40. Furthermore, parametric analysis, sensitivity analysis, and uncertainty analysis are performed to provide more in depth understanding of the LCCP of the systems.

4.4.1.2. System model

The EnergyPlus 4181 m^2 single-story supermarket model used in this study is based on the new construction reference supermarket model developed by the U.S. Department

of Energy (Deru, et al., 2011). The analysis is done for six US cities representing different climate zones, as shown in Table 4.1. Moreover, the system lifetime is assumed to be 20 years with service interval of 2 years. The annual leakage rate, refrigerant loss at end-of-life, service leakage rate, and reused refrigerant are 10%, 10%, 5%, and 85%, respectively (Abdelaziz, et al., 2012).

Table 4.1: Climate zones and cities used in the LCCP analysis

Climate Zone	City	Annual Average Temperature (°C)	Average Hourly Emission Rate for Electricity Production ($kgCO_2/kWh$)
1A	Miami, FL	24.9	0.678
2B	Phoenix, AZ	23.8	0.757
3B	Los Angeles, CA	17.3	0.351
4B	Albuquerque, NM	14.2	1.1
5A	Chicago, IL	10.0	0.638
8	Fairbanks, AK	-2.1	0.774

Note that the remaining leakage rates that appear in Eq. (4.1-4.11), but which do not have a value mentioned in this section, are assumed to be zero. The GWP and blend composition for the different refrigerants is shown in Table 4.2 where the GWP of the refrigerants are obtained from AHRI (Amrane, 2013) and refrigerant manufacturers (Motta, 2011). The total refrigerant charge in each of the systems is based on data provided by PG&E (Pacific Gas and Electric Company, 2011).

Table 4.2: Blend composition and GWP values of the used refrigerants

Refrigerant	Composition (Mass %)	GWP
CO_2	CO_2 (100)	1
N-40	R-32/R-125/R-134a/R-1234yf (25/25/20/30)	1273
L-40	R-32/R-152a/R-1234yf/R-1234ze (40/10/20/30)	285
R-404A	R-125/R-134a/R-143a (44/4/52)	3943

4.4.1.2.1. Multiplex DX System (S1)

The multiplex DX system, shown in Figure 4.2a, consists of a MT/ LT DX compressor rack with mechanical subcooling and an air-cooled condenser. Two such systems are used to satisfy the refrigeration loads of the supermarket, and the refrigeration load and refrigerant charge for each system is given in Table 4.3. This system is analyzed with R-404A and N-40A as working fluids.

4.4.1.2.2. Cascade N-40/CO_2 System (S2)

The cascade N-40/CO_2 system, shown in Figure 4.2b, consists of a primary DX system using the refrigerant N-40, which cools a LT CO_2 DX system and a MT CO_2 secondary loop. The cascade system rejects heat through an air-cooled condenser. The MT loads are cooled with a pumped CO_2 secondary loop while the LT loads are cooled by the LT CO_2 DX system. Two such systems are used to satisfy the refrigeration loads of the supermarket, and the refrigeration load and refrigerant charge for each system are given in Table 4.3.

.

4.4.1.2.3. Transcritical CO_2 Booster System (S3)

In the transcritical CO_2 Booster System, shown in Figure 4.2c, both the MT land LT loads are served by direct expansion of CO_2. The heat rejection from the system occurs either supercritically or subcritically, depending upon the outdoor ambient temperature, through an air-cooled gas cooler. Two such systems are used to satisfy the refrigeration loads of the supermarket, and the refrigeration load and refrigerant charge for each system are given in Table 4.3.

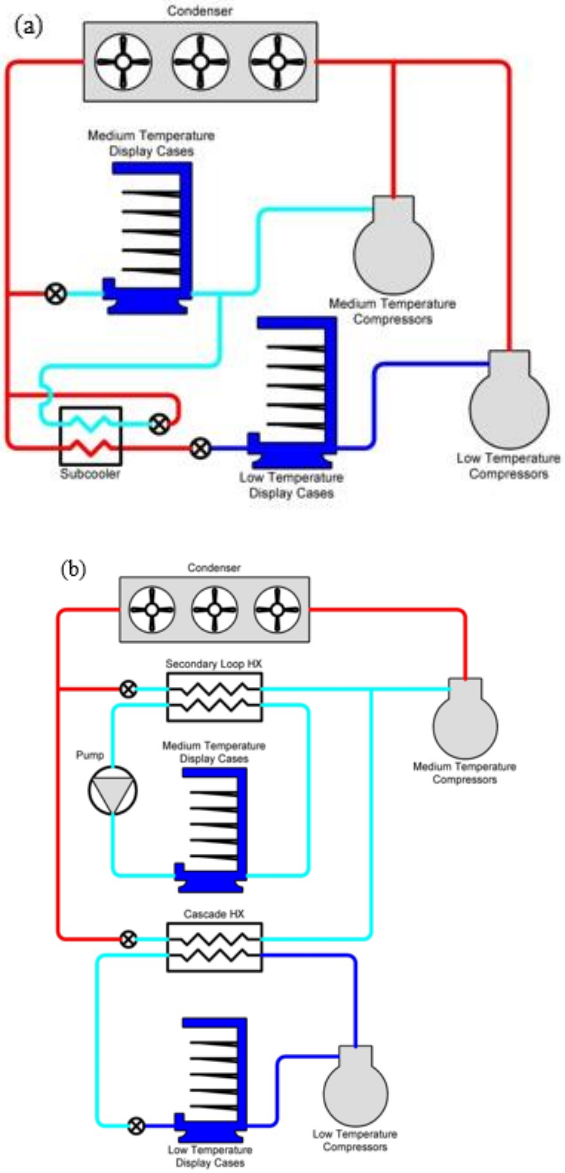

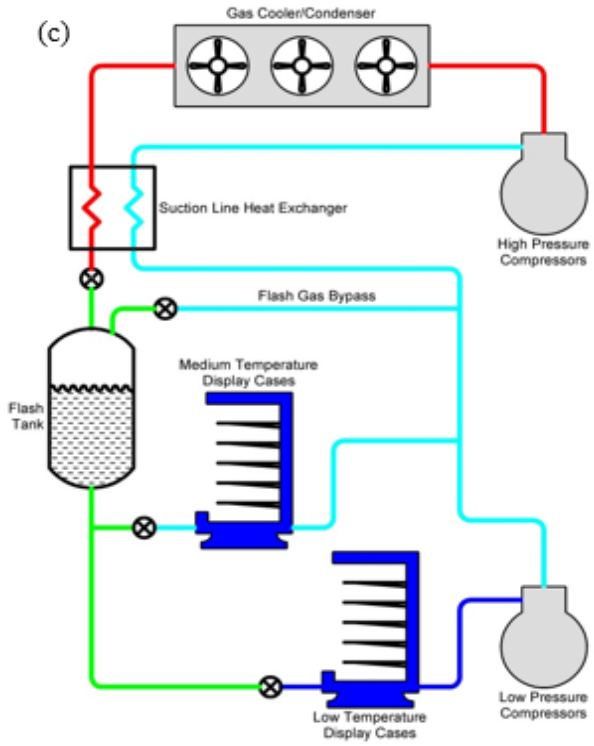

Figure 4.2: Schematic of the systems: (a) S1, (b) S2, and (b) S3

4.4.1.2.4. Secondary (MT) / Central DX (LT) System (S4)

For the secondary circuit system, the MT loads are served by a secondary circuit which uses propylene glycol cooled by a DX system using L-40. The LT loads are satisfied with a separate centralized DX system utilizing N-40. The refrigeration load and refrigerant charge for each compressor rack is given in Table 4.3.

Table 4.3: Load and charge of the systems

System	Subsystem	Refrigeration Load (kW)	Refrigerant Charge (kg)
S1	Multiplex DX System 1	MT: 167.1, LT: 64.6	1038
	Multiplex DX System 2	MT: 52.8, LT: 23.4	340
	Total	307.9	1378
S2	Cascade System 1	MT: 167.1, LT: 64.6	N-40: 625, CO_2: 340
	Cascade System 2	MT: 52.8, LT: 23.4	N-40: 205, CO_2: 110
	Total	307.9	N-40: 830, CO_2: 450
S3	CO_2 Booster System 1	MT: 118.6, LT: 64.6	520
	CO_2 Booster System 2	MT: 101.2, LT: 23.4	170
	Total	307.9	690
S4	MT1	167.1	209
	MT2	52.8	66
	LT1	64.6	290
	LT2	23.4	104
	Total	307.9	669

4.4.1.2.5. EnergyPlus Modeling Assumptions

In this section, some of the modeling assumptions used in the EnergyPlus are provided.

- The evaporating temperatures for the three refrigeration system types are shown in Table 4.4. Each system is modeled with two MT suction groups and two LT suction groups. It was assumed that the evaporating temperatures of the CO_2-

based systems were 1.1°C higher than that of the HFC-based systems due to the better transport properties of carbon dioxide.

Table 4.4: Evaporating temperatures for the three refrigeration systems

System	Compressor Rack	Temperature Level	Evaporating Temperature (°C)
S1	Rack A	MT	-2.80
	Rack B	LT	-20.0
	Rack C	MT	-2.80
	Rack D	LT	-28.3
S2	Rack A	MT	-1.70
	Rack B	LT	-18.0
	Rack C	MT	-1.70
	Rack D	LT	-27.2
S3	Rack A	MT	-1.70
	Rack A	LT	-18.0
	Rack B	MT	-1.70
	Rack B	LT	-27.2

- For systems S1 and S2, the suction line pressure drop was assumed to be 17 kPa (2.5 psi) while the discharge line pressure drop was assumed to be 8.5 kPa (1.2 psi). The suction gas temperature at the compressor inlet was assumed to be the saturated evaporator temperature plus the display case superheat. The

display case superheat was assumed to be 4 K for systems S1 and S2 and 10 K for system S3.

- System S1 contains a subcooler for each LT compressor rack. The temperature of the liquid refrigerant exiting the subcooler was set to 10°C (50°F). No subcoolers were used in the cascade system (system S2). System S3 contains a liquid-suction heat exchanger just after the gas cooler. The effectiveness of this heat exchanger was assumed to be 0.4.
- The difference between the saturated condensing temperature and the ambient air for systems S1 and S2 were approximately 4 K for ambient temperatures greater than or equal to 20°C (68°F). In addition, the minimum condensing temperature for Systems S1 and S2 was set at 22°C (72°F), which is typical of R-404A DX systems today due to the limitations of widely used thermostatic expansion valves at low condensing pressures. However, it is noted that the use of electric expansion valves (EEVs) would allow for lower condensing temperatures in DX or cascade systems. A lower condensing temperature, around 10°C for example, would significantly improve the COP of these systems in cold climates. No subcooling was assumed at the exit of the condensers.
- For system S3, it was assumed that the temperature difference between the gas cooler outlet and the ambient air was 3 K for transcritical operation and 10 K for subcritical operation. During subcritical operation, the minimum condensing temperature for System S3 was set at 10°C (50°F). Note that due to the high operating pressures of CO_2 systems, it is possible to have an

acceptable pressure drop across the expansion valves at lower condensing temperatures than would be possible with HFC-based systems that use thermostatic expansion valves.

- For all systems, the performance of the compressors was determined from compressor maps obtained from the manufacturers. The compressors used in the simulations are listed in Table 4.5. Inefficiencies occurring during part load operation were ignored. The performance of the N40 compressors was based on R404A compressor performance by assuming that N40 capacity was 100% of R404A capacity and N40 power was 93% of R404A power.
- For all systems, the fan power (for evaporators and condensers/gas cooler) was taken into account.

Table 4.5: Compressor models used in simulations

Manufacturer	Refrigerant	Temperature Level	Model
Copeland (Emerson)	R-404A N-40 L-40	MT	3DA3R10ML 4DBXR20ML 4DJ3R28ML ZF13KVE
		LT	2DA3F23KL 4DL3F63KE
Bitzer	CO_2	MT	4HTC-15K
		LT	2FSL-4K 2HSK-3K

4.4.1.3. Results and discussion

4.4.1.3.1. LCCP Analysis

Figure 4.3 shows the direct emissions of the four refrigeration systems (S1, S2, S3, and S4). The direct emissions are dependent on the system refrigerant (GWP of refrigerant), and charge mass and are not affected by the system location. Hence, S3 has the lowest direct emissions due to its low refrigerant GWP and charge mass. Although S4 has slightly lower charge mass than S3, it has higher direct emissions than S3 as S4 utilizes a refrigerant with a much higher GWP. The baseline S1 has the highest direct emissions as it has the highest charge using and the highest GWP refrigerant (R-404A).

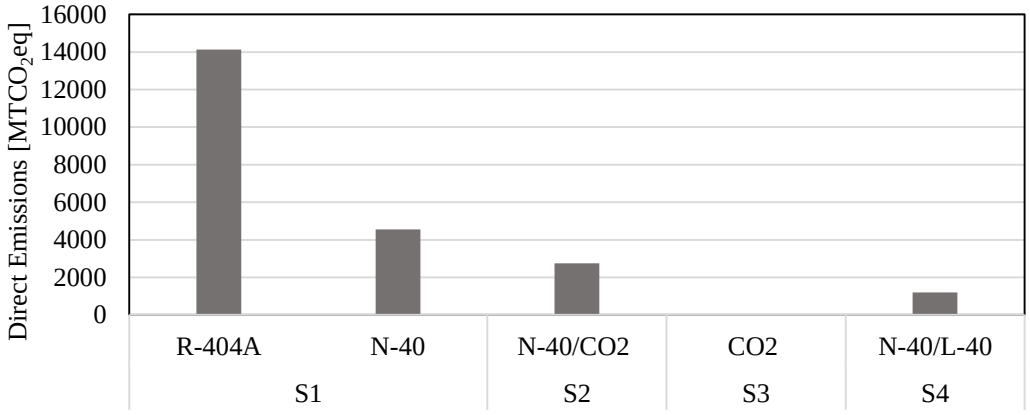

Figure 4.3: Direct emissions of the four refrigeration systems

Figure 4.4 shows the indirect emissions in the six studied cities for the various refrigeration systems. It is clear that while system location does not affect the direct emissions, it does affect the indirect emissions. This is due to differences in the system performance, the weather data (leading to different hourly system power draw) and the hourly emission rate for electricity production. In Figure 4.4, it is noticed that in cold climates such as Fairbanks, the energy consumption of system S3 is much closer to the

other systems than in warmer climates such as Miami. This is because the CO_2 does not perform in warm climates as efficiently as in cold climates as shown in Figure 4.5 (the figure was generated using weather data for Chicago, IL). Thus, system S3 tends to have higher indirect emissions than the other systems in warmer climates. Also, it is worth noting that the indirect emissions in Los Angeles are much lower than the other cities for all systems although it might have higher annual electricity consumption (e.g. than Fairbanks). This is because the hourly emission rate for electricity production is low for Los Angeles as shown in Table 4.1. It is recognized that for all climates, the secondary circuit system (S4) tend to have the lowest electricity consumption and hence indirect emissions. On the other hand, almost for all climates, especially the hot climates such as Miami and Phoenix, the transcritical CO_2 booster system (S3) results in higher electricity consumption and as such high indirect emissions.

Figure 4.6 shows the total emissions in the six studied cities for the various refrigeration systems. For cities in cold and temperate climates, the slightly higher indirect emissions of the transcritical CO_2 booster system are outweighed by its lower direct emissions. Thus, for these climates, S3 has the lowest total emissions. On the other hand, for cities in hot climates such as Miami and Phoenix the higher direct emissions of the secondary circuit system (compared to S3) are outweighed by its lower indirect emissions. Hence, S4 is more environmentally friendly in the hot climates. Overall, the secondary circuit system offers a good trade-off between emissions and electricity consumption making it more attractive for most climates. On the other hand, the multiplex DX system utilizing R-404A has the highest total emissions.

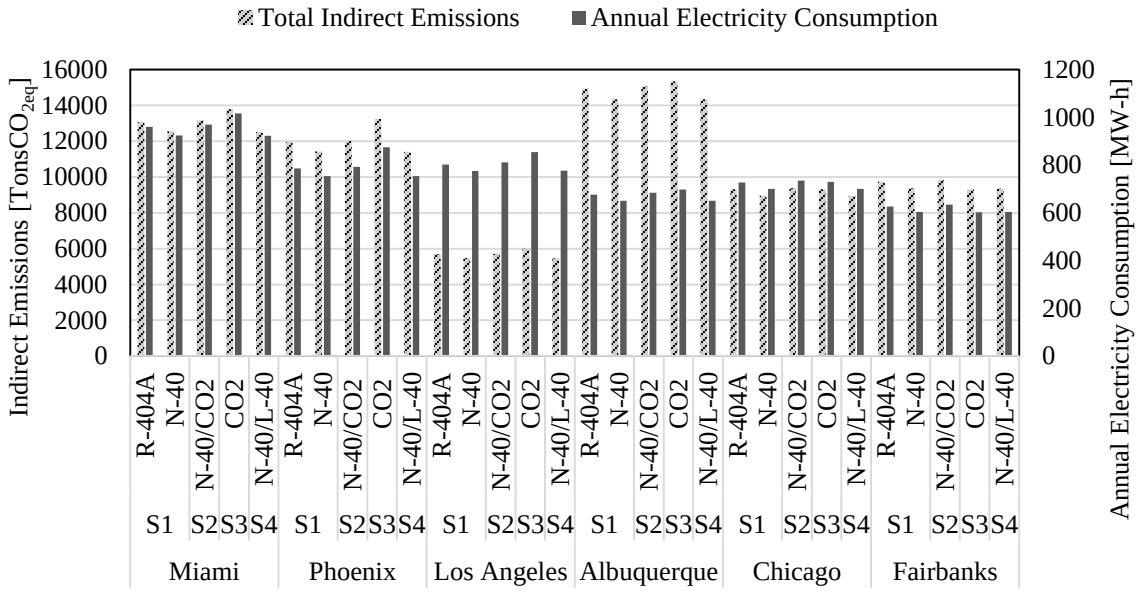

Figure 4.4: Total indirect emissions and annual electricity consumption of the four refrigeration systems

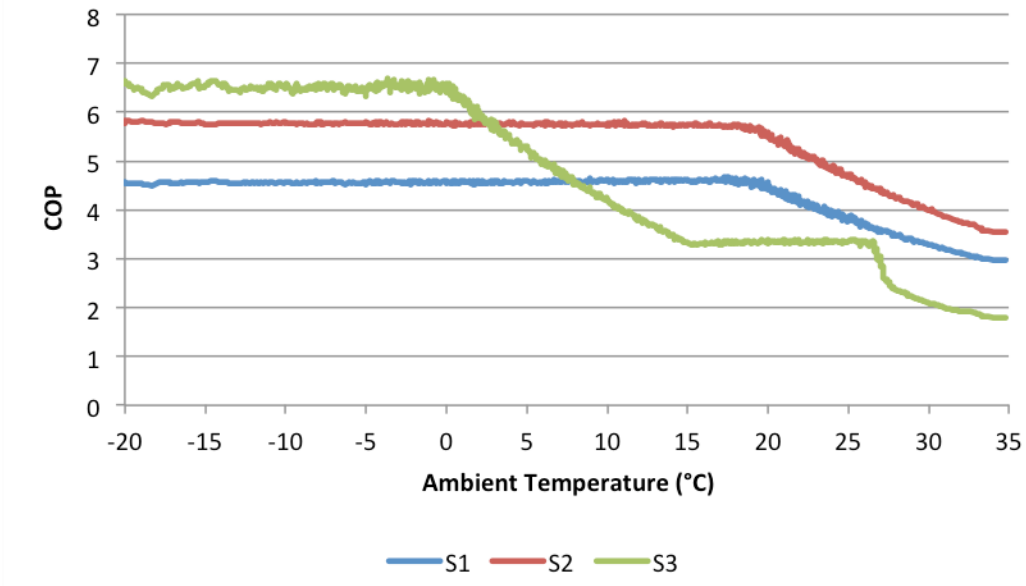

Figure 4.5: variation of the COP with the ambient temperature

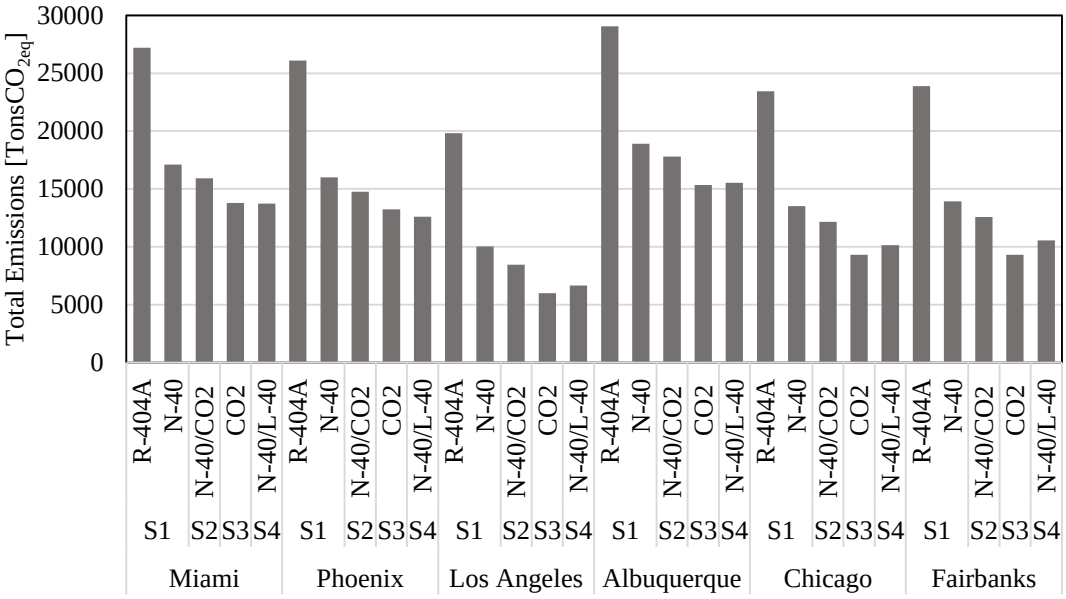

Figure 4.6: Total emissions of the four refrigeration systems

4.4.1.3.2. Parametric Analysis

A parametric analysis of the effect of changing the annual leak rate of the system on the total emissions of systems S1, S3 and S4 in Chicago is performed. Figure 4.7 shows a comparison of the results for the three systems. The direct emissions are the major contributor for LCCP CO_{2eq} emissions in supermarket systems, therefore, using lower GWP refrigerants, or more leak-tight systems result in considerable decrease in the system's total emissions. For CO_2 systems, such as S3 the impact of reducing the annual leak rate is negligible. On the other side, for systems using refrigerants with high or moderate GWP values (such as S1 utilizing R404-A), reducing the annual leak rate has large impact on the total emissions. As previously discussed, for the base annual leakage rate (10%) in Chicago, S4 has higher total emissions than S3 although S4 has lower indirect emissions than S3. This is because of the much lower direct emissions, mainly due to annual leak rate, of S3 compared to S4. As shown in

Figure 4.7, if the annual leak rate is lower than 2%, the higher direct emissions of the S4 compared to S3 is outweighed by its lower indirect emissions. Hence, for low annual leak rates, S4 tends to become more environmentally friendly than all other studied refrigeration systems in all climates.

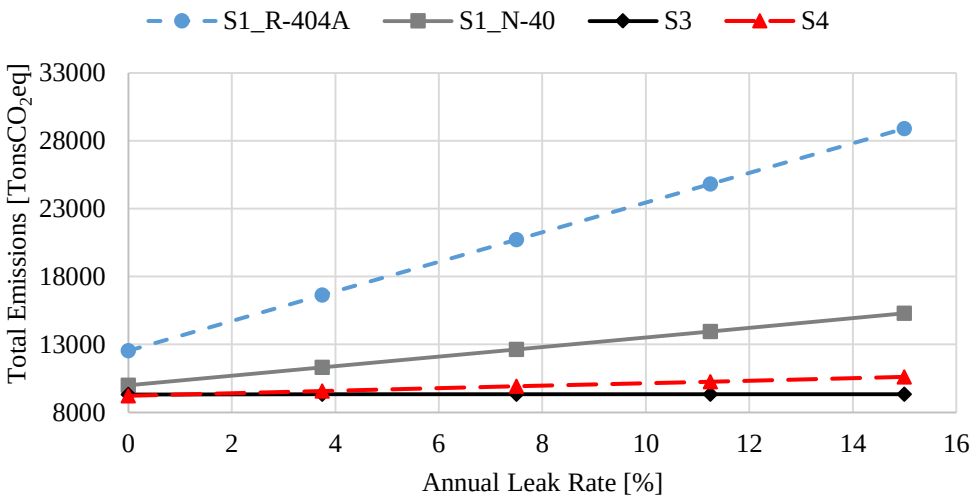

Figure 4.7: Sensitivity analysis of refrigerant charge and electricity production emissions

4.4.1.3.3. Sensitivity Analysis

A sensitivity analysis is performed to determine the effect of a 10% change in the refrigerant charge and the hourly emission rate for electricity production on the total CO_{2eq} emissions of systems S1, and S3 in Miami, and Los Angeles. Figure 4.8 a and b show a comparison of the results for the two systems in the two cities. As noted earlier for supermarket refrigeration systems, refrigerant GWP and charge mass have a strong impact on LCCP. Thus, the LCCP for systems with higher direct emissions (i.e. utilizing refrigerants with higher GWP, or having larger charge mass) tends to be more sensitive to charge variation than systems with lower direct emissions (i.e. utilizing lower GWP refrigerants or having smaller charge mass), as shown in Figure 4.8a.

Moreover, using low GWP refrigerants or smaller system charge reduces the direct emissions, hence the impact of indirect emissions on LCCP becomes more prevalent. As such, the sensitivity of LCCP to variation in electricity production emission rates becomes more noticeable for low GWP refrigerants or smaller charge mass systems, as shown in Figure 4.8b. Moreover, for cities with low hourly emission rates for electricity production, such as Los Angeles, the contribution of direct emissions to total emissions is higher than for other cities. Thus, the LCCP for cities such as Los Angeles tend to have higher sensitivity to charge variation.

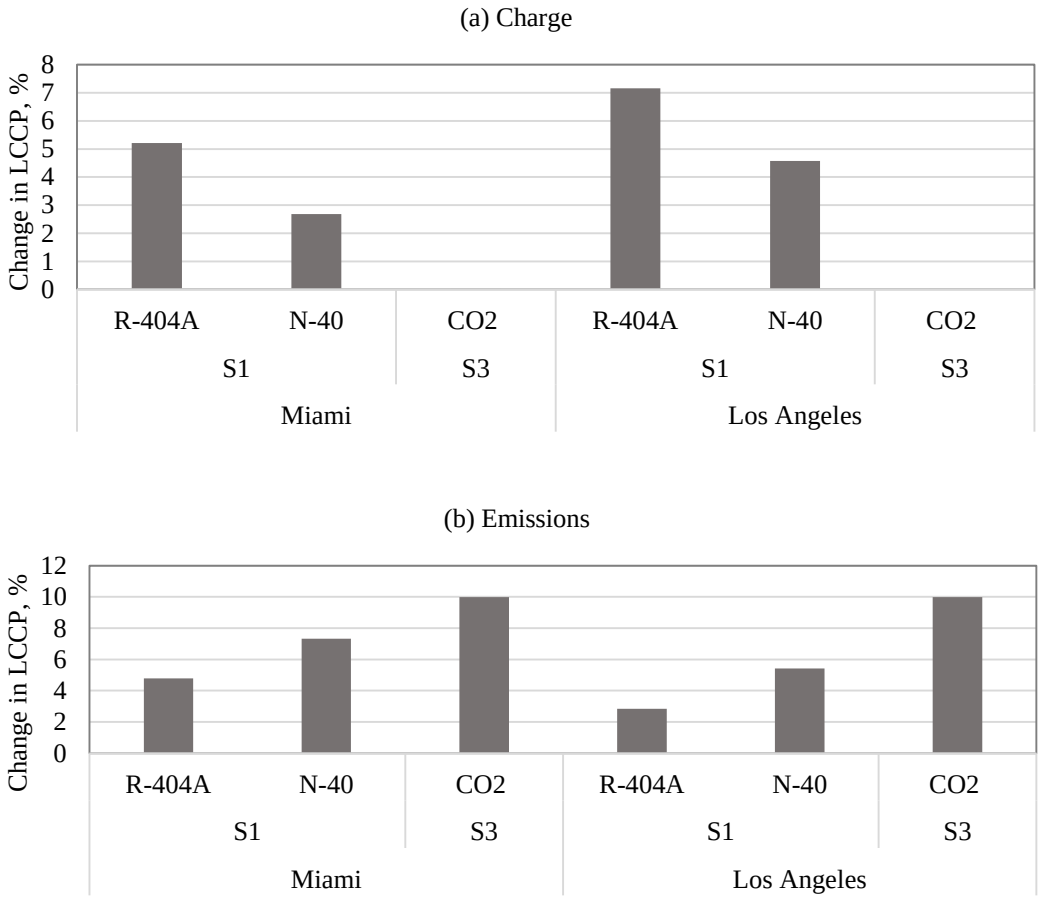

Figure 4.8: Sensitivity of LCCP to a 10% change in (a) refrigerant charge and (b) electricity production emissions

4.4.1.3.4. Uncertainty Analysis

An uncertainty study is performed on S1 located in Chicago and Los Angeles when using R-404A and N-40 to determine the effect of the uncertainty of the inputs on the LCCP results. The inputs included in the study are the service and annual leakage rates, refrigerant loss at end-of-life, percentage of reused refrigerant, system charge, hourly emission rate for electricity production, and refrigerant's GWP. The analysis is performed for three different cases. For the 3 cases the uncertainty values for reused refrigerant, service leakage rate, refrigerant loss at end-of-life, and annual leakage rate are assumed at 20%, and the charge uncertainty is assumed to be 5%. The power plant emission, and the refrigerant GWP uncertainties were varied. For cases 1, 2, and 3 the power plant emission uncertainty are 5%, 5%, and 20% respectively, and the refrigerant GWP uncertainty was 20%, 5%, and 5% respectively.

The resulting uncertainties of the system's LCCP, as a result of uncertainties of the inputs, are shown in Table 4.6. The partial derivatives of the total emissions with respect to each of the input parameters are shown in Figure 4.8 accompanied by the percentage difference between the derivatives values when utilizing N-40 compared to R-404A. The partial derivatives do not change for any of the three cases. This is simply because the derivatives do not depend on the magnitude of uncertainty of the inputs but rather on the baseline design itself. Thus, changing the location from Chicago to Seattle only causes a change in the partial derivative which depends on the location such as the derivative of the total emissions with respect to hourly emission rate for electricity production. Also, the results show that shifting to a low GWP refrigerant causes a noticeable drop in the impact of the uncertainty in the inputs related to the direct

emissions (service leakage rate, refrigerant loss at end-of-life, annual leakage rate, and system's charge) on the total emissions. This results in more dominant impact of the power plant emissions uncertainty on the uncertainty of the total system emissions. Thus, for the low GWP refrigerant (N-40) in Chicago for case 3, the uncertainty of the system's total emissions is higher than for R-404A. Finally, performing the same uncertainty analysis for S3 in Los Angeles results in LCCP uncertainty of 5%, 5%, and 19.98% for cases 1, 2, and 3, respectively. This is due to the small direct emissions of this system which makes the uncertainty in the power plant emissions much more dominant than in the case of other systems. This causes the uncertainty in the transcritical CO_2 booster system's LCCP to follow the value of the uncertainty in the power plant emissions.

Table 4.6: Uncertainties (%) of the system's LCCP

Case 1				Case 2				Case 3			
Chicago		Los Angeles		Chicago		Los Angeles		Chicago		Los Angeles	
R-404A	N-40	R-404A	N-40	R-404A	N-40	R-404A	N-40	R-404A	N-40	R-404A	N-40
15.82	9.40	18.64	12.17	10.69	6.76	12.52	8.40	13.15	14.47	13.68	13.45

Table 4.7: Partial derivatives of the total emissions with respect to each of the input parameters

	Chicago			Seattle		
	Partial derivative			Partial derivative		
	R-404A	N-40	% difference	N-40	R-404A	% difference
Reused refrigerant	-2.3E+04	-1.1E+04	-52.10	-2.3E+04	-1.1E+04	-52.10
Service leakage rate	5.4E+07	1.8E+07	-67.71	5.4E+07	1.8E+07	-67.71
Refrigerant loss at end-of-life	5.4E+06	1.8E+06	-67.71	5.4E+06	1.8E+06	-67.71
Annual leakage rate	1.1E+08	3.5E+07	-67.65	1.1E+08	3.5E+07	-67.65
Charge	1.0E+04	3.3E+03	-67.66	1.0E+04	3.3E+03	-67.66
Power plant emission	1.45E+07	1.40E+07	-3.62	1.61E+07	1.55E+07	-3.36
Refrigerant GWP	3.6E+03	3.6E+03	0	3.6E+03	3.6E+03	0

4.4.1.4. Conclusion

The LCCP tool was used to compare the environmental impact of four different supermarket refrigeration systems in six US cities. Comparing the total emissions for different cities suggests that the transcritical CO_2 booster system has the lowest CO_2 equivalent emissions, according to this analysis, in cold and temperate climates with annual leak rate higher than 2% although it has higher energy consumption. Also, the secondary circuit N-40/L-40 system is found to offer a good balance between emissions and electricity consumption for hot climates with annual leak rate of 10%, and for all climates for annual leak rate less than 2%. The parametric analysis showed that shifting towards low GWP refrigerants decreases the effect of the annual leak rate on the total system emissions. Moreover, the sensitivity analysis showed that shifting towards low GWP refrigerants, or more charge conservative systems increases the effect of the hourly emission rate for electricity production on the total system emissions. Finally, an uncertainty analysis was performed showing that using low GWP refrigerants, or more charge conservative systems causes a noticeable drop in the impact of the uncertainty in the inputs related to the direct emissions.

4.4.2. Total Emissions from HVACR Systems in the US

4.4.2.1. Introduction

In this study, the LCCP tool is used to evaluate the total emissions from the most common residential HVAC, and commercial refrigeration systems in the US. The focus on residential HVAC systems is imperative due to their prevalence in the market and high energy consumption. Thus, they have high indirect emissions in addition to largely contributing to the total emissions of all the residential and commercial refrigeration

and air conditioning systems. On the other hand, commercial refrigeration systems have a large refrigerant charge and high leakage rates, which leads to high direct emissions. This gives these systems the potential to benefit significantly in the short term by shifting to low GWP refrigerants. This evaluation is performed for the currently used refrigerants by accounting for the differences in energy consumption of the systems in the different climates. Then, the total emissions will be re-evaluated after shifting to low GWP refrigerants (R-32, D2Y60, and L-41a for residential HVAC, and N-40, and L-40 for commercial refrigeration systems).

4.4.2.2. Commercial Refrigeration

There are different types of systems that are used in commercial refrigeration, such as supermarket refrigeration systems, walk-in coolers and freezers, ice machines, and refrigerated vending machines. However, the supermarket refrigeration systems account for the largest portion of the total emissions from the commercial refrigeration systems due to their high charge, annual leak rate, and energy consumption. In this section, the total LCCP from the three main supermarket refrigeration systems used is calculated. These are the centralized DX, distributed, and secondary circuit systems. The number of available supermarket systems as of 2010 is 36149 (Food Marketing Institute, 2010), out of which around 70% (25,304), 26% (9,399) and 4% (1,446) are centralized DX, distributed, and secondary circuit, respectively (ICF Consulting for U.S. EPA's Stratospheric Protection Division, 2005). The LCCP calculations are done for six US cities, shown in Table 4.8, representing different climates.

The hourly emission rate for electricity production is assumed to be equal to the average rate obtained from location-specific standardized reference datasets for emissions

(Deru & Torcellini, 2007). This National Renewable Energy Laboratory (NREL) dataset has one average value for each state (obtained based on the different electricity grids covering the state) in the US which is used for each hour in the year. This assumption is made due to lack of available data on hourly emission rate for electricity production. This NREL emission database is selected as it uses data from several sources to derive the energy and emission factors for electricity generation. This includes the NREL US Life Cycle Inventory (LCI) Database (National Renewable Energy Laboratory, 2005) and the US Environmental Protection Agency (EPA) Emissions & Generation Resource Integrated Database (eGRID) (U.S. Environmental Protection Agency, 2007). It is worth noting here that although different databases might have different emission factors than those used in this study, the aim of this study is to show the potential savings in total emissions in the US when shifting to more environmentally friendly systems and lower GWP refrigerants. Based on the uncertainty analysis for similar LCCP analysis of supermarket refrigeration systems, shown in section 4.4.1.3, an uncertainty of 20% in emission factors can causes a difference of up to 20% in the total emissions of the system. However, this results in less than 2% difference between the uncertainties of different systems in the same weather. In other words, while using a different emissions database can make a noticeable difference in the absolute value of calculated total emissions in one location or over the US, it is unlikely to affect the trends and conclusions shown in the paper (i.e. when comparing the same system in different locations or different systems in the same location).

The aim of this analysis is to include the variation in the weather data and emission rates for each kWh of electricity produced throughout the US in the results. It is assumed that the number of supermarkets in each city as compared to the total number of supermarkets is equal to the fraction of the floor space in the corresponding census region to the total floor space over the US (U.S. Energy Information Administration, 2012). However, if more than one city fall within the same census region, the fraction (and hence number of supermarkets) is divided between them according to the population ratio of these cities.

Table 4.8: Climate zones and cities used in the LCCP analysis

Climate Zone	City	Annual Average Temperature (°C)
1A	Miami, FL	24.9
2B	Phoenix, AZ	23.8
3B	Los Angeles, CA	17.3
4B	Albuquerque, NM	14.2
5A	Chicago, IL	10.0
8	Fairbanks, AK	-2.1

The centralized DX system (referred to as S1), distributed system (referred to as S2), and secondary circuit system (referred to as S3) are studied using the baseline refrigerant R-404A, and the low GWP alternative N-40 (N-40/L-40 for S3). The GWP and blend composition for the different refrigerants is shown in Table 4.9.

EnergyPlus (U.S. Department of Energy, 2012) is used for the hourly energy consumption calculations. The 4181 m^2 single-story supermarket model used in this

study is based on the new construction reference supermarket model developed by the U.S. Department of Energy (Deru, et al., 2011). A representative refrigeration load of 308 kW is assumed to be served by each of the three systems with a corresponding charge of 1378 kg, 690 kg, and 669 kg, for S1, S2, and S3, respectively. The system lifetime is assumed to be 20 years with service interval of 2 years. Also, the annual leakage rate, refrigerant loss at end-of-life, service leakage rate, and reused refrigerant are 10%, 10%, 5%, and 85%, respectively (Abdelaziz, et al., 2012). Note that any other leakage rates used in the LCCP calculations, which do not have a value mentioned in this section, are assumed to be zero.

Table 4.9: Blend composition and GWP values of the used refrigerants

Refrigerant	Composition (Mass %)	GWP
R-404A	R-125/R-134a/R-143a (44/4/52)	3,922
R-407F	R-32/R-125/R-134a (30/30/40)	1,824
L-40	R-32/R-152a/R-1234yf/R-1234ze (40/10/20/30)	285
N-40	R-32/R-125/R-134a/R-1234yf (25/25/20/30)	1,300
R-410A	R-32/R-125 (50/50)	2,088
R-32	R-32 (100)	675
D2Y60	R-32/R-1234yf (40/60)	272
L-41a	R-32/R-1234yf/R-1234ze(E) (73/15/12)	494

Figure 4.9 shows the total emissions for one unit of each of the three systems in each of the climate zones using the baseline refrigerant R-404A and the low GWP blend N-40.

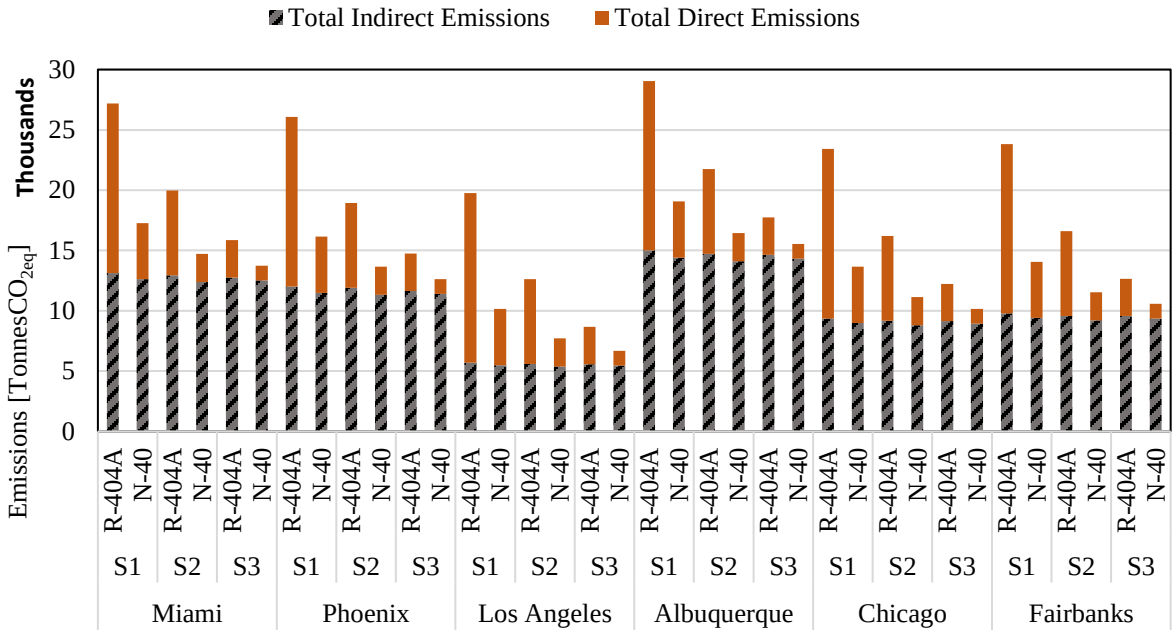

Figure 4.9: Total emissions of supermarket refrigeration systems (Beshr, et al., 2014).

Table 4.10 shows the total emissions ($TonnesCO_{2eq}$) of the supermarket refrigeration systems in four different cases: using R-404A in the current ratio of the system types (S1, S2, and S3), replacing R-404A with N-40 in all the systems, replacing all systems with S2 utilizing N-40, and replacing all systems with S3 utilizing N-40/L-40. Although a system's location does not affect the direct emissions, it affects the indirect emissions. This is due to differences in the weather data (leading to different hourly system electricity consumption) and the hourly emission rate for electricity production between the different cities. It is found that shifting from R-404A to N-40 and using the current system ratio between S1, S2, and S3, causes a drop in the total emissions from 843 Million $TonnesCO_{2eq}$ to 527.7 Million $TonnesCO_{2eq}$ over the lifetime of the system (20 years). This drop in total emissions of 37.4% is a result of 3.92% drop in indirect emissions and 66.76% drop in the direct emissions. The noticeable impact of shifting to low GWP refrigerants in supermarket refrigeration systems on the total

emissions is due to their high charge and annual leak rate, especially for the centralized DX system (emissions reduction is 40%, 30%, and 14% for S1, S2, and S3, respectively). Also, shifting towards S3 for all supermarkets results in a further drop in emissions from 527.7 Million TonnesCO_{2eq} to 417.6 Million TonnesCO_{2eq} over the lifetime of the system (13.1% drop in total emissions), which is 50.5% lower than the baseline case.

Figure 4.10 shows the distribution of total emissions from the supermarket refrigeration systems within the US. It is clear that the south census region (represented by Miami in this study) has the highest emissions. This is due to the relatively high number of supermarket refrigeration units in the south region compared to most of the other regions (e.g. 3.7 times the number of units in the pacific region), and the high total emissions from a single supermarket refrigeration unit in Miami. Although the number of units in the northeast and Midwest regions (represented by Chicago) is even more than the south region, the total emissions in the south region is higher because of the higher total emissions from a single unit in Miami compared to Chicago. However, the pacific region (represented by Los Angeles and Fairbanks in this study) has the lowest emissions. This is due to the low number of supermarket refrigeration units in the pacific region, and the low total emissions from a single supermarket refrigeration unit in some pacific cities such as Los Angeles, as shown in Figure 4.9. It is worth noting that a similar trend is seen among the different regions for all the cases shown in Table 4.10.

Table 4.10: Total emissions (Million TonnesCO2eq) for each supermarket refrigeration system

	Baseline (R-404A)	S1/S2/S3 (N-40)	S2 (N-40)	S3 (N-40)
Miami	348.7	234.4	209.5	195.6
Phoenix	69.8	43.9	39.1	36.1
Los Angeles	112.7	60.6	28.8	25.0
Albuquerque	11.0	4.7	15.7	14.8
Chicago	297.3	183.8	159.2	145.3
Fairbanks	3.5	0.3	0.9	0.8
Total	843.0	527.7	453.1	417.6

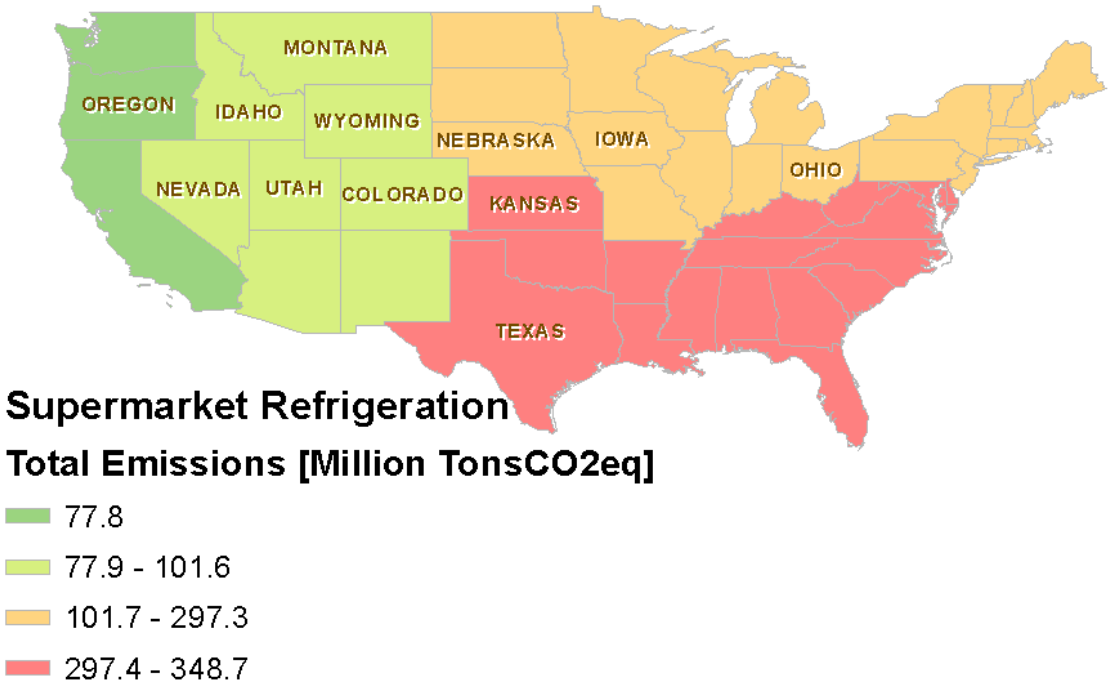

Figure 4.10: Distribution of total emissions from supermarket refrigeration systems using R-404A over the US regions

4.4.2.3. Residential HVAC

There are different types of systems that are used in residential HVAC such as residential unitary air-conditioning (AC) / heat pump (HP) systems, self-contained air conditioning systems, ground source heat pump systems, and dehumidifiers. However, the AC/HP systems account for the largest portion of the total emissions from the residential HVAC systems due to the large portion of installed units, and high annual leak rate. In this section, the total LCCP from an AC/HP system used for cooling and heating is calculated. The number of available AC/HP systems as of 2010 is 70,860,000 out of which 10,320,000 are AC (cooling only) units (U.S. Department of Energy, Building Technologies Program, 2012). The LCCP calculations were done for the same six US cities, shown in Table 4.8, representing different climates.

The hourly emission rate for electricity production is assumed to be equal to the average rate obtained from location-specific standardized reference datasets for emissions (Deru & Torcellini, 2007). This NREL dataset has one average value for each state (obtained based on the different electricity grids covering the state) in the US which is used for each hour in the year. This assumption is made due to lack of available data on hourly emission rate for electricity production. Also, this NREL emission database is selected as it uses data from several sources to derive the energy and emission factors for electricity generation. This includes the NREL LCI Database (National Renewable Energy Laboratory, 2005) and the EPA eGRID (U.S. Environmental Protection Agency, 2007). It is assumed that the number of systems in each city as compared to the total number of systems is equal to the fraction of the homes in the corresponding census region to the total number of homes over the US (U.S. Energy Information

Administration, 2012). However, if more than one city fall within the same census region, the fraction (and hence number of AC/HP systems) is divided equally among them.

The AC/HP system is studied using the baseline refrigerant R-410A, and the low GWP alternatives R-32, D2Y60, and L-41a. The LCCP of the system in the cooling only mode is used to calculate the LCCP of the AC systems while the addition of the cooling and heating modes is used to calculate the emissions of the AC/HP systems. The GWP and blend composition for the different refrigerants is shown in Table 4.9.

The simulated AC/HP system is similar to the system experimentally tested in the AHRI low GWP AREP report #20 (Alabdulkarem, et al., 2013). The system uses R-410A as the baseline refrigerant with a system charge of 4.54 kg. The AHRI standard 210/240 (ANSI/AHRI, 2008) is used for hourly load calculations. VapCyc (Winkler, et al., 2008) is used in the LCCP tool for the electricity consumption calculation. As per the AHRI standard 210/240 (ANSI/AHRI, 2008), if the ambient temperature is higher than 291.5 K (65°F), the system operates in cooling mode while for lower ambient temperatures, the system operates in the heating mode. The system's lifetime is assumed to be 15 years, with a service interval of 5 years. Also, the annual leakage rate, refrigerant loss at end-of-life, service leakage rate, and reused refrigerant are 12%, 65%, 5%, and 35%, respectively (ICF International, Prepared for the U.S. Environmental Protection Agency, 2009). Note that any other leakage rates used in the LCCP calculations, but which do not have a value mentioned in this section, are assumed to be zero.

Figure 4.11 shows the total emissions for one AC/HP unit of each of the refrigerants in each of the studied climate zones. The indirect emissions in Los Angeles are much lower than the other cities for all the refrigerants, which is mainly due to two factors. First, this city has a mild climate, therefore the heat pump will operate for shorter periods and the system's annual electricity consumption will be lower compared to the other cities. The second reason is that the hourly emission rate for electricity production is low for this city. For example, the emission rate in Phoenix is about 2 times that of Los Angeles. Also, Figure 4.11 shows that for the AC/HP system, unlike the supermarket refrigeration systems, the direct emissions represent a small fraction of the total emissions of a single unit of the system. Thus, the percentage drop in total emissions from the AC/HP system when using low GWP refrigerants is expected to be lower than the drop from the supermarket refrigeration systems. However, this occurs only if the low GWP refrigerant used in the AC/HP provides the same performance as the high GWP refrigerant. If the low GWP refrigerant provides better performance than the high GWP refrigerant, the total emissions of the system using the low GWP refrigerant would decrease significantly, and vice versa.

For all cities, L-41produces the lowest total emissions. Although L-41a does not have the lowest GWP and direct emissions (D2Y60 has the lowest GWP and direct emissions), it shows comparable system performance, low energy consumption, and indirect emissions. Thus, selecting the more environmentally friendly system's refrigerant depends not only on the refrigerant's GWP, but also its effect on the system's performance (electricity consumption).

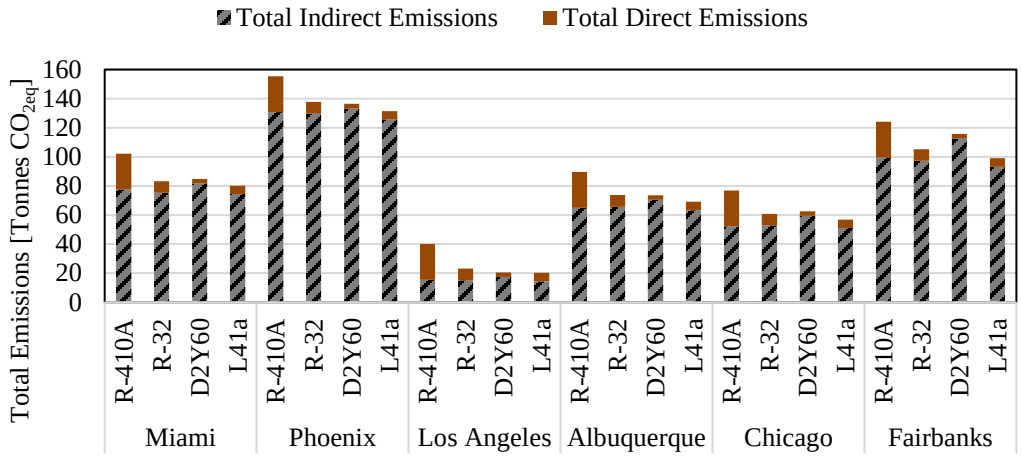

Figure 4.11: ASHP System's total emissions

Table 4.11 shows the total emissions (TonnesCO_{2eq}) for the AC/HP system after considering all the units in each city. Shifting from R-410A to L-41a causes a drop in the total emissions from 5.22 Billion TonnesCO_{2eq} to 3.76 Billion TonnesCO_{2eq} over the lifetime of the system (15 years). This drop in total emissions of 28.0% is a result of 3.7% drop in the indirect emissions and 74% drop in the direct emissions.

Figure 4.12 shows the distribution of total emissions from the AC/HP systems within the US. The south region (represented by Miami in this study) has the highest emissions, although Miami does not have the highest total emissions for a single AC/HP unit, as shown in Figure 4.11. This is mainly because of the high number of AC/HP units in the south region compared to other regions (e.g. 3.4 times the number of units in the pacific region). Although the number of units in the northeast and Midwest regions (represented by Chicago) is more than the south region, the total emissions in the south region is higher due to the higher total emissions from a single unit in Miami compared to Chicago. Additionally, the pacific region (represented by Los Angeles and Fairbanks in this study) has the lowest emissions. This is due to the

low number of AC/HP units in the pacific region, and the low total emissions from a single AC/HP unit in some pacific cities such as Los Angeles, as shown in Figure 4.11. However, both refrigerants (R-410A and L-41a) show a similar trend among different regions.

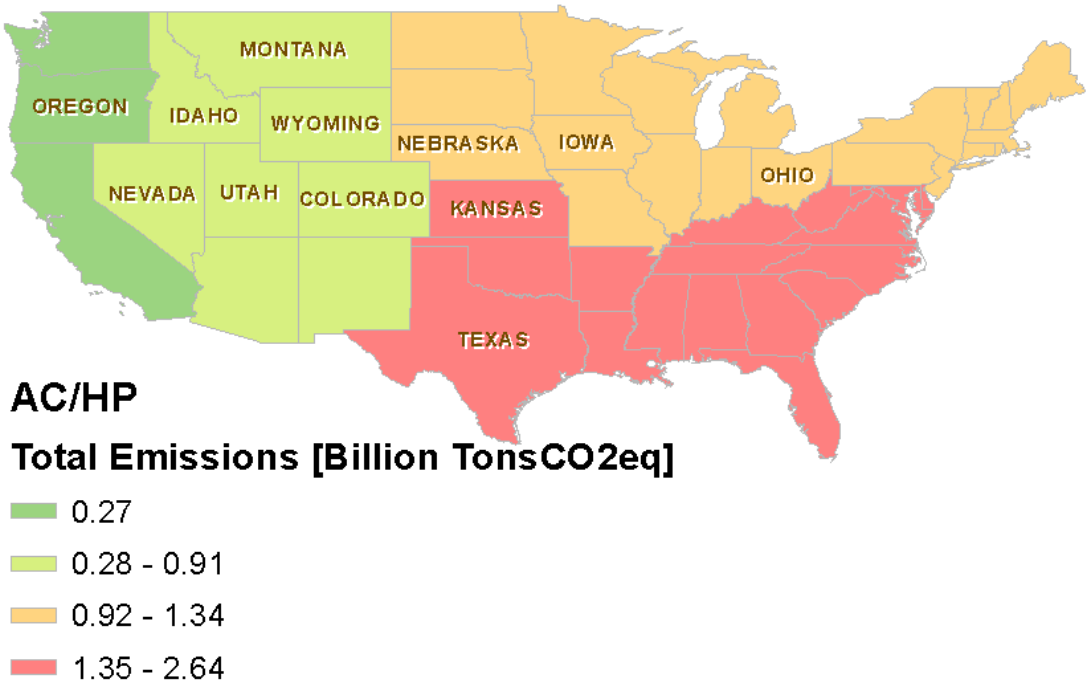

Figure 4.12: Distribution of total emissions from AC/HP systems using R-410A over the US regions

Although the LCCP of a single supermarket refrigeration unit is much higher than the LCCP of an AC/HP unit, the total emissions from the residential HVAC systems is much higher (8.5 times) than the total emissions from the commercial refrigeration systems. This is due to the large number of units of residential HVAC systems compared to the commercial refrigeration system.

Table 4.11: Total emissions (Billion TonnesCO2eq) for AC/HP system

	R-410A	**L-41a**
Miami	2.64	2.06
Phoenix	0.85	0.71
Los Angeles	0.22	0.07
Albuquerque	0.17	0.13
Chicago	1.34	0.77
Fairbanks	0.007	0.003
Total	**5.22**	**3.76**

4.4.2.4. Conclusion

In this study, the LCCP tool is used to calculate the drop-in total emissions from refrigeration, air conditioning, and heat pumping when shifting to low GWP refrigerants. The study is performed in 6 US cities representing different climates. The LCCP of the centralized DX, distributed, and secondary circuit supermarket refrigeration systems is calculated using the baseline R-404A and the low GWP alternative N-40. The drop in the total emissions from the supermarket systems is 50.5%, almost all of which is due to drop in the direct emissions. Furthermore, a residential AC/HP system is simulated using the baseline R-410A and the low GWP alternatives R-32, D2Y60, and N-40. Among the three latter refrigerants, the N-40 shows a good balance between the competitive system performance (energy consumption), and the low GWP (direct emissions). The drop in the total emissions from the AC/HP is 28.01%. The combined drop in total emissions from all the studied systems is 30.43% when shifting from the baseline to low GWP refrigerants, and

towards the more environmentally friendly refrigeration systems. Hence, using S3 supermarket refrigeration systems utilizing N-40 and an AC/HP system utilizing L-41a causes an annual drop in emissions of 118.8 Million TonnesCO_{2eq}.

5. Summary and Conclusions

The first objective of this thesis is to develop a new component-model based steady state vapor compression systems solver that can handle arbitrary cycles and multiple fluid loops. The second objective is to use this solver to design and optimize vapor compression systems using next generation components. The third objective is to develop a modular LCCP evaluation and design based tool for vapor compression systems. All of the objectives are complete and the conclusions are as follow:

5.1.VapCyc Solver

- A new component-model based steady state vapor compression systems solver is developed. This solver can handle arbitrary system configurations with large number of components (more than 500), multiple refrigerants without compromising modeling speed or robustness. Moreover, this solver supports user-defined fluids, and user-defined convergence criteria.
- The solver methodology is demonstrated for different cycles including:
    - Basic four components vapor compression cycle
    - Variable refrigerant flow system
    - Simple cycle with additional compressors in parallel
    - Simple cycle with suction line heat exchanger
    - Vapor injection heat pump system with a flash tank
    - Cascade system
- The solver is also validated using the following systems:
    - Residential ASHP system

- Vapor injection heat pump system
- Two-stage CO_2 supermarket refrigeration system with mechanical subcooler

5.2.Optimization Study

- The comprehensive solver is used to perform a multi-objective optimization of an ASHP system to determine the potential system performance improvements and material savings from using small diameter tubes in the HXs. The objectives of the optimization are minimizing the HXs cost and maximizing the COP of the system.
- By using small diameter tubes (3-5 mm):
  - The cost can be reduced by 44% and 47% for R-410A, and R-32, respectively for the same COP
  - The COP can be improved by 17%, and 15% for R-410A, and R-32, respectively for the same HXs cost
  - The system charge can be reduced by 33%

5.3.LCCP Framework

- A modular LCCP evaluation and design based framework for vapor compression systems is developed. This tool can be coupled with any vapor compression system simulation tool including VapCyc.
- The LCCP framework provides insightful analysis of the effect of shifting towards lower GWP refrigerants and more environmentally friendly HVACR systems for both commercial and residential scales in different climates.

- The LCCP tool was used to compare the environmental impact of four different supermarket refrigeration systems in six US cities. This study shows that:
    - For annual leak rate higher than 2%, the transcritical CO_2 booster system has the lowest total LCCP in cold and temperate climates
    - The secondary circuit N-40/L-40 system offers a good balance between emissions and energy consumption for hot climates with annual leak rate of 10%, and for all climates for annual leak rate less than 2%
- A residential AC/HP system is simulated using the baseline R-410A and the low GWP alternatives R-32, D2Y60, and N-40 in six US cities. This study shows that N-40 shows a good balance between the system performance (energy consumption), and the low GWP (direct emissions).
- The total LCCP from HVACR systems in the US is estimated using the developed LCCP framework. The study shows that by shifting to lower GWP refrigerants and more environmentally friendly HVACR systems:
    - The drop in the total emissions from the supermarket systems is 50.5%
    - The drop in the total emissions from the AC/HP is 28.01%
    - The combined drop in total emissions from all the studied systems is 30.43%

6. List of Contributions and Future Work

6.1.Contributions

The list of contributions include:

- Developing a new comprehensive component-based vapor compression system steady state solver that can handle arbitrary system configurations as well as primary and secondary refrigerant/fluid flow circuits. This helps evaluate the performance of any newly proposed arbitrary system, hence, reducing the engineering time of developing high efficiency advanced heat pump technology.
- Using the comprehensive solver to design and optimize vapor compression systems using next generation components. This includes using lower GWP refrigerants and heat exchangers with small diameter tubes. These optimized systems have substantial material, charge, emissions, and cost reduction and/or higher COP, and SEER.
- Developing an open source modular LCCP evaluation and design based tool for vapor compression systems. This tool can be coupled with any vapor compression system simulation tool. This allows for LCCP-based design and optimization of vapor compression systems to minimize the environmental impact of such systems. Moreover, it provides useful information about different challenges such as the selection of appropriate systems for various climates and the choice of next generation lower GWP refrigerants. Also, this LCCP framework is expected to be the basis for a new international guideline for evaluation and comparison of systems based on their LCCP.

6.2.Future Work

Although the comprehensive solver presented in this thesis is capable of simulating advanced vapor compression systems, there is still some room for additions and improvements to the solver. The future work for the comprehensive VapCyc solver includes but is not limited to:

- Develop new guess value calculation algorithm to enhance the robustness and computational efficiency of the solver. Currently, the guess values of the comprehensive solver are all based on the input values with no further improvement.
- Develop a design feedback algorithm. This algorithm can early predict the simulation failure and failure reason. This helps identify potential problems in the system design. It also provides feedback to the numerical solver during the solver iterations which helps to improve the solver robustness and reduce the engineering time. Furthermore, this algorithm identifies potential system performance improvements.
- Develop a cycle decomposition algorithm and study its effect on the solver robustness and computational efficiency. For some complex cycle configurations, it might be more time efficient and robust for the system solver to decompose the cycle to smaller and much simpler cycles. The solver then, at each iteration, solves each of these cycles and passes its results to the next one until the system converges. Thus, a potential cycle decomposition algorithm can be beneficial and needs further investigation.

Appendix A

This appendix contains a description for the different methods and parameters that are implemented in all of the components used in the new solver. The last section also shows the timeline for calling the different methods in the component model from the solver.

A.1. Parameters

A.1.1. BoundaryCondition

This parameter determines the boundary condition of the component. The component boundary condition determines which parameters from the inlet/outlet port states that the component model requires as an input to execute successfully. The comprehensive solver interacts with components that utilize two types of boundary conditions: mass flow based, and pressure based.

For the pressure based components, the inlet pressure and enthalpy, and outlet pressure are required as inputs for the models to execute. These parameters will be passed from the solver to the component prior to execution of the component model. After the component model runs successfully, it passes the inlet and outlet mass flow rates, and the outlet enthalpy to the system solver.

For the mass flow based components, the inlet pressure, enthalpy, and mass flow rate are required as inputs for the models to execute. These parameters will be passed from the solver to the component prior to execution of the component model. After the component model runs successfully, it passes the outlet pressure, enthalpy, and mass flow rate to the system solver.

A.1.2. Charge

For the previous version of the component standard, this parameter contains the charge of the component. This is an output parameter which is set after the successful run of the component model. This parameter is included in the parameters (i.e. information) of each of the fluid groups in the new standard.

A.1.3. DependentProperties

The dependent properties of the component is a list containing information about additional output parameters of the component (i.e. other than the outlet port state, charge, heat, and power consumption). Thus, these properties, as the name implies, are dependent on the successful run of the component. The details for the properties in the list includes the property name, value, quantity, units based on the quantity, and description. The solver cannot change the value of any the dependent properties as it is calculated in the component. The constraints and objectives of a system optimization are based on the list of dependent properties of the system components.

A.1.4. FluidGroups

In the comprehensive solver, a single component can utilize any number of refrigerants (e.g. the cascade heat exchanger has two different refrigerants passing through it). In order to differentiate the refrigerant paths in a component, a fluid group is defined. A single component can have more than one fluid group. The fluid group carries information including the refrigerant, port states (each fluid group has its own number of inlet and outlet ports), charge, work, heat, and power consumption. Every port through which the solver interacts with a component has a port ID which identifies the component ID, fluid group number, and port number.

The previous version of the component standard which is utilized in the arbitrary cycle solver explained in Section 2.2 doesn't support or include fluid groups. This is simply because this solver only works with one refrigerant in the system. Thus, this previous version of the component standard has parameters for the charge, work, heat, and power consumption. It also has a parameter for PortStates rather than FluidGroups. The difference between the two standard is shown in Figure A.1 below.

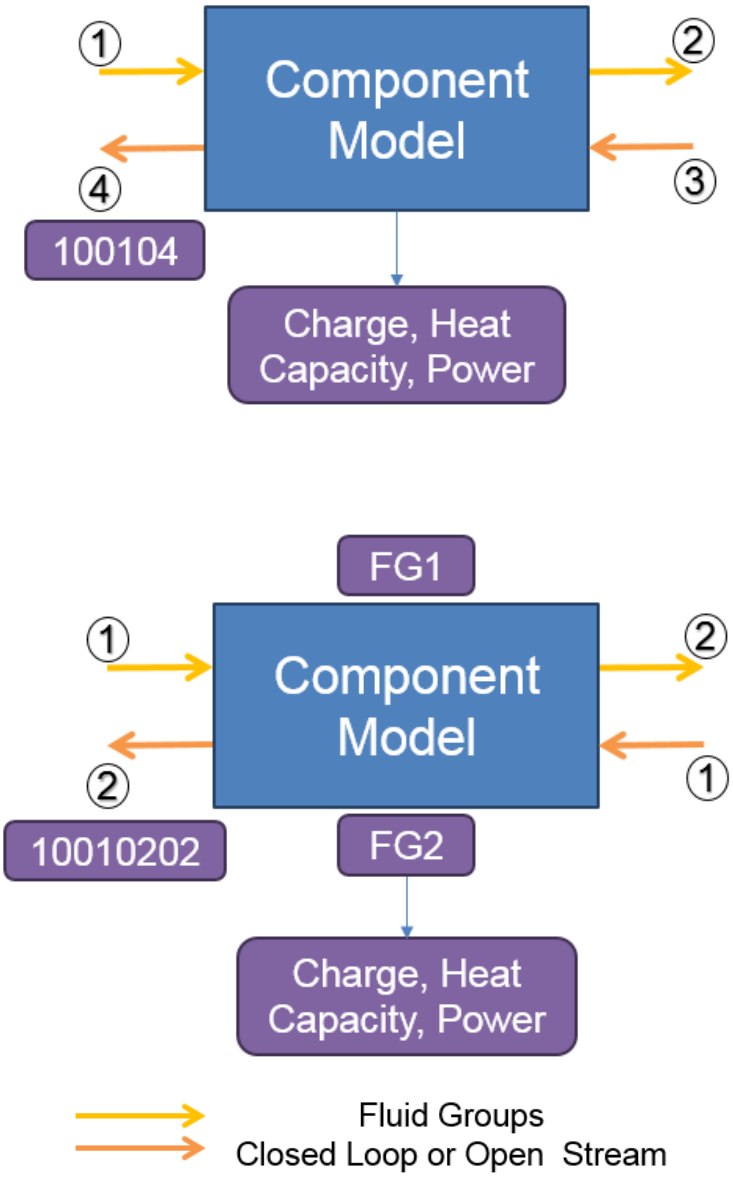

Figure 0.1: Previous (top) and new (bottom) versions of the component standard

A.1.5. FriendlyName

The friendly name of the component is a string which provides the useful name of the component. This name is a meaningful name that gives an insight about the component.

A.1.6. HeatOut

For the previous version of the component standard, this parameter contains the heat out of refrigerant in the component. For a condenser, this value is positive as heat is transferred out of the refrigerant. For an evaporator, this value is negative. This is an output parameter which is set after the successful run of the component model. This parameter is included in the parameters (i.e. information) of each of the fluid groups in the new standard.

A.1.7. HeatOutAirSideNet

For the previous version of the component standard, this parameter contains the heat out of the air (i.e. heat transferred to the refrigerant from the air side). This is an output parameter which is set after the successful run of the component model. This parameter is included in the parameters (i.e. information) of each of the fluid groups in the new standard.

A.1.8. IndependentProperties

The independent properties of the component is a list containing information about some, or all of the input properties of the component. Thus, these properties, as the name implies, are independent on the successful run of the component. The details for the properties in the list includes the property name, value, quantity, units based on the quantity, and description. The solver can change the value of any the independent

properties which in turn changes a corresponding property value in the component. The assigning and using of the independent properties is useful when running a parametric analysis, or system optimization. The variables that can be changed during these two analyses is based on the independent properties list.

A.1.9. Messages

This is a list of strings containing all the messages generated while running the component. These messages can vary between warning messages (which doesn't affect the success of the component run) to an error message causing a failure of the component run. The aim of this parameter is to provide useful information about the component run to the solver. One example of this is returning an error message with run termination if the refrigerant of the selected compressor model is different than the system refrigerant.

A.1.10. PowerConsumption

For the previous version of the component standard, this parameter contains the power consumption of the component. This is an output parameter which is set after the successful run of the component model. This parameter is included in the parameters (i.e. information) of each of the fluid groups in the new standard.

A.1.11. Refrigerant

This has different information about the refrigerant in each of the fluid groups in the component. The refrigerant flowing in each fluid group can be any fluid from any of the following:

- Built in refrigerant (e.g. R-410A)

- User-defined refrigerant
- Air (both dry air and moist air)
- Glycol
- Ammonia water

For a refrigerant mixture, the refrigerant parameter contains the different fluids in the mixture with the normalized mass ratio for each of the fluids.

A.1.12. WorkingFolder

The working folder of the component is the string for a directory which can contain useful information for the component. As an example, if the component model loads a certain file to obtain the required input information (e.g. Microsoft Access file containing the details of the compressor models for a 10 coefficient compressor model), this working folder can be the path of the folder containing this file.

A.2. Methods

A.2.1. BeginSimulation

This method is called before running the non-linear solver. This method can be used to edit any information in the component. One example of the use of this component is the system optimization in Chapter 3 of this thesis. The BeginSimulation method of the heat exchanger component model is used to build the new heat exchanger at every optimization iteration based on the input values for each of the design variables.

A.2.2. EditProperties

This method is the one responsible for the interaction between the component model and its user interface. This method is invoked when the user chooses to edit the inputs

of a component model in the user interface. It is responsible for displaying the user interface for the component showing the current set of values for the inputs of the component model. After editing these input values in the user interface, the new values are passed back to the component model to be used when running the component model.

A.2.3. EndSimulation

This method is called at the end of the simulation. This method can be used to edit any information in the component. One example of the use of this component is when running a parametric analysis on the system. The BeginSimulation method can be used to set a new value for the studied parameter only once at the beginning of the solver runs (e.g. by changing the value of the corresponding independent property). After the simulation is complete, the EndSimulation method can be used to change the studied parameter value back to the original (i.e. baseline) value.

A.2.4. InitializeComponent

This method initializes the component. It returns true if the component is successfully initialized and false if not. The solver will not use the component if it is not initialized. Initializing the component can include adding the list of dependent and independent properties, initializing the refrigerant property calculations, setting the boundary condition, and setting the number of fluid groups in the component and ports in each fluid group.

A.2.5. LoadState

This method is used to load the component inputs from a saved file. This can be used to load the component information as part of the system load method in the solver. It can be also used to load the inputs for an individual component from a saved component file to override the existing set of inputs.

A.2.6. Run

This method executes the component model equations to obtain the results and outlet port states of the component.

A.2.7. SaveState

This method is used to save the component inputs. This can be used to save the component information as part of the system save method in the solver. It can be also used to save the inputs for an individual component to be used in other systems.

A.2.8. TerminateComponent

This method is called when the component model is no longer used. This can be if a component model is unloaded from a system or if the entire system simulation is terminated. This can be used to restore computational memory reserved by the refrigerant property calculations of the component model.

A.3. Solver Timeline

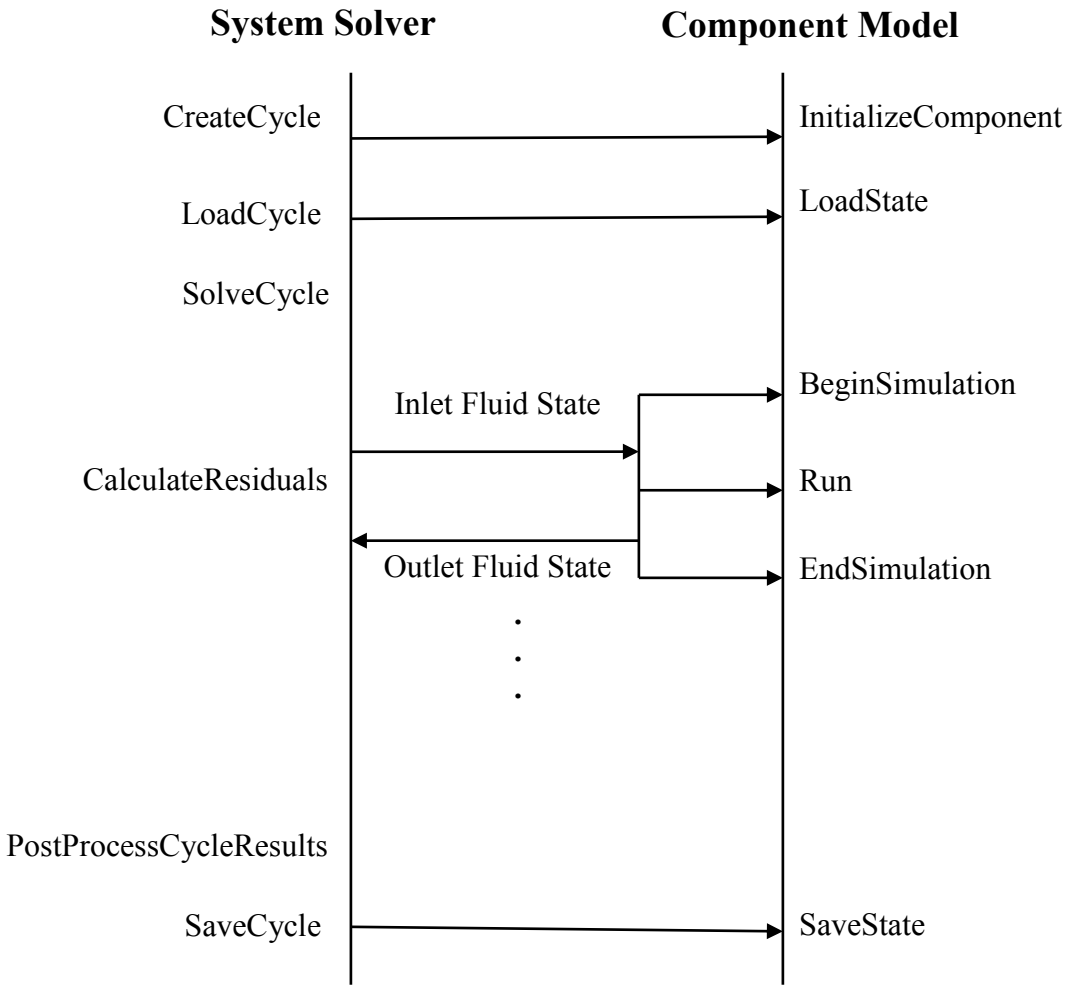

Figure A.2: Solver Timeline

7. Bibliography

Abdelaziz, O., Aute, V., Azarm, S. & Radermacher, R., 2010. Approximation-Assisted Optimization for Novel Compact Heat Exchanger Designs. *HVAC&R Research*, 16(5), pp. 707-728.

Abdelaziz, O., Fricke, B. & Vineyard, E., 2012. *Development of Low Global Warming Potential Refrigerant Solutions for Commercial Refrigeration Systems using a Life Cycle Climate Performance Design Tool.* West Lafayette, Indiana, s.n.

Agrawal, N., Bhattacharyya, S. & Sarkar, J., 2007. Optimization of Two-Stage Transcritical Carbon Dioxide Heat Pump Cycles. *International Journal of Thermal Sciences,* Volume 46, pp. 180-187.

Alabdulkarem, A. et al., 2015. Testing, simulation and soft-optimization of R410A low-GWP alternatives in heat pump system. *International Journal of Refrigeration.*

Alabdulkarem, A., Hwang, Y. & Radermacher, R., 2013. *System Drop-In Tests of Refrigerants R-32, D2Y-60, and L41a in Air Source Heat Pump,* s.l.: Air-Conditioning, Heating, and Refrigeration Institute (AHRI) Low-GWP Alternative Evaluation Program.

Almedia, M. S., Gouveia, M. C., Zdebsky, S. R. & Parise, J. A., 1990. Performance Analysis of a Heat Pump Assisted Drying System. *International Journal of Energy Research,* Volume 14, pp. 397-406.

Amrane, K., 2013. *Overview of AHRI Research on Low-GWP Refrigerants,* s.l.: AHRI Low-GWP Alternative Refrigerants Evaluation Program Presentation.

ANSI/AHRI, 2004. *AHRI 540-2004 Performance Rating Of Positive Displacement Refrigerant Compressors and Compressor Units,* s.l.: s.n.

ANSI/AHRI, 2008. *ANSI/AHRI 210/240-2008 with Addenda 1 and 2, Performance Rating of Unitary Air-Conditioning & Air-Source Heat Pump Equipment,* s.l.: s.n.

Arthur D. Little Inc., 2002. *Global Comparative Analysis of HFC and Alternative Technologies for Refrigeration, Air Conditioning, Foam, Solvent, Aerosol Propellant, and Fire Protection Applications,* s.l.: The Alliance for Responsible Atmospheric Policy.

ASHRAE, 1995. *ANSI/ASHRAE Standard 116, Methods of testing for rating seasonal efficiency of unitary air conditioners and heat pumps,* Atlanta, GA, USA: ASHRAE.

Aute, V. & Radermacher, R., 2014. *TSIOP- Thermal Systems Integration and Optimization Platform, IS-2005-062, Platform Documentation and Codes,* s.l.: University of Maryland.

Bacellar, D., Abdelaziz, O., Aute, V. & Radermacher, R., 2015. *Novel Heat Exchanger Design Using Computational Fluid Dynamics and Approximation Assisted Optimization.* Chicago, IL, s.n.

Bacellar, D., Aute, V. & Radermacher, R., 2014. *CFD-Based Correlation Development for Air Side Performance of Finned and Finless Tube Heat Exchangers with Small Diameter Tubes.* Purdue University, West Lafayette, Indiana, USA, s.n.

Bacellar, D., Aute, V. & Radermacher, R., 2015. *CFD-Based Correlation Development for Air Side Performance of Small Diameter Tube-Fin Heat Exchangers with Wavy Fins.* Yokohama, Japan, s.n.

Belman, J. M., Navarro-Esbri, J., Ginestar, D. & Milian, V., 2009. Steady-state Model of a Variable Speed Vapor Compression System Using R134A as Working Fluid. *International Journal of Energy Research,* 34(11), pp. 933-945.

Beshr, M. et al., 2015. Potential Emissions Savings from Refrigeration and Air Conditioning Systems by Using Low GWP Refrigerants. *International Journal of Life Cycle Assessment*, Volume accepted.

Beshr, M., Aute, V., Fricke, B. & Radermacher, R., 2014. *An Evaluation of the Environmental Impact of Commercial Refrigeration Systems Using Alternative Refrigerants.* London, s.n.

Beshr, M., Aute, V. & Radermacher, R., 2015. Multi-objective Optimization of a Residential Air Source Heat Pump with small-diameter tubes using Genetic Algorithms. *International Journal of Refrigeration*, Volume 67, pp. 134-142.

Beshr, M. et al., 2015. A Comparative Study on the Environmental Impact of Supermarket Refrigeration Systems Using Low GWP Refrigerants. *International Journal of Refrigeration*, Volume 56, pp. 154-164.

Beshr, M., Bush, J., Aute, V. & Radermacher, R., 2016. *Steady State Testing and Modeling of a CO2 Two-Stage Refrigeration System with Mechanical Subcooler.* Edinburgh, UK, s.n.

Bhatti, M. S. & Shah, R. K., 1987. Turbulent and Transition Flow Convective Heat Transfer in Ducts. In: S. Kacak, R. K. Shah & W. Aung, eds. *Handbook of Single Phase Heat Transfer*. New York: John Wiley.

Blanco, D., Nagano, K. & Morimoto, M., 2012. Steady State Vapor Compression Refrigeration Cycle Simulation for a Monovalent Inverter-Driven Water-to-Water Heat Pump with a Desuperheater for Low Energy Houses. *International Journal of Refrigeration*, Volume 35, pp. 1833-1847.

Bourdouxhe, J. P. et al., 1994. A Toolkit for Primary HVAC System Energy Calculation – Part 2: Reciprocating Chiller Models. *ASHRAE Transactions,* 100(2), pp. 774-786.

Browne, M. & Bansal, P., 1998. Steady-State Model of Centrifugal Liquid Chillers. *International Journal of Refrigeration,* Volume 21, pp. 343-358.

Broyden, C. G., 1965. A Class of Methods for Solving Nonlinear Simultaneous Equations. *Mathematics of Computation,* Volume 19, p. 577–593.

Burns, L., Austin, M. & Chen, C., 2013. *System Drop-in Testing of R-410A Replacements in Split System Heat Pump,* s.l.: Air-Conditioning, Heating, and Refrigeration Institute (AHRI) Low-GWP Alternative Evaluation Program.

Cavallini, A. et al., 2003. Condensation Inside and Outside Smooth and Enhanced Tubes - a Review of Recent Research. *International Journal of Refrigeration,* 26(4), pp. 373-292.

Choi, S.-H., Cho, W.-H., Kim, J.-W. & Kim, J.-S., 2004. A Study on the Development of the Wire Woven Heat Exchanger Using Small Diameter Tubes. *Experimental Thermal and Fluid Science,* 28(2-3), pp. 153-158.

Churchill, S. W., 1977. Frictional Equation Spans All Fluid Flow Regimes. *Chemical Engineering Journal,* Volume 84, pp. 91-92.

Corberan, J. M., Gonzalvez, J., Montes, P. & Blasco, R., 2002. *'ART' a Computer Program Code to Assist the Design of Refrigeration and A/C Equipment.* West Lafayette, IN, s.n.

Corberan, J. M., Gonzalvez, J., Urchuegui, J. & Lendoiro, A. N., 2000. *Simulation of an Air-to-Water Reversible Heat Pump.* West Lafayette, IN, s.n.

Dang, C., Daiguji, H., Hihara, E. & Tokunaga, M., 2011. Finned Small Diameter Tube Heat Exchanger. *Transactions of the Japan Society of Refrigerating and Air Conditioning Engineers,* 18(2), pp. 143-151.

Davis, G. L. & Scott, T. C., 1976. *Component Modeling Requirements for Refrigeration System Simulation.* West Lafayette, s.n.

de Lemos, M. J. & Zaparoli, E. L., 1996. *Steady-State Numerical Solution of Vapor Compression Refrigeration Units.* West Lafayette, s.n.

Deb, K., 2001. *Multi-Objective Optimization Using Evolutionary Algorithms.* s.l.:John Wiley & Sons.

Deru, M. et al., 2011. *U.S. Department of Energy Commercial Reference Building Models of the National Building Stock,* Golden, CO: National Renewable Energy Laboratory.

Deru, M. & Torcellini, P., 2007. *Source Energy and Emission Factors for Energy Use in Buildings,* s.l.: National Renewable Energy Laboratory (NREL).

Ding, G. L., 2007. Recent Developments in Simulation Techniques for Vapor-Compression Refrigeration Systems. *International Journal of Refrigeration,* Volume 18, pp. 1119-1133.

Ding, G. et al., 2012. Simulation-based Design Method for Room Air Conditioner with Smaller Diameter Copper Tubes. *International Journal of Air-Conditioning and Refrigeration,* 20(3).

Dittus, F. W. & Boelter, L. M., 1985. Heat Transfer in Automobile Radiators of the Tubular Type. *International Communications in Heat and Mass Transfer,* 12(1), pp. 3-22.

DOE/ORNL, n.d. *DOE/ORNL Heat Pump Design Model.* [Online] Available at: http://web.ornl.gov/~wlj/hpdm/MarkVI.shtml

Domanski, P. A. & Didion, D., 1983. *Computer Modeling of the Vapor Compression Cycle with Constant Flow Area Expansion Device,* Gaithersburg, MD: National Institute of Standards and Technology.

Domanski, P. A., Didion, D. & Chi, J., 2003. *CYCLE_D: NIST Vapor Compression Cycle Design Program, Version 3.0 User Guide,* Gaithersburg, MD: National Institute of Standards and Technology.

Domanski, P. A. & McLinden, M. O., 1992. A Simplified Cycle Simulation Model for the Performance Rating of Refrigerant and Refrigerant Mixtures. *International Journal of Refrigeration,* Volume 15, pp. 81-88.

Eldeeb, R., Aute, V. & Radermacher, R., 2016. *An Improved Approach for Modeling Plate Heat Exchangers Based on Successive Substitution in Alternating Flow Directions.* West Lafayette, s.n.

Ellison, R. D. & Creswick, F. A., 1978. *A Steady-State Computer Design Model for an Air-to-Air Heat Pump, ORNL/CON-16,* Oak Ridge, TN: Energy Division, Oak Ridge National Laboratory.

Emerson Climate Technologies, 2015. *System Design Simulator (SDS) V 8.3.3.* [Online] Available at: http://www.emersonclimate.com/en-us/Services/Design_Testing/Design_Services_Network/Pages/SystemDesignSimulator(SDS).aspx [Accessed 12 8 2015].

Fischer, S. K. & Rice, C. K., 1983. *The Oak Ridge Heat Pump Model: I. A Steady State Computer Design Model for Air-to-Air Heat Pumps, ORNL/CON-80/RI,* Oak Ridge, TN: Energy Division, Oak Ridge National Laboratory.

FKW Research Center for Refrigeration and Heat Pumps, 2013. *Cycle calculation program KMKreis 7.0.* [Online] Available at: http://www.fkw-hannover.de/8.html [Accessed 12 8 2015].

Foli, K. et al., 2006. Optimization of Micro Heat Exchanger: CFD, Analytical Approach and Multi-Objective Evolutionary Algorithms. *International Journal of Heat and Mass Transfer*, 49(5-6), pp. 1090-1099.

Food Marketing Institute, 2010. *Supermarket Facts - Industry Overview 2010,* s.l.: s.n.

Fukushima, T., Arai, A. & Arai, N., 1977. Simulation of Refrigeration Cycle for Air Conditioners. *JSRAE Reito,* Volume 52, pp. 301-314.

Gholap, A. K. & Khan, J. A., 2007. Design and Multi-Objective Optimization of Heat Exchangers for Refrigerators. *Applied Energy,* 84(12), pp. 1226-1239.

Goetzler, W., 2007. Variable Refrigerant Flow Systems. *ASHRAE Journal,* 49(4), pp. 24-31.

Grossman, G. & Gommed, K., 1987. A Computer Model for Simulation of Absorption Systems in Flexible and Modular Form. *ASHRAE Transactions,* 93(2), pp. 2389-2428.

Grossman, G. & Michelson, E., 1985. A Modular Computer Simulation of Absorption Systems. *ASHRAE Transactions,* 91(2B), pp. 1808-1827.

Grossman, G. & Zaltash, A., 2001. ABSIM – Modular Simulation of Advanced Absorption Systems. *International Journal of Refrigeration,* Volume 24, pp. 531-543.

Herbas, T. B. et al., 1993. Steady-State Simulation of Vapour Compression Heat Pumps. *International Journal of Energy Research,* Volume 17, pp. 801-816.

Hiller, C. C. & Glicksman, L. R., 1976. *Improving Heat Pump Performance via Compressor Capacity Control Analysis and Test, Volume 1. Energy Laboratory Reports MIT-EL 76-0001*, Cambridge, MA: MIT Energy Laboratory.

Hui, J. & Spitler, J. D., 2002. A Parameter Estimation Based Model of Water-to-Water Heat Pumps for Use in Energy Calculation Programs. *ASHRAE Transactions,* 108(1), pp. 3-17.

Hwang, Y. & Radermacher, R., 1998. Theoretical Evaluation of Carbon Dioxide Refrigeration Cycle. *HVAC&R Research,* Volume 43, pp. 245-263.

ICF Consulting for U.S. EPA's Stratospheric Protection Division, 2005. *Revised Draft Analysis of U.S. Commercial Supermarket Refrigeration Systems,* s.l.: s.n.

ICF International, Prepared for the U.S. Environmental Protection Agency, 2009. *The U.S. Phaseout of HCFCs: Projected Servicing Needs in the U.S. Air-Conditioning and Refrigeration Sector,* s.l.: s.n.

Incropera, F. P. & DeWitt, D. P., 1996. *Introduction to Heat Transfer.* 3rd ed. New York: John Wiley & Sons.

Intergovernmental Panel on Climate Change, 2013. *Fifth Assesment Report: Climate Change,* Geneva, Switzerland: s.n.

Jiang, H., Aute, V. & Radermacher, R., 2006. CoilDesigner: A General-Purpose Simulation and Design Tool for Air-to-Refrigerant Heat Exchangers. *International Journal of Refrigeration,* 29(4), pp. 601-610.

Jolly, P., Jia, X. & Clements, S., 1990. Heat Pump Assisted Continuous Drying Part 1: Simulation Model. *International Journal of Energy Research,* Volume 14, pp. 757-770.

Joudi, K. A. & Namik, H. M., 2003. Component Matching of a Simple Vapor Compression Refrigeration System. *Energy Conversion and Management,* Volume 44, pp. 975-993.

Jung, D. S., McLinden, M., Radermacher, R. & Didion, D., 1989. A Study of Flow Boiling Heat Transfer with Refrigerant Mixtures. *International Journal of Heat and Mass Transfer*, 32(9), pp. 1751-1764.

Jung, D. S. & Radermacher, R., 1989. Prediction of Pressure Drop During Horizontal Annular Flow Boiling of Pure and Mixed Refrigerants. *International Journal of Heat and Mass Transfer*, 32(12), pp. 2436-2446.

Kasagi, N., Shikazono, N., Suzuki, Y. & Oku, T., 2003. *Assessment of High-Performance Compact Micro Bare-Tube Heat Exchangers for Electronics Equipment Cooling.* University of Newcastle, s.n.

Kasagi, N., Suzuki, Y., Shikazono, N. & Oku, T., 2003. *Optimal Design and Assessment of High Performance Micro Bare-Tube Heat Exchangers.* Crete, s.n., pp. 241-246.

Koury, R., Machado, L. & Ismail, K., 2001. Numerical Simulation of a Variable Speed Refrigeration System. *International Journal of Refrigeration,* Volume 24, pp. 192-200.

Koyama, S., Lee, J. & Yonemoto, R., 2004. An investigation on Void Fraction of Vapor–Liquid Two-Phase Flow for Smooth and Microfin Tubes with R134a at Adiabatic Condition. *International Journal of Multiphase Flow,* Volume 30, pp. 291-310.

Lei, Z. & Yanting, Z., 2013. *System Drop-in Test of Refrigerant R-32 in Split Air-conditioning System,* s.l.: Air-Conditioning, Heating, and Refrigeration Institute (AHRI) Low-GWP Alternative Evaluation Program.

Li, H. & By, B., 2012. *Soft-optimized System Test of Refrigerant R-32 in 3-ton Split System Heat Pump,* s.l.: Air-Conditioning, Heating, and Refrigeration Institute (AHRI) Low-GWP Alternative Evaluation Program.

Lockhart, R. W. & Martinelli, R. C., 1949. Proposed Correlation of Data for Isothermal Two-Phase, Two-Component Flow in Pipes. *Chemical Engineering Progress,* 45(1), pp. 39-48.

Motta, S. F. Y., 2011. *Low-GWP Refrigerants for Air Conditioning and Refrigeration Applications,* s.l.: Honeywell.

Muller, A. C. & Chiou, J., 1988. Review of Various Types of Flow Mal-Distribution in Heat Exchangers. *Heat Transfer Engineering,* 9(2), pp. 36-50.

Najafi, H., Najafi, B. & Hoseinpoori, P., 2011. Energy and Cost Optimization of a Plate and Fin Heat Exchanger Using Genetic Algorithm. *Applied Thermal Engineering,* 31(10), pp. 1839-1847.

National Renewable Energy Laboratory, 2005. *U.S. LCI Database.* [Online]
Available at: www.nrel.gov/lci [Accessed 2016].

National Renewable Energy Laboratory, 2005. *U.S. LCI Database.* [Online]
Available at: www.nrel.gov/lci [Accessed 2016].

National Renewable Energy Laboratory, 2012. *National Solar Radiation Data Base, 1991-2005 Update: Typical Meteorological Year 3,* s.l.: s.n.

Negrão, C. & Hermes, C., 2011. Energy and Cost Savings in Household Refrigerating Appliances: A Simulation-Based Design Approach. *Applied Energy,* 88(9), pp. 3051-3060.

Oak Ridge National Laboratory, and the University of Maryland College Park, 2013. *LCCP Desktop Application v1 Engineering Reference*, s.l.: s.n.

Pacific Gas and Electric Company, 2011. *Supermarket Refrigeration Codes and Standards Enhancement Initiative (CASE),* San Francisco, CA: s.n.

Paitoonsurikarn, S., Kasagi, N. & Suzuki, Y., 2000. *Optimal Design of Micro Bare-Tube Heat Exchanger.* Hong Kong, s.n., pp. 972-979.

Papasavva, S., Hill, W. R. & Andersen, S. O., 2010. GREEN-MAC-LCCP: A Tool for Assessing the Life Cycle Climate Performance of MAC Systems. *Environmental Science & Technology,* 44(19), pp. 7666-7672.

Parise, J. A., 1986. Simulation of Vapour-Compression Heat Pumps. *Simulation,* Volume 46, pp. 71-76.

Paulus, D., Gaggioli, R., Park, H. & Dunbar, W., 1994. *Development of Personal Computer Software for Energy System Simulation.* Chicago, IL, s.n.

Pettersen, J., Hafner, A. & Skaugen, G., 1986. Development of Compact Heat Exchangers for CO2 Air-Conditioning Systems. *International Journal of Refrigeration,* 21(3), pp. 180-193.

Pham, H. & Rajendran, R., 2012. *R32 and HFOs as Low-GWP Refrigerants for Air Conditioning.* Purdue University, West Lafayette, Indiana, USA, s.n.

Qiao, H. et al., 2013. A New Model for Plate Heat Exchangers with Generalized Flow Configurations and Phase Change. *International Journal of Refrigeration,* 36(2), pp. 622-632.

Qiao, H., Aute, V. & Radermacher, R., 2010. *A Review for Numerical Simulation of Vapor Compression Systems.* West Lafayette, s.n.

Rajendran, R., 2013. *Promising Lower GWP Refrigerants In Air Refrigerants In Air-Conditioning Conditioning And Refrigeration Systems,* s.l.: Emerson Climate Technologies.

Richardson, D., 2006. *An Object Oriented Simulation Framework for Steady-State Analysis of Vapor Compression Refrigeration Systems and Components, PhD Dissertation,* s.l.: University of Maryland, College Park.

Richardson, D., Aute, V., Winkler, J. & Radermacher, R., 2004. *Numerical Challenges in Simulation of a Generalized Vapor Compression Refrigeration System.* West Lafayette, IN, s.n.

Richardson, D. H., Jiang, H., Lindsay, D. & Radermacher, R., 2002. *Optimization of Vapor Compression Systems via Simulation.* Purdue University, West Lafayette, Indiana, USA, s.n.

Richardson, D., Jiang, H., Lindsay, D. & Radermacher, R., 2002. *Optimization of Vapor-Compression Systems Via Simulation.* West Lafayette, IN, s.n.

Rigola, J., Raush, G., Pérez-Segarra, C. D. & Oliva, A., 2005. Numerical Simulation and Experimental Validation of Vapour Compression Refrigeration Systems - Special Emphasis on CO2 Trans-critical Cycles. *International Journal of Refrigeration,* 28(8), pp. 1225-1237.

Robinson, D. M. & Groll, E. A., 2000. Theoretical Performance Comparison of CO2 Transcritical Cycle Technology Versus HFC-22 Technology for a Military Packaged Air Conditioner Application. *HVAC&R Research,* Volume 64, pp. 325-348.

Rossi, T. A., 1995. *Detection, Diagnosis, and Evaluation of Faults in Vapor Compression Cycle Equipment, PhD Dissertation,* West Layafette, IN: Department of Mechanical Engineering, Purdue University.

Saji, N. et al., 2001. Development of a Compact Laminar Flow Heat Exchanger with Stainless Steel Micro-Tubes. *Physica C: Superconductivity,* 354(1-4), pp. 148-151.

Sanaye, S. & Hajabdollahi, H., 2010. Thermal-Economic Multi-Objective Optimization of Plate Fin Heat Exchanger Using Genetic Algorithm. *Applied Energy,* 87(6), pp. 1893-1902.

Sanaye, S. & Malekmohammadi, H. R., 2004. Thermal and Economical Optimization of Air Conditioning Units with Vapor Compression Refrigeration System. *Applied Thermal Engineering,* Volume 24, pp. 1807-1825.

Santa, R. & Garbai, L., 2013. The Mathematical Model and Numerical Simulation of the Heat Pump System. *International Journal of Engineering,* Volume 4, pp. 271-280.

Sarkar, J., Bhattacharyya, S. & Gopal, M. R., 2006. Simulation of a CO2 Transcritical Heat Pump Cycle for Simultaneous Cooling and Heating Applications. *International Journal of Refrigeration,* Volume 29, pp. 735-743.

Shao, S., Shi, W., Li, X. & Yan, Q., 2008. Simulation Model for Complex Refrigeration Systems Based on Two-Phase Fluid Network – Part I: Model Development. *International Journal of Refrigeration,* 31(3), pp. 490-499.

Shen, B. & Rice, C. K., 2014. *HVAC System Optimization with a Component Based System Model – New Version of ORNL Heat Pump Design Model, Purdue HVAC/R Optimization short course, International Compressor & refrigeration conferences at Purdue.* West Lafayette, USA: s.n.

Shikazono, N. et al., 2007. *Research and Development of High-Performance Compact Finless Heat Exchangers.* s.l., s.n.

Southern California Edison, 2004. *Investigation of secondary loop supermarket refrigeration systems,* s.l.: California Energy Commission.

Stefanuk, N. M., Aplevich, J. D. & Renksizbulut, M., 1992. Modeling and Simulation of a Superheat-Controlled Water-to-Water Heat Pump. *ASHRAE Transactions,* 98(2), pp. 172-184.

Stoecker, W. F., 1971. A Generalized Program for Steady-State System Simulation. *ASHRAE Transactions,* 77(1), pp. 140-147.

SysMo Ltd, n.d. *SmoWeb - The computational platform.* [Online]

Available at: http://platform.sysmoltd.com/ [Accessed 28 8 2015].

Tassou, S. A., Marquand, C. J. & Wilson, D. R., 1982. Modelling of Variable Speed Air-to-Water Heat Pump Systems. *Journal of the Institute of Energy,* Volume 59, pp. 59-64.

Technical University of Denmark (DTU), n.d. *CoolPack - IPU.* [Online]

Available at: http://en.ipu.dk/Indhold/refrigeration-and-energy-technology/coolpack.aspx [Accessed 28 8 2015].

The Air Conditioning, Heating and Refrigeration Institute, n.d. *AHRI Low-GWP Alternative Refrigerants Evaluation Program.* [Online]. Available at:

http://www.ahrinet.org/ahri+low_gwp+alternative+refrigerants+evaluation+program.aspx.

U.S. Department of Energy, Building Technologies Program, 2012. *Annual Energy Outlook Early Release 2012,* s.l.: s.n.

U.S. Department of Energy, 2010. *Energy Efficiency Trends in Residential and Commercial Buildings,* s.l.: U.S. Department of Energy.

U.S. Department of Energy, 2011. *Alternative Efficiency Determination Methods and Alternate Rating Method.* [Online] Available at: https://www1.eere.energy.gov/buildings/appliance_standards/pdfs/arm_aedms_rfi.pdf [Accessed 2015].

U.S. Department of Energy, 2012. *EnergyPlus Energy Simulation Software.* [Online] Available at: http://apps1.eere.energy.gov/buildings/energyplus/

U.S. Energy Information Administration, 2012. *Commercial Buildings Energy Consumption Survey (CBECS).* [Online] Available at: http://www.eia.gov/consumption/commercial/reports/2012/preliminary/index.cfm [Accessed 12 2014].

U.S. Environmental Protection Agency, 2007. *eGRID 2006 version 2.1. Emissions and Generation Resource Integrated Database.* [Online]
Available at: www.epa.gov/cleanenergy/egrid [Accessed 2016].

U.S. Environmental Protection Agency, 2007. *eGRID 2006 version 2.1. Emissions and Generation Resource Integrated Database.* [Online]
Available at: www.epa.gov/cleanenergy/egrid [Accessed 2016].

UNEP/TEAP, 1999. *The Implications to the Montreal Protocol of the Inclusion of HFCs and PFCs in the Kyoto Protocol,* s.l.: s.n.

United nations environment programme ozone secretariat, 1989. Montreal Protocol on Substances that Deplete the Ozone Layer Final Act 1987. *Journal of Environmental Law,* 1(1), pp. 128-136.

United Nations, 1998. *Kyoto Protocol to the United Nations Framework Convention on Climate Change,* s.l.: United Nations.

University of Maryland, College Park, n.d. *Thermodynamic Cycle Model (TCM)* | *Center for Environmental Energy Engineering.* [Online] Available at: http://www.ceee.umd.edu/consortia/isoc/tcm [Accessed 28 8 2015].

Wang, C.-C., Tsai, Y.-M. & Lu, D.-C., 1998. Comprehensive Study of Convex-Louver and Wavy Fin-and-Tube Heat Exchangers. *Journal of Thermophysics and Heat Transfer,* 12(3), pp. 423-430.

Wang, X., Amrane, K. & Johnson, P., 2012. *Low Global Warming Potential (GWP) Alternative Refrigerants Evaluation Program (Low-GWP AREP).* West Lafayette, IN, s.n.

Webb, R. L. & Kim, N.-H., 2005. *Principles of Enhanced Heat Transfer.* New York: Taylor & Francis.

Winkler, J., Aute, V. & Radermacher, R., 2006. *Component-Based Vapor Compression Simulation Tool with Integrated Multi-Objective Optimization Routines.* Purdue University, West Lafayette, Indiana, USA, s.n.

Winkler, J., Aute, V. & Radermacher, R., 2008. Comprehensive Investigation of Numerical Methods in Simulating a Steady-State Vapor Compression System. *International Journal of Refrigeration,* 31(5), pp. 930-942.

Winkler, J. M., 2009. *Development of a Component Based Simulation Tool for the Steady State and Transient Analysis of Vapor Compression Sysytems, PhD Dissertation,* s.l.: University of Maryland, College Park.

Wu, W. et al., 2012. *Principle of Designing Fin-and-Tube Heat Exchanger With Smaller Tube for Air Condition.* Purdue University, West Lafayette, Indiana, USA, s.n.

Xu, X., Hwang, Y. & Radermacher, R., 2013. Performance Comparison of R410A and R32 in Vapor Injection Cycles. *International Journal of Refrigeration,* 36(3), pp. 892-903.

Zhang, M., Muehlbauer, J., Aute, V. & Radermacher, R., 2011. *Life Cycle Climate Performance Model for Residential Heat Pump System,* s.l.: Air-Conditioning, Heating and Refrigeration Technology Institute, Inc. (AHRTI).

Zhao, P. C., Ding, G. L., Zhang, L. & Zhao, L., 2003. Simulation of a Geothermal Heat Pump with Non-Azeotropic Mixture. *Applied Thermal Engineering,* Volume 23, pp. 1515-1524.